Mechanisms of Clearance of MHC I-deficient Tumors Induced by STING Agonists

By

Christopher James Nicolai

A thesis submitted in partial satisfaction of the

requirements for the degree of

Doctor of Philosophy

in

Molecular and Cell Biology

in the

Graduate Division

of the

University of California, Berkeley

Committee in charge:
Professor David H. Raulet, Chair
Professor Russell E. Vance
Professor Gregory M. Barton
Professor Daniel K. Nomura

Spring 2020

Abstract

Mechanisms of Clearance of MHC I-deficient Tumors Induced by STING Agonists

by

Christopher James Nicolai

Doctor of Philosophy in Molecular and Cell Biology

University of California, Berkeley

Professor David H. Raulet, Chair

Immunotherapies, such as “checkpoint blockade” have revolutionized modern cancer treatment, greatly increasing patient survival and leading to cures in a significant number of people. These groundbreaking drugs target inhibitory receptors on CD8 T cells, increasing T cell activation and promoting tumor destruction. However, tumors may evade such therapies via loss of MHC molecules or because they contain few/no neoantigens. Therefore, approaches to mobilize immune cells to kill CD8 T cell-resistant tumors are needed to combat these potential escape mechanisms. Natural killer (NK) cells recognize stress-induced ligands on tumor cells and do not require that tumors display neoantigens. CD4 T cells recognize epitopes presented by MHC II molecules that can serve as alternative targets for anti-tumor responses and are capable of activating other immune cells within the tumor microenvironment to kill tumor cells. Therefore, immunotherapies that mobilize NK cells or CD4 T cells have potential for targeting tumors resistant to CD8 T cells.

Cyclic-dinucleotides (CDNs) are a class of immunostimulatory molecules that bind to the STING protein and induce type I interferons (IFN) and other pro-inflammatory mediators. Recently, in mouse transplantable tumor models, it was shown that intratumoral CDN injections stimulate powerful CD8 T cell-mediated tumor rejection, often leading to long-lasting tumor regression and protection from rechallenge. Compounds that activate the STING pathway are currently being tested in clinical trials for treating cancer.

My thesis work examines the potential of CDNs to mobilize anti-tumor immune responses against MHC I-deficient tumors. The data show that CDNs trigger potent tumor rejection in several different tumor models, independent of CD8 T cells. The antitumor effects are dependent on NK and in some cases CD4 T cells, which can mediate rejection independently of each other. CDNs enhanced NK cell activation, cytotoxicity, and antitumor effects in part by inducing type I IFN (IFN). IFN acted in part directly on NK cells *in vivo*, and in part indirectly via dendritic cells. Upon applying CDNs *in vivo*, dendritic cells (DCs) upregulated IL-15Rα in an IFN-dependent manner, and IL-15 action was important for CDN-induced NK activation and tumor control. Mice lacking IFNAR specifically on DCs had reduced NK cell activation and tumor control.

CD4 T cells also mediate potent antitumor responses in some tumor models, independently of CD8 T cells and, in the primary response, independently of NK cells, B cells, and γδ T cells. CDN treatments led to increased tumor-specific priming of CD4 T cells and enhanced effector functions, such as production of IFN-γ, IL-2, and TNFα. Tumor-specific CD4 T cells in tumors treated with CDNs had a less exhausted, Th1-like phenotype, with increased production of IFN-γ, which was necessary for the antitumor response. Mice that cleared their primary tumors exhibited a long-lasting antitumor memory response, which was dependent on CD4 T cells, IFN-γ and partially dependent on B cells, myeloid cells and, albeit to a minor extent, NK cells. Interestingly, the antitumor response did not rely on MHC II expression by the tumor cells, suggesting that CD4 T cells either initiate antitumor effects indirectly, without direct recognition of the tumor cell by CD4 T cells, or engage ligands other than conventional MHC II (and MHC I) on tumor cells.

In the final chapter of the thesis I described several genetic screens in cell lines aimed at identifying novel cellular ligands for NK cell activating receptors. The screens employed chimeric antigen receptor (CAR) T cells that incorporate NK cell activating receptors (NK CAR T cells) as selecting agents against human tumor cell lines mutagenized with a retroviral gene-trap or stably expressing CRISPR-Cas9 and a genome-wide gRNA library. I successfully generated multiple NK CAR T cells and performed several screens using NKp44 and NKp46 CAR T cells. These screens resulted in lists of genes, that when mutated, were enriched in the surviving cellular population. Future work will be needed to validate the hits from these screens and perform additional screens if necessary.

This thesis aims to identify mechanisms of immune cell activation induced by STING agonists as well as to unearth novel mechanisms of NK cell tumor recognition. This work is significant because it addresses CD8 T cell-independent immunological rejection of MHC-deficient tumors induced by CDNs and mediated by NK and CD4 T cells. A greater understanding of mechanisms leading to immunological clearance of MHC-deficient tumors will be necessary to develop approaches to overcome mechanisms tumors employ to escape CD8 T cell control and to design rational combination therapies with existing anti-cancer drugs. Therapeutics that activate NK cells and CD4 T cells may represent next-generation approaches to cancer immunotherapy.

Table of Contents

List of Figures

Acknowledgements

There are many in my life who I would like to thank. Without your help, guidance, support, and love I would not be the person that I am today.

First, I would like to thank Vashon Island, and the friends I made growing up there. Perhaps more than anything else you shaped who I am. Thank you for exploring the woods, building forts on the beach, pirate rafts, purple Sharks, Harry Springer, choco tacos, lunchtime basketball, snatching lawn gnomes, FAPC, E-brake slides, Last Ditch Effort, bonfires, Jensen fireworks, gravel pit helicopters, towers of power, Bluffs Deluxe, T missions, rocking in the Jam Room, Sasquatch, Seahawks trips, and for everything still yet to come. OI! I'm lucky know to you all.

I would next like to thank the architects of my undergraduate experiences at the University of Washington. Thank you, Pretty Girl, for helping me with paper sciences, mohawks, and having 2 AM waffles at IHOP. Thanks for Ciao Bella, Coach Carter, and helping me with (doing) my Spanish homework. Most of all thanks for marrying me (more on that later). Thank you, buddies of the 848 house. You accepted me into your family and I am forever grateful. We were softball champions, Dante's pool and beer pong hustlers, and Husky tailgaters. I'll never forget rushing the field against USC. Thanks for rope swings at Magnuson, trust falls, Dinner Club, enraging our neighbors with our parties, long talks around the fire in the backyard, Mazatlán, and 4th of July at the crate. Smell the bat.

After graduation I got my first (real) job that would end up influencing both my scientific interests as well as my career direction. Thank you Immune Design for steering me toward the field of tumor immunology and cancer immunotherapy. Thanks for giving me the opportunity to take on responsibility within the company and creating an environment where I was capable of succeeding. Most of all thank you for great friends aligned toward a common goal. Thanks for Quarter Lounge and Siam. I would especially like to thank Semih Tareen, my mentor and friend, for teaching me how to conduct a proper experiment, how to think scientifically, and how to present effectively to a group.

With my passion for this field sparked, I decided to go to the laboratory of David Raulet at the University of California, Berkeley for my graduate education, and there are many who were instrumental during my progression through my PhD. First I would like the thank my co-ton, Djem Kissiov. We rotated in the lab together, joined together, and became great friends over the course of our time in the lab. I always enjoyed our discussions about our projects, and although we studied different subjects, thank you for always being engaged and offering insightful advice whenever I came to you for help. I would also like to thank Michele Ardolino and Thornton Thompson for teaching me flow cytometry and for helping me analyze my initial experiments, thoughtful discussions, and planning future studies. It was truly a pleasure to work with you. Thank you Assaf Marcus, my baymate, for challenging me and thoughtful data interpretation. Thank you Natalie Wolf for being an excellent rotation student and friend, and for carrying the torch of STING activation in the tumor microenvironment! Thank you Lily Zhang for being my (and everyone else's) lab mom. Lab would fall apart without you. Also thank you to Lily's daughter Joanna, for babysitting Henry and allowing Katey and I do go to dinner and a

movie. Thank you to members of my thesis committee, Russell Vance, Greg Barton, and Dan Nomura. Your guidance and thoughtful discussions were instrumental in formulating my thesis project. Finally, I would like to thank my mentor and thesis chair, David Raulet. Thank you, David, for being the perfect mentor for me. You were hands-off when I needed to explore and your door was always open when I needed help. I will always look back fondly on your words (stories) of wisdom in all matters of things, from science to basketball. Thank you for allowing me to always follow the data and for letting me shape my own destiny.

Above all else I would like to thank my loving and supportive family. Thank you to my parents, Phil and Joanne Nicolai, for always being incredibly supportive and for constantly pushing me to be my best, whether it be in sports or academics. Your love and guidance instilled in me a great wonder for the natural world, as well as the self-confidence and determination necessary to complete my PhD. You made me the person I am today and I truly could not have done (let alone start) this without you. Thank you for my life and for setting an example for parenting that I am attempting to recreate with my own children. I hope I am able to do as good of a job as you did for me. Thank you to my brother, Michael. Thanks for being a friend growing up. Building forts on the beach, wrestling in the living room, and fourth of July firework shows are memories I will cherish forever. I love you, bro.

Finally I would like to thank the newest members of my family. Thank you, Katey. From the moment I saw you I loved you. At first I didn't know your actual name, so you were dubbed Pretty Girl during discussion with my friends. Thankfully I didn't have to wait too long to meet you. The most important decision of my life was deciding to take a break from studying for my paper science midterm and going up to the 4th floor breakroom of the Mercer Dormitory to hang out. As I joined my friends at a table, my heart skipped a beat. You, Pretty Girl, were there, at a different table across the room. Somehow I managed to get you to give me a mohawk (I still have no idea how I managed to pull that off) which led to us talking all evening long. The night culminated with a 2AM run to IHOP for pancakes. Thank you for that and everything that was to come. You are responsible for all of the best days of my life. Thank you for marrying me. Thank you for moving to Berkeley with me. This PhD truly belongs to you, too, because without your support I would not have been able to complete it. Most importantly, thank you for giving me the most important things in my life, our children Henry and Lily. To Henry and Lily, my definition of love changed when you both were born and you have given purpose to everything I do. Thank you. I dedicate this dissertation, my PhD, and my life to you.

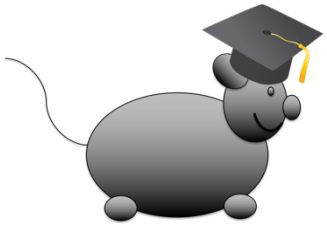

Chapter 1
Introduction

Overview of the Immune System

We are constantly under attack. Every minute of every day since birth we are exposed to a variety of bacteria, viruses, and fungi that would like nothing more than to live, feed, and replicate within us. Their ultimate goal is simple: to pass on their genetic material to the next generation, thus increasing their genetic footprint within this world. One can hardly blame them, for we (and every other living creature) are also trying to accomplish the same thing. In some contexts, these interactions lead to mutually beneficial relationships, such as in the gut when bacteria and viruses, in exchange for food and a nice place to live, help us digest and absorb nutrients. However, in other situations these interactions can have devastating consequences. For example, according to the World Health Organization, in 2018 the intracellular bacterium *Mycobacterium tuberculosis* caused 10 million new cases of active tuberculosis, and killed 1.5 million people. Our defense against such attacks is our immune system.

The immune system is a collection of tissues, cells, and molecules which function to protect us from infectious agents. In order to do this, it must act quickly to recognize potential threats and eliminate them before infections get out of control. It must also act selectively to ensure specific recognition of harmful microbes while leaving our own tissues intact. Overactive or non-selective immune responses can lead to autoimmune diseases which may be just as deadly as the initial microbial infection. Thus, the immune system must be highly regulated to ensure a quick and specific response lasting only a finite time to maintain optimal host health.

Innate and Adaptive Immunity

The immune system is composed of two branches: the innate and the adaptive. The innate immune response acts rapidly, within the first few minutes to hours after insult to the host. It is composed of physical barriers as well as cells such as dendritic cells, macrophages, neutrophils, and natural killer (NK) cells. Innate immune recognition of pathogens is achieved via germline-encoded pattern-recognition receptors (PRRs). PRRs recognize common components of microbes not normally found in mammalian cells, such as bacterial cell wall components and flagella, or bacterial and viral nucleic acid. These are called pathogen-associated molecular patterns (PAMPs). In addition, PRRs also recognize normal components of mammalian cells located abnormally, which may occur in times of tissue damage or stress. These are called damage-associated molecular patterns (DAMPs) and include extracellular ATP and cytosolic DNA. When triggered, PRRs elicit a series of responses to promote cytokine production, trafficking of innate immune cells, and initiate adaptive immune responses to protect against the infection. The innate immune system acts rapidly in order to keep the initial infection under control. Its ability to broadly recognize many different microbial components is balanced by its relative lack of specificity. In order to achieve highly specific immune responses against a limitless number of antigens and to ultimately clear serious infections, the immune system utilizes the adaptive immune system.

Adaptive immunity, in contrast to innate immunity, takes more time to develop (on the order of a few days to one week after infection) but is much more specific to an individual pathogen. To achieve this high degree of specificity the cells of the adaptive immune system, T cells and B cells, undergo genetic recombination at the loci encoding their antigen receptors.

This process creates a large pool of T cells and B cells with the potential to recognize a near infinite number of antigens. When T or B cells recognize their cognate antigen, they initiate effector functions and clonally expand several thousand-fold, leading to elimination of the pathogen. After an immune response has subsided, a subset of T and B cells remain with ability to respond much more rapidly to a second infection. This capacity for immunological memory is a key feature of adaptive immunity.

The Immune System and Cancer

Historically the immune system has been studied in the context of infectious disease, but it has become increasingly clear that the immune system also plays an important role in the prevention and control of cancer. Cancer is a genetic disease in which cells acquire the ability to proliferate uncontrollably. All cancers share a common core of essential characteristics that enable their existence. These include sustained proliferative signaling and replicative immortality, resistance to growth suppressors and apoptosis, induction of angiogenesis, and tissue invasion and metastasis (Hanahan and Weinberg, 2000). More recently it has become appreciated that cancer cells must reprogram host energetic pathways to facilitate sustained growth and that they must also overcome the host immune system (Hanahan and Weinberg, 2011).

In order to generate effective antitumor immune responses, the immune system must differentiate between cancerous and noncancerous cells. Recognition of tumors by the immune system can occur through several mechanisms. Nonmutated proteins can be recognized when they are overexpressed by tumor cells or when they become expressed on cells which do not normally express them, such as with aberrantly expressed developmental genes. Mutations within the cancer cell genome can also be recognized. Cancer cells, being genetically unstable, will generate mutations which may cause changes in the protein sequence, thus generating novel antigens not found in noncancer cells. These “neoantigens” can then bind to MHC molecules and stimulate productive antitumor adaptive immune responses mediated by T cells and B cells (Schumacher and Schreiber, 2015).

The innate immune system can also recognize cancer cells. Stressed and dying tumor cells often release molecules (DAMPs) that are detected by PRRs on innate immune cells, triggering inflammation. An example that will be discussed later in detail is cytosolic DNA, which is frequently found within tumors. Cytosolic DNA triggers production of cyclic GMP-AMP (cGAMP) which can be detected by innate immune cells and stimulate antitumor responses (Marcus et al., 2018). In addition, excessive proliferation and DNA damage associated with tumorigenesis cause induction of cell-intrinsic molecular stress pathways, leading to upregulation of abnormally-expressed cell surface molecules that sensitize tumors to innate immune attack, especially by NK cells (Marcus et al., 2014).

Natural Killer cells

Natural killer (NK) cells are lymphocytes of the innate immune system and originate from the common lymphoid progenitor cell in the bone marrow. NK cells were initially named for their ability to spontaneously lyse susceptible tumor cell lines *in vitro* without prior

immunization (Herberman et al., 1975; Kiessling et al., 1975). This finding was in direct contrast with what was known about T cells, which require antigen-specific priming to lyse targets, and the name "natural killer" was given to this newly discovered population of cells. Since their discovery, NK cells have been found to be key mediators of both antiviral and antitumor immunity *in vivo* (Cerwenka and Lanier, 2001). NK cell cytotoxicity is thought to be primarily mediated via the release of granules containing perforin and granzymes which can penetrate target cells to induce apoptosis. In addition, NK cells can also upregulate death receptors, such as TRAIL and FasL, which also induce apoptosis in target cells (Trapani and Smyth, 2002). Besides their killing ability, activated NK cells can release a variety of chemokines and cytokines, such as interferon-gamma (IFN-γ), that enable them to recruit other immune cells and to have immunomodulatory effects, such as promoting adaptive immune responses (Vivier et al., 2011). Triggering of NK cell effector functions is ultimately determined by a balance of signals deriving from a variety of germline-encoded activating and inhibitory receptors, all of which contribute to the overall activation of the cell (Raulet and Vance, 2006).

NK cell activating and inhibitory receptors

NK cells express numerous activating and inhibitory receptors, all which influence the overall activation of the cell. The most studied activating receptor is NKG2D. NKG2D is a lectin-like type 2 transmembrane protein and is expressed on all NK cells. After engagement, NKG2D utilizes the adapter proteins DAP10 and DAP12 to initiate an intracellular signaling cascade culminating in various cellular effector functions, such as production of IFN-γ and killing of the target cell (Marcus et al., 2014). NKG2D recognizes numerous ligands which include MULT1 and the RAE-1 and H60 families in mice and MICA, MICB, and the ULBP family in humans (Raulet et al., 2013). These ligands are not usually expressed, or are expressed at very low levels on normal, healthy cells, but can be induced by cell stress pathways induced by ER stress and DNA damage, which often occur during tumorigenesis and viral infections.

Another group of NK activating receptors are the natural cytotoxicity receptors (NCRs), NKp30, NKp44 and NKp46. Similar to NKG2D, when engaged these receptors stimulate target cell killing and IFN-γ production via signaling cascades propagated through adapter proteins such as CD3ζ, FcεRIγ, and DAP12 (Marcus et al., 2014). Unlike NKG2D, the ligands for the NCRs are less understood. B7-H6 and BAT3 are proposed ligands for NKp30 (Brandt et al., 2009; Pogge von Strandmann et al., 2007) and an isoform variant of MLL5 has been reported to be a ligand for NKp44 (Baychelier et al., 2013). The ligand for NKp46 is much less clear. One report implicated viral hemagglutinin as a ligand for NKp46 (Mandelboim et al., 2001), but the cellular ligand remains unknown. Other important NK activating receptors include the SLAM family, DNAM-1, and CD16, the latter of which binds the Fc domain of antibodies and is important for antibody-dependent cellular cytotoxicity (ADCC) (Marcus et al., 2014).

NK cells also possess activating receptors for soluble and membrane bound cytokines, most notably IL-2, IL-12, IL-15, IL-18, and IL-21. These cytokines function to promote NK cell proliferation and enhance activation and effector functions (Vivier et al., 2011). IL-15, which is trans-presented by IL-15Rα-expressing cells, such as dendritic cells and macrophages (Mortier et al., 2009; Mortier et al., 2008), is particularly important for NK cells and is necessary for NK cell development and homeostasis. Type I interferon (IFN) is another soluble mediator of NK

cell function, important for enhancing NK cell activation and effector functions and acts both directly on NK cells (Martinez et al., 2008) and indirectly by inducing production of IL-15 (Lucas et al., 2007).

In addition to activating receptors, NK cells also express numerous inhibitory receptors. The major class of inhibitory receptors on NK cells bind to MHC class I (MHC I) molecules and are the killer cell immunoglobulin-like receptors (KIRs) in humans and the Ly49 receptors in mice (Karlhofer et al., 1992; Moretta et al., 1996). Another inhibitory receptor, the CD94/NKG2A heterodimer, recognizes non-classical MHC I molecules (HLA-E in humans and Qa-1b in mice) (Vance et al., 1998). When engaged, these receptors negatively regulate NK cell effector functions via immunoreceptor tyrosine-based inhibitory motifs (ITIMs), which recruit phosphatases that limit signal transduction initiated by activating stimuli. The ability to recognize MHC I, which confers capacity to detect its absence, is known as "missing self recognition". This is a key aspect of NK cell biology as virus-infected cells and tumors may lose MHC I in order to evade CD8 T cell recognition. However, this evasion comes with a cost, as loss of MHC I causes NK cells to become less inhibited when engaging these cells, making them more sensitive to NK mediated-killing (Karre, 2008).

Other inhibitory receptors found on NK cells include the checkpoint molecules PD-1, Tim-3, Lag-3, TIGIT, and CD96. These are typically expressed on activated NK cells and T cells and serve to restrain cellular effector functions (Guillerey et al., 2016). There is currently much excitement surrounding these molecules as a means to treat cancer which will be discussed in greater detail below.

Tumor surveillance by NK cells

NK cells are important mediators of antitumor immunity in both mice and humans. Initial studies showed that these cells were capable of killing multiple tumor cell lines *in vitro* and that incubation with IL-2 was capable of enhancing these effects (Wu and Lanier, 2003). The importance of NK cells for tumor surveillance *in vivo* was subsequently shown using the NK cell depleting antibodies anti-NK1.1 and anti-asialo-GM-1, where mice depleted of NK cells were more susceptible to both transplantable (Seaman et al., 1987) and carcinogen-induced tumors (Smyth et al., 2001). Further *in vivo* evidence for tumor surveillance by NK cells involves comparisons of spontaneous and carcinogen-induced tumor formation in *Rag2*$^{-/-}$ mice, which lack T cells and B cells but have NK cells, and *Rag2*$^{-/-}$*Stat1*$^{-/-}$ mice which also lack the ability to respond to interferons, a potent activator of NK cell effector functions. Compared to *Rag2*$^{-/-}$ mice, *Rag2*$^{-/-}$*Stat1*$^{-/-}$ mice developed tumors faster (Shankaran et al., 2001), suggesting NK cells may play a role in limiting tumor formation.

Additional evidence for the importance of NK cells in tumor surveillance comes from mice lacking NK cell activating receptors. As mentioned above, many tumors express NK cell activating ligands due to induction of cellular stress pathways. Consistent with a role for NK cells in tumor surveillance, mice lacking NK cell-activating receptors are more susceptible to tumor development. For example, mice lacking NKG2D were shown to be more susceptible to both TRAMP and *Eμ-Myc* transgenic mouse cancer models (Guerra et al., 2008). In a separate study, mice lacking NKp46 were found to be more susceptible to tumor lung metastasis (Glasner

et al., 2012). These studies highlight the important role NK cells play in cancer immunosurveillance. As basic knowledge of NK cell biology increases so does excitement about the opportunity to design NK cell-based immunotherapies for cancer.

Harnessing the immune system to treat cancer

A brief history and current therapies

In 2011, the U.S. Food and Drug Administration (FDA) granted approval of a monoclonal antibody targeting CTLA-4 for the treatment of metastatic melanoma. Shortly thereafter, in 2014, approval was granted for a second monoclonal antibody, targeting PD-1, for the same disease. These drugs marked a great departure from traditional cancer therapies, such as chemotherapy and radiation, in that they targeted the immune system, and not the cancer cells themselves, to treat cancer. Collectively termed "checkpoint inhibitors", these antibodies function to block inhibitory receptors found on tumor-targeting cytotoxic lymphocytes, thus "removing the brakes" on the cell and enhancing cellular functions and tumor killing (Hirano et al., 2005; Leach et al., 1996). These drugs have since led to unprecedented responses in patients with a variety of cancers, some of which experience long-lasting antitumor immunity and who appear to be in complete remission with no obvious signs of cancer (Ribas and Wolchok, 2018; Sharma and Allison, 2015a). These results were so stunning that in 2013, *Science Magazine* named cancer immunotherapy as its "breakthrough of the year", and in 2018, the Nobel Prize in medicine was awarded to James Allison and Tasuku Honjo for their extraordinary and pioneering work on immune checkpoint molecules and how their inhibition can be used to treat cancer.

Perhaps the first example of attempts to activate the immune system to treat cancer can be attributed to a surgeon in the late 1800s named William Coley. Coley observed that some patients' tumors had appeared to disappear after they had contracted bacterial infections near the site of the tumor. He hypothesized that inflammation, induced by the infection, stimulated antitumoral immune responses and Coley began injecting mixtures of heat-killed bacteria directly into tumors. Amazingly, many of the patients he injected responded to the treatment and some were even reportedly cured. Soon "Coley's Toxin", as the heat-killed bacteria mixture came to be known, began to be used for the treatment of bone and soft-tissue sarcomas. However, its use was short-lived and despite some treatment successes, there was widespread skepticism in the medical community surrounding Coley's Toxin and eventually the approach lost favor to other forms of therapies, such as radiation and chemotherapy. Sadly, by the 1960's, use of Coley's toxin was banned in the United States (McCarthy, 2006).

Coley's Toxin may have lost favor but the idea of harnessing the immune system to treat malignancy had not. IL-2 is an important cytokine capable of driving proliferation and activation of lymphocytes such as T cells and NK cells. After promising preclinical studies in mice, high-dose recombinant IL-2 (rIL-2) was given to patients with metastatic melanoma and renal carcinoma. These and subsequent studies proved high-dose rIL-2 to be an effective treatment in some patients and it was FDA approved for treating metastatic renal cancer in 1992 and metastatic melanoma in 1998 (Rosenberg, 2014). These were important studies because they

showed definitively that activating immune system could be a viable treatment for cancer even if the benefit was small with rIL-2 alone.

rIL-2 had only proved modestly effective and its scope was limited to just a few types of cancer. The major breakthrough in cancer immunotherapy came with the discovery of checkpoint blocking monoclonal antibodies. As described above, these antibodies are designed to block inhibitory receptors expressed by activated immune cells, such as T cells and NK cells, and limit the amount of negative signal they receive, thus increase their effector functions and tumor killing capacity. The first checkpoint inhibitor to be used clinically was an antibody targeting CTLA-4. CTLA-4 is expressed on T regulatory cells (Tregs) and on activated T cells and binds B7-1 and B7-2, thereby preventing their interaction with the costimulatory molecule CD28, thus limiting T cell responses (Krummel and Allison, 1995). Consistent with these observations, administration of a CTLA-4-blocking monoclonal antibody in tumor-bearing mice led to complete tumor regressions. Furthermore the mice were protected from tumor rechallenge, confirming establishment of long-term antitumor immunity (Leach et al., 1996). The success of targeting CTLA-4 as a tumor therapy in preclinical mouse models led to human clinical trials in metastatic melanoma, where it was shown that patients receiving anti-CTLA-4 had significantly enhanced overall survival (Hodi et al., 2010). Amazingly, more than a decade after stopping anti CTLA-4 therapy, many of these original patients are still in remission (Eroglu et al., 2015; Schadendorf et al., 2015).

The success of anti-CTLA-4 launched an effort to find other checkpoint molecules that may be targeted for the treatment of cancer. The first of these were PD-1 and its ligand, PD-L1. Similar to CTLA-4, PD-1 is upregulated on activated lymphocytes and functions to restrain their effector functions and killing ability. When engaged by PD-L1, PD-1 recruits the tyrosine phosphatase SHP-2 to its cytoplasmic domain which dephosphorylates signaling molecules downstream of activating receptors, thus inhibiting signal transduction and leading to cell inactivation and contributing to an overall exhausted cell phenotype (Baumeister et al., 2016). The ligand of PD-1, PD-L1, is induced during inflammation, especially by interferons, and it can be expressed by many cell types including endothelial, epithelial, and even other immune cells within tumors, as well as the tumor cells themselves (Sharma and Allison, 2015b). PD-1 is also highly expressed within tumors and this led to trials evaluating whether antibodies blocking PD-1 or PD-L1 have antitumor clinical benefit. The trials have proved incredibly successful and to date PD-1, or PD-L1-targeting antibodies are approved in 11 different cancer indications (Ribas and Wolchok, 2018). As these drugs target different signaling pathways, it was hypothesized that combining them might achieve a synergistic effect. This was soon confirmed in mouse preclinical studies (Curran et al., 2010; Mangsbo et al., 2010), which led to human trials confirming the additional benefit of combination therapies in both advanced and untreated melanoma (Larkin et al., 2015; Wolchok et al., 2013).

The massive success of CTLA-4 and PD-1/PD-L1 monoclonal antibodies for the treatment of cancer has led to a search to find other inhibitory pathways that may also be targeted. Lag-3, Tim-3, TIGIT, and VISTA are examples of surface-bound inhibitory receptors on induced on activates lymphocytes that are currently being evaluated and may represent the next generation of checkpoint immunotherapies (Baumeister et al., 2016).

Another class of emerging cancer immunotherapeutics showing promise are cellular-based adoptive transfer therapies (ACTs), especially using chimeric antigen receptor T (CAR T) cells. The first adoptive transfer therapies were for metastatic melanoma. These involved harvesting tumor-infiltrating lymphocytes from patient tumors, expanding the cells *ex vivo* using IL-2, and then transferring them back into the original patient after undergoing a lymphodepletion regimen (Rosenberg and Restifo, 2015). These initial studies were important because they showed ACT could be a viable treatment, at least for melanoma. Next-generation ACT therapies involve genetically altering the tropism of the adopted T cells to a known antigen by introducing either an artificial T cell receptor (TCR) or a chimeric antigen receptor (CAR). CARs are molecules combining a receptor, most commonly the single-chain variable fragment (scFv) from an antibody, with a signaling domain derived from the TCR and other costimulatory molecules (June and Sadelain, 2018). These CARs can then be incorporated into T cells, thus generating CAR T cells, which are targeted to surface-expressed tumor antigens via the scFv and when engaged trigger T cell activation and killing. The first clinical success using CAR T cells were using CARs targeting CD19, which is highly expressed in B cell leukemias and lymphomas. CD19 CAR T cell therapy is proving to be incredibly successful, especially in children and adults with relapsed B-cell acute lymphoblastic leukemia (ALL), with complete remissions in over 70% of patients (Park et al., 2016). The clinical success of CD19 CAR T cells has led to FDA approval for their use in refractory pre-B cell ALL and diffuse large B cell lymphoma (June et al., 2018).

Tumor immune evasion mechanisms

The recent advances in cancer immunotherapy discussed above have revolutionized modern cancer treatment and have resulted in unprecedented remissions in many patients with several different types of cancer. As a result, immunotherapy is now a first-line treatment for several different cancers, including melanoma and non-small-cell lung cancer. As amazing as these results have been, the fact is most patients do not respond to current immunotherapies and there are some cancers which are completely refractory. A major goal of ongoing research is to determine how tumors evade antitumor immune responses and how to circumvent those evasion mechanisms.

One way tumors may escape the immune system is by setting up complex tumor microenvironments (TMEs) that inhibit immune cell infiltration and function. For example, oncogenes, which are important drivers of tumor cell growth, have been found to influence infiltration of tumors by immune cells. Recently it was shown in preclinical mouse melanoma models that activation of the WNT-β-catenin signaling pathway within tumor cells correlated with a lack of *Batf3* $CD103^+$ dendritic cells (DCs) in the TME (Spranger et al., 2015). *Batf3* DCs are key players in promoting adaptive CD8 T cell responses (Hildner et al., 2008). The β-catenin-induced paucity of DCs within these tumors led to decreased infiltration of antitumor T cells and resulted in increased resistance to immunotherapeutic checkpoint blockade (Spranger et al., 2015).

Even if immune cells are able to penetrate into the tumor, their function is often suppressed. This dysfunctional state is termed exhaustion, or anergy, and has been reported for both CD8 T cells and NK cells in human cancer patients (Costello et al., 2002; Epling-Burnette

et al., 2007; Wherry and Kurachi, 2015). One suppression mechanism which has already been discussed is induction of checkpoint molecules. These are induced on activated T cells and NK cells within tumors and function to dampen signals received from activating receptors. Many types of tumors or cells within the tumor environment can express ligands for these inhibitory receptors and their engagement promotes immune cell dysfunction and exhaustion (Hsu et al., 2018; Ribas and Wolchok, 2018; Zhang et al., 2018).

Another mechanism of immune cell dysfunction, or anergy, within tumors is chronic activating receptor stimulation. This was shown for CD8 T cells using an inducible liver cancer mouse model with a defined tumor antigen (Schietinger et al., 2016). In this study, tumor-specific T cells become dysfunctional early on during tumorigenesis, and while initially reversible, T cell dysfunction eventually enters a fixed state. Interestingly, only the T cells that were specific for the defined tumor antigen were rendered anergic, while T cells recognizing an irrelevant antigen remained functional. This study suggests that persistent TCR stimulation, rather than microenvironmental factors, is the main driver of T cell anergy.

NK cells can also become anergic through chronic stimulation of activating receptors, such as NKG2D and Ly49H (Oppenheim et al., 2005; Sun and Lanier, 2008). Tumors often express ligands for NK cell activating receptors and it is possible that under these conditions NK cells are exposed to anergy-inducing chronic stimulation. In addition, MHC I loss, which is common in tumors (Garrido et al., 2016), can also result in chronic stimulation of NK cells due to loss of inhibitory Ly49 receptor or KIR engagement. Evidence for tumor-induced NK cell anergy *in vivo* comes from a study employing MHC I-deficient tumors. This study found that NK cells within MHC I-deficient tumors had impaired signaling and functional responses when compared to NK cells in MHC I-sufficient tumors and that this functional defect could be reversed with addition of NK cell-activating cytokines (Ardolino et al., 2014).

Tumors may also evade antitumor immune responses by losing the ability to be recognized by attacking cells. CD8 T cells recognize non-self-peptides bound to MHC I molecules. Tumor cells are often genetically unstable and as a result can generate mutated peptides, termed neoantigens, capable of binding MHC I and stimulating T cell responses (Schumacher and Schreiber, 2015). However, there is significant variability in the overall number of mutations in the spectrum of human cancer (Alexandrov et al., 2013) and it is possible that some patient tumors may not have neoantigens capable of being bound by their respective MHC molecules and recognized by CD8 T cells and thus may be resistant to T cell-mediated attack. Indeed, accumulating evidence suggests that successful responses to checkpoint blockade therapies correlate with overall tumor mutational burden (Le et al., 2015; Rizvi et al., 2015; Yarchoan et al., 2017) and the majority of clinically approved immunotherapies are for cancers with relatively high numbers of mutations. Another way tumors may evade CD8 T cells is through selective loss of MHC I molecules (Garrido and Algarra, 2001). Tumors are known to lose MHC I as a means to avoid T cell recognition and several studies have shown that tumors from patients who are unresponsive to immunotherapy exhibit loss of MHC I (Garrido et al., 2016), in some cases through mutations in β_2-microglobulin (Restifo et al., 1996; Rodig et al., 2018; Sade-Feldman et al., 2017; Zaretsky et al., 2016), which is necessary to ensure proper folding and surface expression of MHC I. Tumors have also been shown to lose specific MHC alleles, in some cases from events that result in loss of MHC heterozygosity, presumably to

escape recognition of strong neoantigens presented by those alleles (McGranahan et al., 2017). This is an especially interesting evasion mechanism as a partial loss of MHC would limit the number of neoantigens capable of being displayed by tumors while maintaining capacity to engage NK cell inhibitory receptors, thus limiting the anti-tumor activity of NK cells.

Tumors can also evade NK cell recognition via the loss of NK cell-activating ligands, most notably those for NKG2D. Using a spontaneous prostate cancer model, one study found that spontaneous prostate tumors that arose in NKG2D knockout (KO) mice had high cell surface expression of NKG2D ligands whereas such tumors that arose in WT mice lacked NKG2D ligands (Guerra et al., 2008), suggesting that the presence of NKG2D was enabling selection for loss of NKG2D ligands on the developing tumors. Another study found that 3' methylcholanthrene (MCA)-induced sarcomas tended to express higher amounts of the NKG2D ligand, H60a when induced in immune-deficient mice compared to WT mice. When cell lines were produced from the sarcomas, some had variable expression of H60a and when implanted into *Rag2*$^{-/-}$ mice, the resulting tumors had lost H60a expression (O'Sullivan et al., 2011). These data suggested that NK cells were imposing NKG2D-mediated selective pressure on the growing tumors leading to the outgrowth of tumor variants that had lost H60a expression.

Altering the function of myeloid cells, especially macrophages, is another way tumors can suppress antitumor immune responses. For example, tumor-infiltrating myeloid cells can produce the enzyme indole 2,3-deoxygenase (IDO) which catabolizes tryptophan. Tryptophan is essential for T cell function and its depletion inhibits cell proliferation and leads to T cell anergy and apoptosis (Platten et al., 2012). Finally, regulatory T cells (Tregs) also play important roles in immune suppression. Tregs can inhibit immune function through several mechanisms, such as: limiting the amount of extracellular IL-2 available for conventional T cells and NK cells; expressing CTLA-4 in order to engage B7-1 and B7-2, thereby preventing their engagement of CD28 on conventional T cells; producing immune-suppressive cytokines such as IL-10 and TGF-β (Tanaka and Sakaguchi, 2017). Understanding the immune evasion mechanisms employed by tumors will be crucial to developing next generation immunotherapies.

Utilizing NK cells for cancer immunotherapy

Many of the therapies in the clinic are designed to target CD8 T cells, but NK cells also have potent tumor-killing abilities and there is much excitement around harnessing NK cells to treat cancer. In one approach NK cells are extracted and expanded *ex vivo* with NK cell activating cytokines, such as IL-12, IL-18, and IL-15, and then adoptively transferred back into patients (Guillerey et al., 2016). In some cases the activated NK cell are engineered to express CARs prior to their adoptive transfer, thus conferring specificity to a desired tumor antigen such as CD19 (Shimasaki et al., 2020). NK-activating cytokines have also shown promise when administered *in vivo.* One study found that injecting IL-12+IL-18 or IL-2 was able to overcome NK cell anergy within MHC I-deficient tumors and enhance antitumor NK cells effector functions (Ardolino et al., 2014).

Like T cells, NK cells also express numerous inhibitory receptors that can limit their antitumor activity and strategies aimed at blocking these interactions are being pursued. As described above, NK cells are inhibited by MHC molecules via their KIRs and NKG2A/CD94

complexes. Monoclonal antibodies blocking KIRs and NKG2A/CD94 have shown promise in preclinical studies (Andre et al., 2018; Romagne et al., 2009) and are currently being evaluated the clinical trials (Vey et al., 2012). In addition, antibodies blocking "classical" checkpoint molecules, such as PD-1, TIGIT, and CD96 have also been successful preclinical studies, enhancing NK cell activation and promoting tumor clearance (Blake et al., 2016; Hsu et al., 2018). Therapies blocking many of these checkpoint molecules are already being developed because of their potential for mobilizing T cells and it is likely these will also augment NK cell antitumor functions. Indeed, it is plausible that some of the activity of the currently approved checkpoint drugs is due to their effects in mobilizing NK cells.

Finally, antibodies targeting surface molecules on tumors can also stimulate NK cell-mediated tumor killing. Examples that are already widely used in the clinic are antibodies targeting CD20 and HER2 (Weiner et al., 2010), which can trigger NK ADCC through the Fc-binding activating receptor CD16. Recently, more sophisticated molecules targeting NK cells to tumors have been developed. These include bi- and tri-specific antibodies which link CD16, NKG2D, or NKp46 on NK cells with tumor antigens to promote NK activation, cytokine production, and tumor killing ability (Gauthier et al., 2019; Gleason et al., 2012). In some cases, these molecules are engineered to incorporate NK cell activating cytokines, such as IL-15, for enhanced NK cell activation (Vallera et al., 2016). NK cells are powerful mediators of antitumor immunity and these examples illustrate the excitement surrounding NK cell-based immunotherapies.

The cGAS-STING pathway and its emerging role in antitumor immunity

As discussed above, the innate immune system utilizes germline-encoded PRRs to detect PAMPs or DAMPs. A relatively newly discovered PRR system is the cGAS-STING pathway. The cGAS-STING pathway senses cytosolic DNA, resulting in production of type I IFN and proinflammatory cytokines and chemokines (Chen et al., 2016; Ishikawa et al., 2009). Upon binding double-stranded DNA, the cytosolic enzyme cGAS generates the second messenger 2'3' cyclic GMP-AMP (cGAMP) from ATP and GTP (Ablasser et al., 2013a; Chen et al., 2016; Diner et al., 2013). cGAMP then binds and activates the endoplasmic reticulum membrane protein STING (Chen et al., 2016; Ishikawa et al., 2009), triggering its trafficking to the Golgi. STING's C-terminal tail then recruits the kinase TBK1 which phosphorylates the transcription factor IRF3, allowing its dimerization and translocation to the nucleus. The cGAS-STING pathway also activates NF-κB, but interestingly, the exact mechanism of this remains unclear (Ablasser and Chen, 2019). Upon activation, IRF3 and NF-κB translocate to the nucleus and initiate transcription of numerous cytokines and chemokines (Chen et al., 2016).

Early on it was clear that the cGAS-STING pathway was crucial for host defense against pathogens, especially viruses. Protection against many DNA viruses, such as herpes simplex virus, vaccinia virus, and cytomegalovirus is dependent on type I IFN and mice genetically deficient for either cGAS or STING are unable to mount sufficient antiviral responses, are unable to produce type I IFN, and ultimately succumb to their infections more easily than WT mice (Chen et al., 2016).

The cGAS-STING pathway also plays a role in autoimmunity. The cGAS enzyme is capable of recognizing any double stranded DNA, regardless of origin, raising the possibility that perturbations in host DNA localization could trigger the pathway, leading to unwanted inflammation. An example is the autoinflammatory disease Aicardi-Goutières syndrome (AGS). AGS is characterized by high levels of systemic type I IFN and many patients with AGS have been found to have mutations in TREX1, an exonuclease that degrades cytosolic DNA (Chen et al., 2016). Mice deficient for *Trex1* exhibit a similar pathology to AGS, with systemic inflammation and high amounts of serum type I IFN, and ultimately die within a few months of birth. Interestingly crossing *Trex1*$^{-/-}$ mice to *Sting*$^{-/-}$, *cGAS*$^{-/-}$, or *Irf3*$^{-/-}$ mice completely alleviates the symptoms and rescues the animals from death, implicating cytosolic DNA and the cGAS-STING pathway in this autoimmune disease (Gall et al., 2012; Gray et al., 2015).

The cGAS-STING pathway also has important implications for cancer surveillance and therapy. Mice lacking functional STING are more susceptible to both transplanted (Marcus et al., 2018; Woo et al., 2014) and carcinogen-induced tumors (Zhu et al., 2014) and NK cells and CD8 T cells have both been shown to be important for STING-dependent antitumor immune responses (Deng et al., 2014; Marcus et al., 2018; Woo et al., 2014). Major mediators of STING-dependent antitumoral effects are thought to be type I IFNs, which play major roles in both T cell and NK cell-mediated cancer immunosurveillance (Diamond et al., 2011; Swann et al., 2007), as well as efficacy of cancer immunotherapies in general (Critchley-Thorne et al., 2009; Fuertes et al., 2013; Zitvogel et al., 2015). Indeed, an intratumoral type I IFN gene signature has been found to correlate with positive clinical outcomes for human patients in a variety of cancers (Fuertes et al., 2011; Ulloa-Montoya et al., 2013). In support of this hypothesis, early studies found that the defect in tumor rejection in STING-deficient mice was associated with decreased CD8 T cell priming, with both dendritic cells and Type I IFN being important for this process (Deng et al., 2014; Woo et al., 2014).

The source of DNA for activation of the pathway, in the context of antitumor immunity, is thought to be tumor-cell derived (Klarquist et al., 2014; Marcus et al., 2018; Ohkuri et al., 2014; Woo et al., 2014). A hallmark of cancer is the ability to replicate indefinitely and often without all the normal checkpoints that ensure orderly DNA replication. This can lead to replicative stress, resulting in DNA double-strand breaks, activation of the DNA-damage response (DDR) (Marcus et al., 2014), and leakage of DNA into the cytosol, thus triggering production of cGAMP (Lam et al., 2014). Tumor-derived cGAMP can act on STING within tumor cells to induce expression of NK cell activating ligands, like RAE-1 (Lam et al., 2014), or to promote the senescence-associated secretory phenotype (Li and Chen, 2018). However, cGAMP can also be transferred to non-tumor cells (Marcus et al., 2018), via potentially several mechanisms including traversing gap junctions (Ablasser et al., 2013b), via the SLC19A1 folate transporter (Luteijn et al., 2019; Ritchie et al., 2019), and via LRRC8 volume-regulated anion channels (Zhou et al., 2020) to trigger STING activation.

Although several tumor cell lines have been found to contain cytosolic DNA (Ho et al., 2016; Lam et al., 2014; Shen et al., 2015), the amounts of cGAMP made or transferred appear to be limiting for inducing a maximally potent antitumor immune response. However, injections of cGAMP or other STING agonists directly into tumors has been shown to induce a powerful antitumor immune response, leading to tumor rejection in several tumor transplant models of

cancer (Corrales et al., 2015; Curran et al., 2016; Demaria et al., 2015; Francica et al., 2018; Fu et al., 2015; Sivick et al., 2018). Based on these findings, STING agonists are currently being tested for anticancer therapeutic activity in clinical trials.

Overall thesis question and dissertation overview

Immune-therapeutics have revolutionized modern cancer treatment, greatly increasing patient survival and leading to long-term remission in a significant number of people. Despite these successes, the fact is that the large majority of cancer patients do not respond to currently approved therapies. Many of these drugs act by unleashing the awesome destructive power of CD8 T cells, increasing their activation and proliferation, or altering their tropism, to promote tumor destruction. However, tumors may evade CD8 T cells through the loss of tumor MHC molecules or because some tumors may contain few/no neoantigens. These tumors will likely be resistant to current therapies. Therefore, approaches to mobilize immune cells to kill CD8 T cell-resistant tumors are needed to combat these potential escape mechanisms.

Cyclic-dinucleotides (CDNs) are a class of immunostimulatory molecules that bind to the STING protein and induce type I IFN and other pro-inflammatory mediators. Recently, in mouse transplantable tumor models, it was shown that intratumoral CDN injections trigger tumor regressions and resulted in long-lasting antitumor immunity. The antitumor effects of CDN-based therapies have been primarily attributed to CD8 T cells (Curran et al., 2016; Demaria et al., 2015; Sivick et al., 2018) and their impact on other cells remains poorly defined.

My thesis work examines the potential of CDNs to mobilize antitumor immune responses against CD8 T cell-resistant tumors. As a model, I have employed *B2m*$^{-/-}$, MHC I-deficient tumor cell lines, which are resistant to killing by CD8 T cells. This is also a clinically relevant model as tumor cells are known to lose MHC I as a means to escape CD8 T cell recognition, and in many cases, loss of MHC I is achieved via mutations in *B2M*. In chapter 3 of this dissertation, I detail the role of NK cells in mediating tumor rejection after CDN therapy, focusing primarily on the mechanisms of NK cell activation mediated by CDN-induced type I IFNs. In chapter 4, I examine the role of CD4 T cells and find that they can also mediate powerful antitumor responses independently of CD8 T cells, NK cells, and B cells, illuminating potentially novel mechanisms of CD4 T cell-mediated tumor control. Finally, in chapter 5 I will describe the design and implementation of a screen I developed to identify novel NK cell-activating ligands on tumors cells. While this may seem somewhat unrelated to the previous chapters, identifying novel ligands for NK cell activating receptors will be important for the design and implementation of future NK cell-based immunotherapies, including STING agonists.

This project is significant because it addresses CD8 T cell-independent immunological rejection of MHC-deficient tumors induced by CDNs – a promising new mode of cancer therapy. A greater understanding of mechanisms leading to immunological clearance of MHC-deficient tumors will be necessary to bypass mechanisms tumors employ to escape CD8 T cells and to design rational combination therapies with existing anti-cancer drugs.

Chapter 2
Methodology

Mouse strains

Mice were maintained at the University of California, Berkeley. C57BL/6J, CD45.1-congenic (B6.SJL-*Ptprc*^{a} *Pepc*^{b}/BoyJ), *Rag2*$^{-/-}$, *Rag2*$^{-/-}$*Il2rg*$^{-/-}$, *Prf1*$^{-/-}$, *Ifnar1*$^{-/-}$, *Tnfrsf1a*$^{-/-}$, *Tnfrsf1b*$^{-/-}$, *Ighm*$^{-/-}$, *Tcrd*$^{-/-}$, *Ifng*$^{-/-}$, *Ifngr1*$^{-/-}$, MHC II KO (*H2-Ab1*$^{-/-}$, *H2-Aa*$^{-/-}$, *H2-Eb1*$^{-/-}$, *H2-Eb2*$^{-/-}$, *H2-Ea*$^{-/-}$) (all on the B6 background), and BALB/c mice were purchased from the Jackson Laboratory. *Ncr1*^{iCre} and *Sting*$^{gt/gt}$ mice were generous gifts from Eric Vivier and Russell Vance, respectively. NK-DTA mice were generated by breeding *Ncr1*^{iCre} mice to *Rosa26*$^{LSL\text{-}DTA}$ mice (Jackson Laboratories). *Ncr1*$^{iCre/+}$, *Ifnar1*$^{fl/fl}$ and *CD11c-Cre, Ifnar1*$^{fl/fl}$ mice were generated by breeding *Ncr1*^{iCre} and *CD11c (Itgax)-Cre-eGFP* (Jackson Laboratories) mice to *Ifnar1*$^{fl/fl}$ mice (Jackson Laboratories). *Rag2*$^{-/-}$ *Prf1*$^{-/-}$ mice were generated in our lab by breeding *Rag2*$^{-/-}$ and *Prf1*$^{-/-}$ mice together. *Tnfrsf1a*$^{-/-}$*Tnfrsf1b*$^{-/-}$ (TNFR1/2 dKO) were generated in Greg Barton's lab by breeding *Tnfrsf1a*$^{-/-}$ and *Tnfrsf1b*$^{-/-}$ mice together. All mice used were aged 8-30 weeks. All experiments were approved by the UC Berkeley Animal Care and Use Committee.

Cell lines and culture conditions

RMA (obtained from Michael Bevan, who received it from Dr. K. Karre, Karolinska Institute, Stockholm, Sweden), CT26 (obtained from Aduro Biotech), 4T1 (obtained from Dr. Robert Weinberg), and C1498 (purchased from ATCC) were cultured in RPMI 1640 (ThermoFisher). B16-F10 (obtained from the UC Berkeley Cell Culture Facility) and MC-38 (obtained from Dr. James Allison) were cultured in DMEM (ThermoFisher). In all cases media contained 5% FBS (Omega Scientific), 0.2 mg/ml glutamine (Sigma-Aldrich), 100 U/ml penicillin (Thermo Fisher Scientific), 100 μg/ml streptomycin (Thermo Fisher Scientific), 10 μg/ml gentamycin sulfate (Lonza), 50 μM β-mercaptoethanol (EMD Biosciences), and 20 mM HEPES (Thermo Fisher Scientific), and the cells were cultured in 5% CO_2. *B2m*$^{-/-}$, *Ifnar1*$^{-/-}$, *Fas*$^{-/-}$, *Ifngr1*$^{-/-}$, or *Ab1*$^{-/-}$ cell lines were generated using CRISPR-Cas9 (described below). All cells tested negative for mycoplasma contamination.

Generation of edited cell lines using CRISPR-Cas9

Plasmids containing Cas9 and *B2m*-targeting guide sequence (shown below) were generated and described previously (Ardolino et al., 2014). The *Ifnar1*-, *Fas*-, *Ifngr1*-, *Tnfrsf1a*-, *Tnfrsf1b*-, and *Ab1*-targeting CRISPR-Cas9 plasmids were generated by cloning their guide sequences (shown below*)* into PX330 or PX458 (Addgene) following the "Zhang lab general cloning protocol" located on the addgene website and provided by the Zhang Lab at the Massachusetts Institute of Technology. To generate knockout cell lines, plasmids were transiently transfected using either lipofectamine 2000 (ThermoFisher) (CT26, 4T1, B16-F10, and MC-38) or by nucleofection (RMA and C1498) (Kit T, Lonza). In some cases, GFP^{+} (for PX458) cells were sorted one day after nucleofection to ensure that all cells in culture received the Cas9 plasmid. One week later, MHC I, IFNAR1, FAS, IFNγR1, TNFR1, TNFR2, or MHC II-deficient cells were sorted using a FACS Aria cell sorter. For B16-F10, cells were incubated with 100 ng/ml IFNβ (Biolegend) overnight before sorting in order to easily distinguish MHC I^{+} and MHC I^{-} cells. For generating *Ab1*$^{-/-}$ cells, a plasmid containing CIITA-GFP (obtained from Dr. Cheong-Hee Chang) was nucleofected prior to sorting to easily distinguish MHC II^{+} and MHC II^{-} cells.

CRISPR-Cas9 guide sequences:
B2m: AGTCGTCAGCATGGCTCGCT
Ifnar1: GCTGGTGGCCGGGGCGCCTT
Fas: CTGCAGACATGCTGTGGATC
Ifngr1: ATTAGAACATTCGTCGGTAC
Ab1: TCGTATGCGCTGCGTCCCGT
Tnfrsf1a: CTGATGGGGATACATCCATC
Tnfrsf1b: GAGATCTGGCACTCGTACCC

In vivo tumor growth experiments

Cells were washed and (ThermoFisher) resuspended in PBS and 100 µl containing 4 x 10^6 cells (unless otherwise noted) were injected subcutaneously. Tumor growth was measured using calipers and graphed using the ellipsoid formula: $V = (\pi/6)ABC$. In some experiments, mice were NK-depleted by intraperitoneal (i.p.) injection of 250 µg anti-NK1.1 (clone PK136, purified in our laboratory) or 100 µl anti-asialo-GM1 (Biolegend) for C57BL/6J and BALB/c mice, respectively. Mice were CD8 and CD4-depleted by i.p. injection of 250 µg anti-CD8b.2 (clone 53-5.8, Leinco) or 250 ug anti-CD4 (clone GK1.5, Leinco), respectively. Whole rat Ig (Jackson Immunoresearch) was used as a control. Depleting or control antibodies were injected 2 and 1 days before tumor inoculation and continued weekly thereafter. Depletions were confirmed by flow cytometry. 5 days after tumor inoculation, when tumors were ~50-150 mm^3, mice were injected i.t. with PBS or 1x 50 µg c-di-AMP (RMA-*B2m*$^{-/-}$, B16-F10-*B2m*$^{-/-}$, C1498-*B2m*$^{-/-}$, MC38-*B2m*$^{-/-}$) or 3 x 25 µg c-di-AMP (CT26-*B2m*$^{-/-}$, 4T1-*B2m*$^{-/-}$) in a total volume of 100 µl (PBS).

In some experiments, mice received 500 µg anti-IFNAR1 (clone MAR1-5A3, Leinco), 200 µg anti-TNF-α (clone TN3-19.12, Leinco), 200 µg anti-IFN-γ (clone XMG1.2, Leinco), 100 µg anti-GR-1 (clone RB6-8C5, Leinco), 200 µg anti-Ly6G (clone 1A8, Leinco), 200 µg anti-IL-5 (clone TRFK5, Leinco), 200 µl Clodronate Liposomes (Liposoma), or control rat IgG i.p. on day -1, day 0, and twice weekly thereafter. In some experiments, mice received 5 µg anti-IL-15/15R (clone GRW15PLZ, Thermo Fisher Scientific) or control rat IgG i.p. on day -1, once again i.t. mixed with CDN on day 0, and again i.p. on days 1 and 2.

For serum transfer experiments, mice were bled from either the tail or blood was collected via cardiac puncture. Serum was pooled from several mice and 200 µl was injected IP beginning on the day of tumor injection and every 2 days thereafter for a total of 4 serum injections.

Flow Cytometry

Single cell suspensions of spleens and lymph nodes were generated by passing cells through a 40 µm filter. Red blood cells were removed from spleens using ACK buffer. Tumors were chopped with a razor blade and dissociated in a gentleMACS Dissociator (Miltenyi) before passage through an 80 µm filter. For assessing NK activation, cell suspensions were incubated for 4 hours in medium containing Brefeldin A (Biolegend), Monensin (Biolegend) and CD107a

antibodies before surface and intracellular staining. In some experiments, PMA (50 ng/ml, Sigma) + Ionomycin (1 mg/ml, Sigma) was used to stimulate cells. LIVE/DEAD stain (ThermoFisher) was used to exclude dead cells. FcγRII/III receptors were blocked with 2.4G2 hybridoma supernatant (prepared in the lab). Staining with fluorochrome- or biotin-conjugated antibodies occurred at 4 degrees C for 30 min in FACS buffer (2.5% FBS and 0.02% Sodium Azide in PBS). When necessary, fluorochrome-conjugated streptavidin was added. For intracellular staining, cells were fixed and permeabilized using Cytofix/Cytoperm buffer (BD Biosciences) and stained with fluorochrome-conjugated antibodies for 30 min at 4 degrees C in Perm/Wash buffer (BD Biosciences). Transcription factor staining was done using the FOXP3/Transcription Factor Staining Buffer Set (eBioscience) according to the manufacturers protocol. Specifically, cells were fixed and permeabilized using FoxP3 Fix/Perm Buffer and stained with fluorochrome-conjugated antibodies for 30 min at 4 degrees C in Foxp3 Perm Buffer. Flow cytometry was performed using an LSR Fortessa, or X20 (BD Biosciences). Data analyzed with FlowJo (Tree Star).

Tetramer staining of GP70 tumor-specific CD4 T cells

Spleens of Naïve or RMA-*B2m*$^{-/-}$ tumor-bearing mice were harvested approximately one week after CDN or PBS treatment, single cell suspensions were made, and ACK-treated as described above. Splenocytes were then stained in triplicate with a PE-conjugated MHC II I-A^{b} tetramer containing the MuLV env$_{123\text{-}141}$ epitope EPLTSLTPRCNTAWNRLKL, which was kindly provided by the Tetramer Core Facility at the National Institutes of Health. Tetramer staining was done in 100 µl RPMI media in a round-bottom 96 well plate at a dilution of 1:400 for 3 hours at 37 degrees C. Tetramer-stained splenocytes were then stained with Live/Dead, 2.4G2, and surface markers as described above. Triplicate samples were pooled prior to running flow cytometry.

Peptide stimulation assay

Spleens of Naïve or RMA-*B2m*$^{-/-}$ tumor-bearing mice were harvested approximately one week after CDN or PBS treatment, single cell suspensions were made, and treated with ACK to lyse red blood cells. Splenocytes were then added in triplicate to a round-bottom 96 well plate in 100 µl RPMI media gp70 peptide (DEPLTSLTPRCNTAWNRLKL, from Peptide 2.0) at a concentration of 5 µg/ml. One hour later, Brefeldin A (Biolegend) and Monensin (Biolegend) were added to the stimulation mix. 4 hours later, cells were stained with Live/Dead, 2.4G2, and surface markers as described above. Triplicate samples were pooled prior to running flow cytometry.

Antibodies

For flow cytometry we used the following antibodies: Biolegend: anti-CD45 (30-F11), anti-CD45.1 (A20), anti-CD45.2 (104), anti-CD3ε (145-2C11), anti-CD4 (GK1.5), anti-CD8α (53-6.7), anti CD44 (IM7) anti-CD11b (M1/70), anti-CD11c (N418), anti-CD19 (6D5), anti-F4/80 (BM8), anti-Ly6C (HK1.4), anti-Ly6G (1A8), anti-NKp46 (29A1.4), anti-NK1.1 (PK136), anti-Sca-1 (D7), anti-Ter119 (TER-119), anti-Ki67 (SolA15), anti-CD107a (1D4B), anti-I-A/I-E

(M5/114.15.2), anti-IFN-γ (XMG1.2), anti-IL-2 (JES6-5H4), anti-TNF-α (MP6-XT22), anti-IFNAR1 (MAR1-5A3), anti-DR5 (MD5-1), anti-mouse IgG (poly4053), anti-T-bet (4B10), anti-FOXP3 (MF-14), anti-PD-1 (29F.1A12), anti-Tim-3 (RMT3-23), anti-Lag-3 (C9B7W), and anti-TIGIT (1G9). BD Pharmingen: anti-H-2K^{b} (AF6-88.5), anti-Fas (Jo2). BD Horizon: anti-Granzyme B (GB11). R&D Systems: anti-IL-15Rα (BAF551). Miltenyi Biotec: anti-TOX (REA473). ThermoFisher Scientific: anti-Eomes (Dan11mag).

Ex vivo cytotoxicity assay

Cytotoxicity by splenocytes was assessed with a standard 4-hour ^{51}Cr-release assay. ~24 hours after CDN or PBS treatment of tumors, spleens were harvested and treated with ACK buffer. Pooled splenocytes from 4-6 mice were employed as effector cells. Triplicate samples of 10^4 ^{51}Cr-labeled RMA-*B2m*$^{-/-}$ cells per 96-well V-bottom plate well were incubated with splenocytes at the indicated E:T ratios for 4 hrs before determining the percent ^{51}Cr release in the supernatant. % specific lysis = 100 x (experimental - spontaneous release$_{Avg}$)/(maximum release$_{Avg}$ - spontaneous release$_{Avg}$), where maximum release was release with addition of Triton-X 100 (final concentration 2.5%).

Where shown, pooled splenocytes were NK-depleted by incubating on ice for 30 min with anti-NKp46-Biotin (Biolegend) and anti-NK1.1-Biotin (Biolegend) followed by 20 min incubation with streptavidin magnetic beads (Biolegend), and magnetic removal of bead-bound cells. Depletion (>95%) was confirmed by flow cytometry.

RNA isolation, reverse transcription, and qPCR

Total RNA was isolated from cells in culture or from tumors dissociated using the gentleMACS dissociator (Miltenyi) using the RNeasy Mini Kit (Qiagen) and treated with DNase I (Qiagen). In some cases, cells were treated overnight with recombinant murine IFN-γ (100 ng/ml, Biolegend). cDNA was generated using the iScript reverse transcription kit (BioRad). Quantitative real-time PCR was done using SsoFast EvaGreen Supermix (BioRad) with 25 ng of cDNA per reaction in a CFX96 Thermocycler (BioRad). *Gapdh* and *Ubc* were used as references.

Primer sequences:
Gapdh F: TGTGTCCGTCGTGGATCTGA, R: TTGCTGTTGAAGTCGCAGGAG
Ubc F: GCCCAGTGTTACCACCAAGA, R: CCCATCACACCCAAGAACAA
Ifnb1 F: ATGAACTCCACCAGCAGACAG, R: ACCACCATCCAGGCGTAGC
Il15 F: GTGACTTTCATCCCAGTTGC, R: TTCCTTGCAGCCAGATTCTG
Il15ra F: CCCACAGTTCCAAAATGACGA, R: GCTGCCTTGATTTGATGTACCAG
Irf1 F: CAGAGGAAAGAGAGAAAGTCC, R: CACACGGTGACAGTGCTGG

ELISA

Tumors of ~100 mm^3 were treated with PBS or 50 μg CDN. 6 hours later serum was harvested and IFNβ was quantified by ELISA (Biolegend) following the manufacturer's instructions.

Bone marrow chimeras

Recipient mice were irradiated with 10 Gy (5 Gy + 5 Gy on consecutive days). After the second round of irradiation on day 2, 10^7 donor bone marrow cells suspended in 100 µl PBS were injected intravenously into the tail vein. For mixed bone marrow chimeras, donor bone marrow from each group was mixed equally (5 x 10^6 cell each/mouse) before injection. For WT/*Ifnar1*$^{-/-}$ chimeras, WT mice were B6-CD45.1 and the *Ifnar1*$^{-/-}$ donors were on the B6 background (CD45.2). For WT/*Ifng*$^{-/-}$, *Rag2*$^{-/-}$/*Ifng*$^{-/-}$, and *Ifng*$^{-/-}$ chimeras, WT mice were B6 background (CD45.2) and all recipients were B6-CD45.1. After 8 weeks, chimerism was assessed by staining blood cells for CD45.1 and CD45.2 expression and analyzing by flow cytometry, and mice were employed for experiments.

Generating NK chimeric antigen receptor T cells

Constructs encoding the extracellular domain of human NKp30, NKp44, or NKp46 fused to the transmembrane and intracellular signaling domains of CD28 and intracellular signaling domain of CD3ζ were ordered from Integrated DNA Technologies and cloned into a lentiviral vector backbone with an EF-1α promoter and an IRES-mCherry sequence, which was a gift from Claudia Cattoglio in the Tijan Lab at UC Berkeley. Virus was generated by transfecting these plasmids, along with the PSPAX2 packaging plasmid and VSV-G envelope plasmid, into 293T cells. 48 hours after transfection, virus-containing supernatant was harvested and filtered through a 0.45 µm filter. For transduction 5 x 10^6 PBMCs were stimulated with anti-CD3/CD28 beads (ThermoFisher) for 4 hours following the manufacturer's instructions. The cells and beads were then pelleted and resuspended in 2 ml of viral supernatant containing polybrene at 10 µg/ml and IL-2 at 50 U/ml. The cells were then spinfected in a 6 well plate at 30 degrees C for 1.5 hours at 2,500 RPM. The cells were then incubated overnight at 37 degrees C. The next day the transduction was repeated. One day after the second transduction the media was changed with fresh RPMI media containing IL-2 at 50 U/ml. Two days later (3 days after beads were initially added), the beads were removed and fresh IL-2-containg RPMI media was added. Three days later the cells were sorted on mCherry. In some instances the cells were additionally sorted on CD4 or CD8.

Expanding NK CAR T cells using the rapid expansion protocol (REP)

This protocol was provided by Tom Schmitt of the Greenberg Lab. 2.5 x 10^5 NK CAR T cells were combined with 25 x 10^6 irradiated PBMCs (3500 rads), 5 x 10^6 irradiated TM-LCL cells (7000rads, a generous gift from Dr. P. Greenberg), and 30ng/ml anti-CD3 (clone OKT3) in an upright T25 flask in a total volume of 25 ml RPMI media. The next day IL-2 was added to a achieve a final concentration of 50 U/ml. 4 days later the cells were pelleted and resuspended in fresh media containing 50 U/ml IL-2. For the next 7-10 days the culture was monitored and fresh IL-2 was added twice/week. The cells were split as needed, making sure to keep the cells at ~1-1.5 x 10^6 cells/ml. The cells were used for assays or another REP 12-20 days after beginning the first REP.

NK CAR T cell stimulation assays

Antibodies specific for NKp30, NKp44, or NKp46 were added to a high-binding flat bottom 96 well plate at 5 μg/ml in PBS overnight at 4 degrees C. The next day the plates were washed and 1-2 x 10^5 NK CAR T cells were added to the wells. For tumor cell stimulations 10^5 tumor cells were used to stimulate 10^5 NK CAR T cells per well in a round bottom 96 well plate. All stimulations occurred in the presence of Brefeldin A (Biolegend), Monensin (Biolegend), and in some cases anti-CD107a. In some experiments, PMA (50 ng/ml, Sigma) + Ionomycin (1 mg/ml, Sigma) was used to stimulate cells. LIVE/DEAD stain (ThermoFisher) was used to exclude dead cells. Intracellular cytokine staining for IFN-γ and TNF-α was done as described above.

NK CAR T cells cytotoxicity assay

Cytotoxicity by NK CAR T cells was assessed with a standard 4-hour ^{51}Cr-release assay. NK CAR T cells, generated as described above, were employed as effector cells. Triplicate samples of 10^4 ^{51}Cr-labeled Hap1 or HCT116 cells per 96-well V-bottom plate well were incubated with NK CAR T cells at the indicated E:T ratios for 4 hrs before determining the percent ^{51}Cr release in the supernatant. % specific lysis = 100 x (experimental - spontaneous $release_{Avg}$)/(maximum $release_{Avg}$ - spontaneous $release_{Avg}$), where maximum release was release with addition of Triton-X 100 (final concentration 2.5%).

Statistics

Statistics were performed using Prism (GraphPad). For tumor growth and survival, two-way ANOVA and Log-rank (Mantel-Cox) tests were used. For NK activation and qPCR, unpaired two-tailed students T tests or one-way ANOVA followed by Tukey's multiple comparisons tests were used when data fit a Normal distribution. For nonparametric data, the Kruskal-Wallis test with Dunn's multiple comparisons was used. Two-way ANOVA was used for cytotoxicity and in some instances the areas under the curves were compared using paired two-tailed Student's T tests. Significance is indicated as: *P < 0.05; **P<0.01; ***P < 0.001; ****P<0.0001.

Chapter 3
STING agonists trigger NK cell-dependent clearance of CD8 T cell-resistant tumors

Portions of this chapter were adapted and/or reprinted with permission from "Nicolai, C.J., Wolf, N., Chang, I.C., Kirn, G., Marcus, A., Ndubaku, C.O., McWhirter, S.M., and Raulet, D.H. NK cells mediate clearance of CD8(+) T cell-resistant tumors in response to STING agonists. Science Immunology, 20 Mar 2020. Vol. 5, Issue 45. DOI: 10.1126/sciimmunol.aaz2738."

Abstract

Several immunotherapy approaches that mobilize CD8 T cell responses stimulate tumor rejection, and some, such as checkpoint blockade, have been approved for several cancer indications and show impressive increases in patient survival. However, tumors may evade CD8 T cell recognition via loss of MHC molecules or because they contain few/no neoantigens. Therefore, approaches are needed to combat CD8 T cell-resistant cancers. STING-activating cyclic-di-nucleotides (CDN) are a new class of immune-stimulating agents that stimulate impressive CD8 T cell-mediated tumor rejection in preclinical tumor models and are now being tested in clinical trials. Here we demonstrate powerful CDN-induced, natural killer (NK) cell-mediated tumor rejection in numerous tumor models, independent of CD8 T cells. CDNs enhanced NK cell activation, cytotoxicity, and antitumor effects in part by inducing type I IFN (IFN). IFN acted in part directly on NK cells *in vivo*, and in part indirectly via the induction of IL-15 and IL-15 receptors, which were important for CDN-induced NK activation and tumor control. Upon applying CDNs *in vivo*, dendritic cells (DCs) upregulated IL-15Rα in an IFN-dependent manner. Mice lacking IFNAR specifically on DCs had reduced NK cell activation and tumor control. Therapeutics that activate NK cells, such as CDNs, checkpoint inhibitors, NK cell engagers, and cytokines, may represent next-generation approaches to cancer immunotherapy.

Introduction

Recent breakthroughs in tumor immunology have provided novel immune-based therapeutics, extending patient lives and in some cases resulting in what appear to be permanent remissions (Ribas and Wolchok, 2018; Sharma and Allison, 2015a). Most immunotherapy protocols aim to augment CD8 T cell responses by targeting immune inhibitory pathways, leading to greater T cell activation and tumor destruction (Hirano et al., 2005; Leach et al., 1996). However, tumors may evade the CD8 T cell response via selective or complete loss of MHC class I expression (Garrido et al., 2016; McGranahan et al., 2017; Roemer et al., 2016) or because they express few or no neoantigens (Alexandrov and Stratton, 2014), and may consequently be refractory to CD8 T cell-dependent therapies. Therefore, knowledge of how the immune system can be mobilized to kill CD8 T cell-resistant tumors is needed to address these potential escape mechanisms and design next generation immunotherapies.

Natural Killer (NK) cells are cytotoxic innate lymphocytes that are important for killing virus-infected cells and tumor cells (Cerwenka and Lanier, 2001; Marcus et al., 2014; Vivier et al., 2011). Unlike T cells, which target unique peptide antigens displayed on MHC molecules, NK cells recognize abnormally expressed, stress-induced ligands on unhealthy cells (Cerwenka and Lanier, 2001; Moretta et al., 2001; Raulet et al., 2013; Raulet and Guerra, 2009), and/or cells that have lost MHC class I (Karlhofer et al., 1992; Karre et al., 1986; Moretta et al., 1996; Raulet and Vance, 2006). Furthermore, NK cells produce cytokines and chemokines that enhance recruitment and maturation of dendritic cells (DCs) (Barry et al., 2018; Bottcher et al., 2018),

promoting adaptive immune responses. These features enable NK cells to increase adaptive immune responses to tumors as well as directly kill tumors that have escaped T cell responses, making NK cells exciting targets for immunotherapy.

As discussed in Chapter 1, the cGAS-STING pathway is an innate immune sensing pathway that, in response to cytosolic DNA, produces the second messenger molecule, cGAMP, which binds to STING, promoting activation of IRF3 and NF-κB transcription factors, resulting in production of type I IFN and proinflammatory cytokines and chemokines (Chen et al., 2016). Recently it was shown that injections of cGAMP or other STING agonists directly into tumors induces a powerful antitumor response leading to tumor rejection in various tumor transplant models of cancer (Corrales et al., 2015; Demaria et al., 2015; Francica et al., 2018; Fu et al., 2015; Sivick et al., 2018) and based on these findings, STING agonists are currently being tested in clinical trials.

The antitumor effects of STING agonists have primarily been attributed to CD8 T cells (Curran et al., 2016; Demaria et al., 2015; Sivick et al., 2018), while their impacts on other cells, such as NK cells, remain poorly defined. STING activation potently induces multiple inflammatory mediators, including type I IFNs (Ishikawa et al., 2009), which play central roles in NK cell biology, including maturation, homeostasis, and activation (Swann et al., 2007). In this study, we have investigated the role of NK cells in mediating tumor rejection after cyclic dinucleotide (CDN) therapy, independent of the CD8 T cell response. Our results demonstrate powerful CD8-independent antitumor responses mediated by NK cells that are induced by therapeutic applications of CDNs in numerous cancer models, including both MHC I-deficient and MHC I^+ tumor models.

Results

Successful immunotherapy of MHC class I-deficient tumors by CDNs occurs independently of CD8 T cells.

To examine the CD8 T cell-independent antitumor effects of intratumoral (i.t.) CDN injection, we employed CRISPR-Cas9 to disrupt *B2m* in multiple tumor cell lines, generating cells with severely diminished levels of cell surface MHC I molecules (Figure 1A and 2A). Such tumors have potential clinical relevance in light of evidence that MHC I-deficiency is selected for when T cell responses against tumors are induced, and is common in certain cancers (Garrido et al., 2016; McGranahan et al., 2017; Rodig et al., 2018; Roemer et al., 2016; Sade-Feldman et al., 2017; Zaretsky et al., 2016). Tumors were established with a high dose of MHC I-deficient cells injected subcutaneously in syngeneic mice, and treated i.t. once, or in some cases three times, with mixed-linkage (2'3') RR cyclic di-AMP (hereafter referred to as "CDN") or PBS. The dose of CDN used has been shown to be optimal for CD8 T cell responses (Sivick et al., 2018). CDN injections resulted in regression and severely delayed tumor growth in each of six *B2m*$^{-/-}$ tumor models tested, representing multiple types of cancer (Figure 1B). Notably, in all but one model there was a significant incidence of long-term remissions as a result of single agent i.t. administration of CDN, with no evidence of renewed tumor growth for the remainder of the study (50-100 days). The impact of CDNs was abrogated in *Sting*$^{gt/gt}$ mice in both tumor models subsequently tested, demonstrating the role of host STING in the responses (Figure 1C).

Depletion of CD8 T cells using CD8b.2 antibody (Figure 3A) did not diminish tumor rejection in either of the two models tested, consistent with the absence of MHC I molecules on the tumor cells (Figure 1D). These data showed that i.t. injections of CDNs trigger potent antitumor effects independently of CD8 T cells.

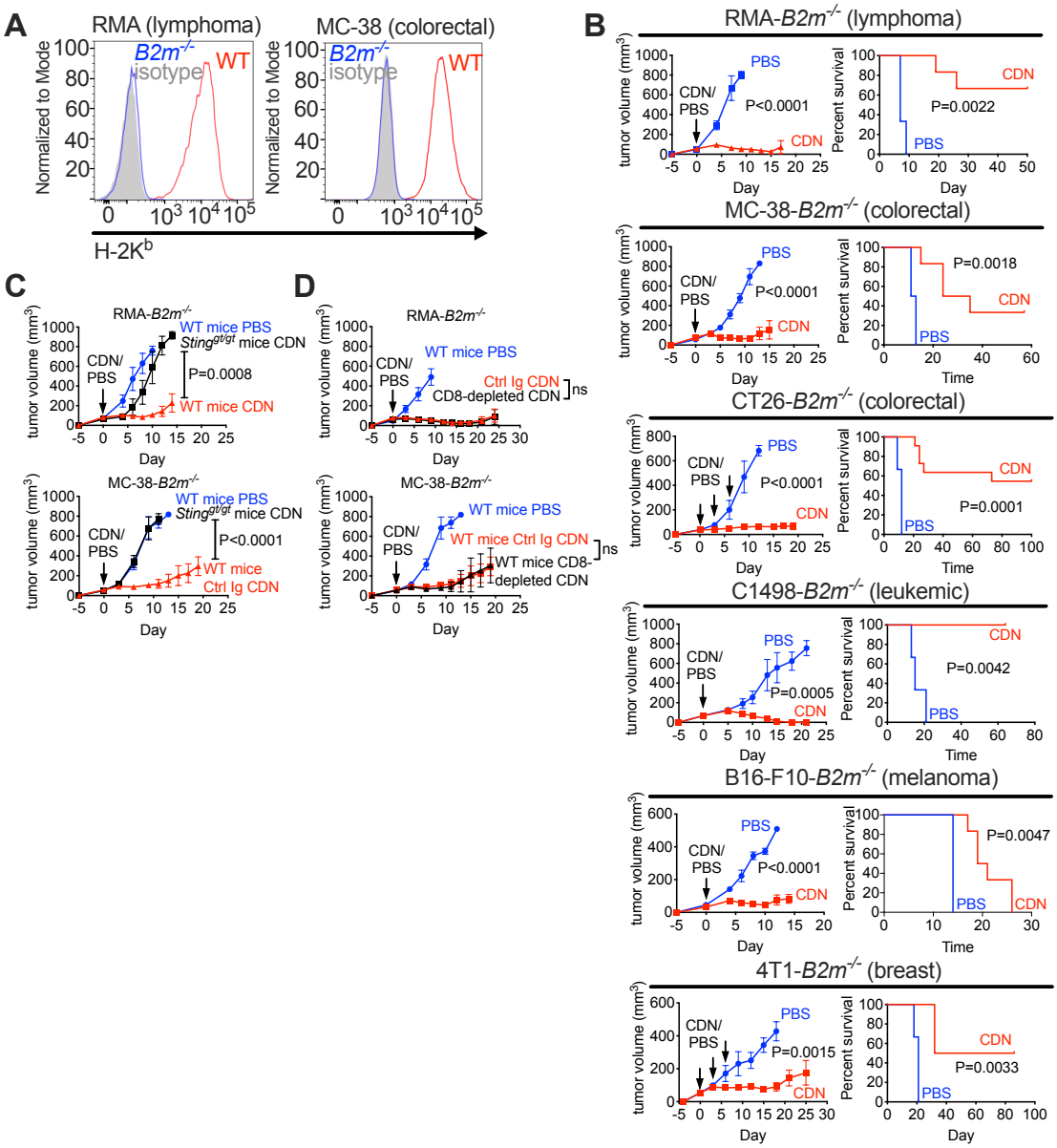

Fig. 1. Rejection of MHC I-deficient tumors induced by intratumoral injections of CDN (2'3' RR c-di-AMP). (**A**) WT and *B2m*$^{-/-}$ tumor cells were stained with MHC class I (H-2K^{b} clone AF6-88.5) or isotype control antibodies. (**B**) Tumor cells were injected s.c. in C57BL/6J or BALB/c (CT26 and 4T1) mice and treated i.t. 5 days later with PBS or once with 50 µg of CDN, or three times with 25 µg CDN over 5 days, indicated by the arrows. Tumor volume and survival was analyzed with 2-way ANOVA and Log-rank (Mantel-Cox) tests, respectively. n=5-11 for CDN-treated mice and 3-4 for PBS-treated mice. Data are representative of 2 independent experiments. (**C**) Tumors were established in C57BL/6J or *Sting*$^{gt/gt}$ mice, treated, and analyzed as in B. n=6 for CDN/WT groups and 3-4 for the other groups. Data are representative of 2 independent experiments. (**D**) Tumors were established, treated, and analyzed as in B. Mice were CD8-depleted or received control rat Ig (see Methods). n=5-8 for the

CDN-treated groups and 3-4 for the PBS-treated group. Data are representative of 2 independent experiments. The MC-38 data in C and D were from the same experiment.

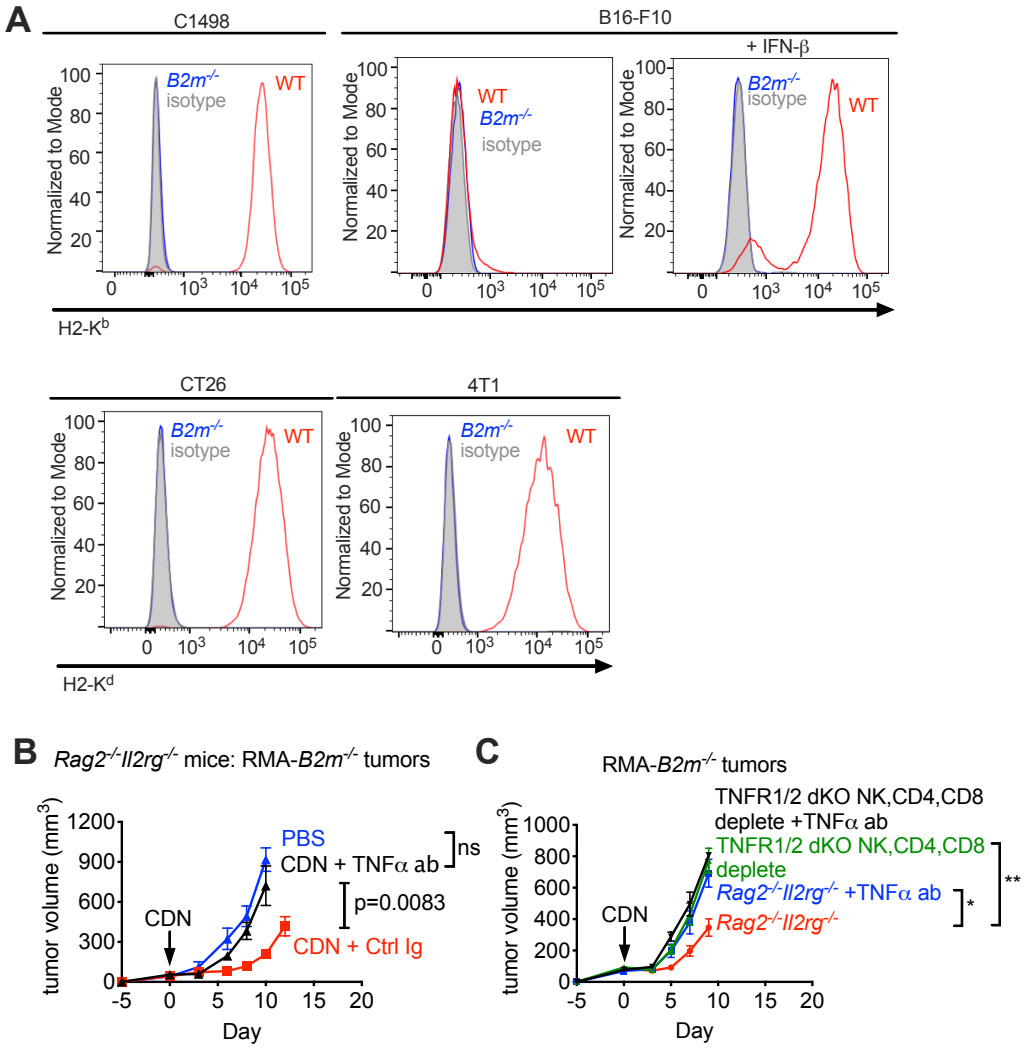

Fig. 2. MHC I expression on *B2m*$^{-/-}$ tumor cell lines and CDN-induced delay in tumor growth in *Rag*$^{-/-}$*Il2rg*$^{-/-}$ mice is TNF-α-dependent. (**A**) MHC I expression on *B2m*$^{-/-}$ tumor cell lines. WT and *B2m*$^{-/-}$ tumor cells were stained with anti-MHC class I (H-2K^{b} clone AF6-88.5 for C1498 and B16-F10 and H-2K^{d} clone SF1-1.1 for CT26 and 4T1) or isotype control. For B16-F10, some cells were incubated with 100 ng/ml IFNβ (Biolegend) for 24 hours before staining. (**B**) CDN-induced delay in tumor growth in *Rag*$^{-/-}$*Il2rg*$^{-/-}$ mice are TNF-α-dependent. RMA-*B2m*$^{-/-}$ tumors were established in *Rag2*$^{-/-}$*Il2rg*$^{-/-}$ mice, treated and analyzed as in Fig. 1B. Some mice were given TNF-α neutralizing antibody or control Ig (see Methods). n=3-4 per group. Representative of two independent experiments. (**C**) TNF-α acts on host cells. RMA-*B2m*$^{-/-}$ tumors were established in *Rag2*$^{-/-}$*Il2rg*$^{-/-}$ mice or TNFR1/2 dKO mice treated with NK, CD4, and CD8 T cell-depleting antibodies and treated and analyzed as in Fig. 1B. Some mice were given TNF-α neutralizing antibody or control Ig (see Methods). n=5 per group. Preliminary data, experiment done only once. *P<0.05; **P<0.01.

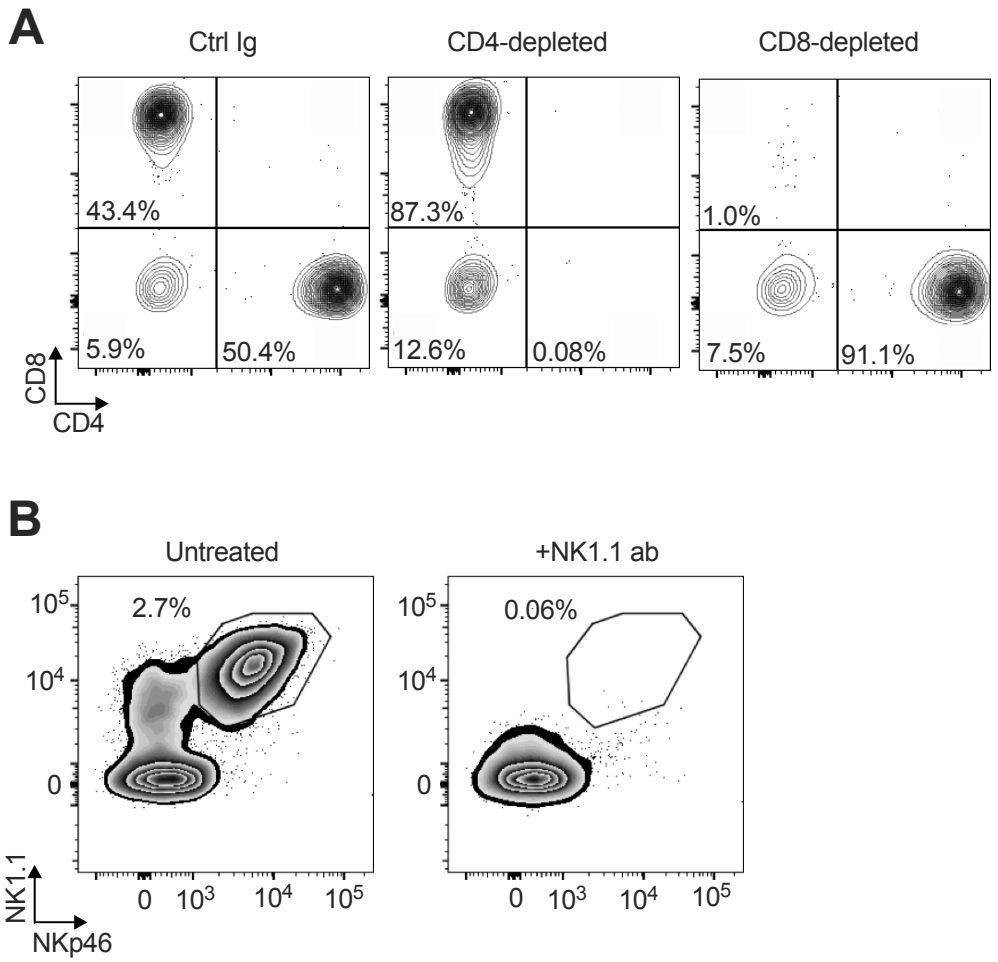

Fig. 3. Verifying *in vivo* depletions. (**A**) Success of T cell depletion protocols. Mice were treated with control Ig (left panel), CD4 T cell-depleting antibodies (center panel) or CD8 T cell-depleting antibodies (left panel) at Day= -2 and Day= -1, as described in methods. On Day=0, Blood was collected, ACK-treated, and stained for viable, $CD3^+$ cells. (**B**) Success of NK cell depletion protocols. Mice were either untreated (left panel) or NK cell-depleted (left panel) at Day= -2 and Day= -1, as described in methods. On Day=0, splenocytes were collected, ACK-treated, and gated on viable, $CD45^+$, CD3-, CD19- cells.

CDN-induced rejection of MHC I-deficient tumors depends on NK cells.

To test the role of NK cells, we depleted mice of NK cells before tumor implantation and subsequent CDN treatment. NK-depletion (Figure 3B) resulted in rapid tumor growth in all five tumor models tested, including MC-38-*B2m*$^{-/-}$ (colorectal), B16-F10-*B2m*$^{-/-}$ (melanoma), CT26-*B2m*$^{-/-}$ (colorectal), C1498-*B2m*$^{-/-}$ (leukemic), and RMA-*B2m*$^{-/-}$ (lymphoma) tumor models (Figure 4A). For the RMA-*B2m*$^{-/-}$ lymphoma line, CDN therapy was also defective in NK-DTA mice, which specifically lack NK cells due to diphtheria toxin expression only in NKp46^{+} cells (Narni-Mancinelli et al., 2011) (Figure 4B). CDN-induced tumor rejection also occurred in *Rag2*$^{-/-}$ mice, which lack T and B cells, but was strongly diminished in NK-depleted *Rag2*$^{-/-}$ mice (Figure 4C), or in *Rag2*$^{-/-}$*Il2rg*$^{-/-}$ mice, which lack NK cells and other innate lymphoid cells in addition to lacking T and B cells (Figure 4D). Thus, CDNs mobilize powerful NK responses against MHC I-deficient tumors that are quite effective in the absence of T and B cells.

Without NK cells, T cells or B cells, as in *Rag2*$^{-/-}$*Il2rg*$^{-/-}$ mice, CDN injections caused a residual delay in tumor growth (Figure 2B, 4C and 4D). Consistent with previous evidence that STING agonists induce an immediate local hemorrhagic necrosis in tumors, mediated by TNF-α (Francica et al., 2018), the CDN-induced delay in the growth of RMA-*B2m*$^{-/-}$ tumors was eliminated when TNF-α was neutralized in *Rag2*$^{-/-}$*Il2rg*$^{-/-}$ mice (Figure 2B). Notably, the delay in tumor growth in *Rag2*$^{-/-}$*Il2rg*$^{-/-}$ mice was transient and none of the mice survived, showing that robust antitumor effects depended on lymphocytes. Furthermore, TNF-α signaling was most important on host cells. NK and T cell-depleted mice lacking both TNF-α receptors (TNFR1/2 dKO) did not exhibit any TNF-α-mediated antitumor effects and tumor growth in these mice was similar to TNF-α–neutralized *Rag2*$^{-/-}$*Il2rg*$^{-/-}$ mice (Figure 2C), suggesting TNF-α acts on host cells. This is consistent with previous reports concluding that STING agonists work in part via TNF-α disrupting the tumor vasculature (Zhao et al., 2002).

Many tumor cells express high MHC I but are nevertheless sensitive to NK cells due to high expression of NK-activating ligands (Jamieson et al., 2002; Raulet and Vance, 2006). An important question was whether CDN-induced, NK-mediated, antitumor effects would be effective against MHC I-high tumor cells that are NK-sensitive. To address this question, we employed the WT (*B2m*$^{+/+}$) MC-38 line, which is MHC I-high (Figure 1A), but which NK cells kill effectively *in vitro* due, at least in part, to the expression of NKG2D ligands by these tumor cells (Jamieson et al., 2002). Remarkably, in *Rag2*$^{-/-}$ mice, which lack all T cells and B cells, CDN treatment was effective in delaying growth of MC-38 tumors and even resulted in a few long-term survivors (Figure 4E). NK depletion resulted in rapid tumor growth and eliminated any long-term survivors. Thus, NK cells can reject MHC I^{+} MC-38 tumor cells after CDN injections, even in the complete absence of T cells. We conclude that CDN-induced NK responses are effective not only against MHC I-deficient tumors but also against tumors that are NK sensitive due, for example, to expression of NK-activating ligands.

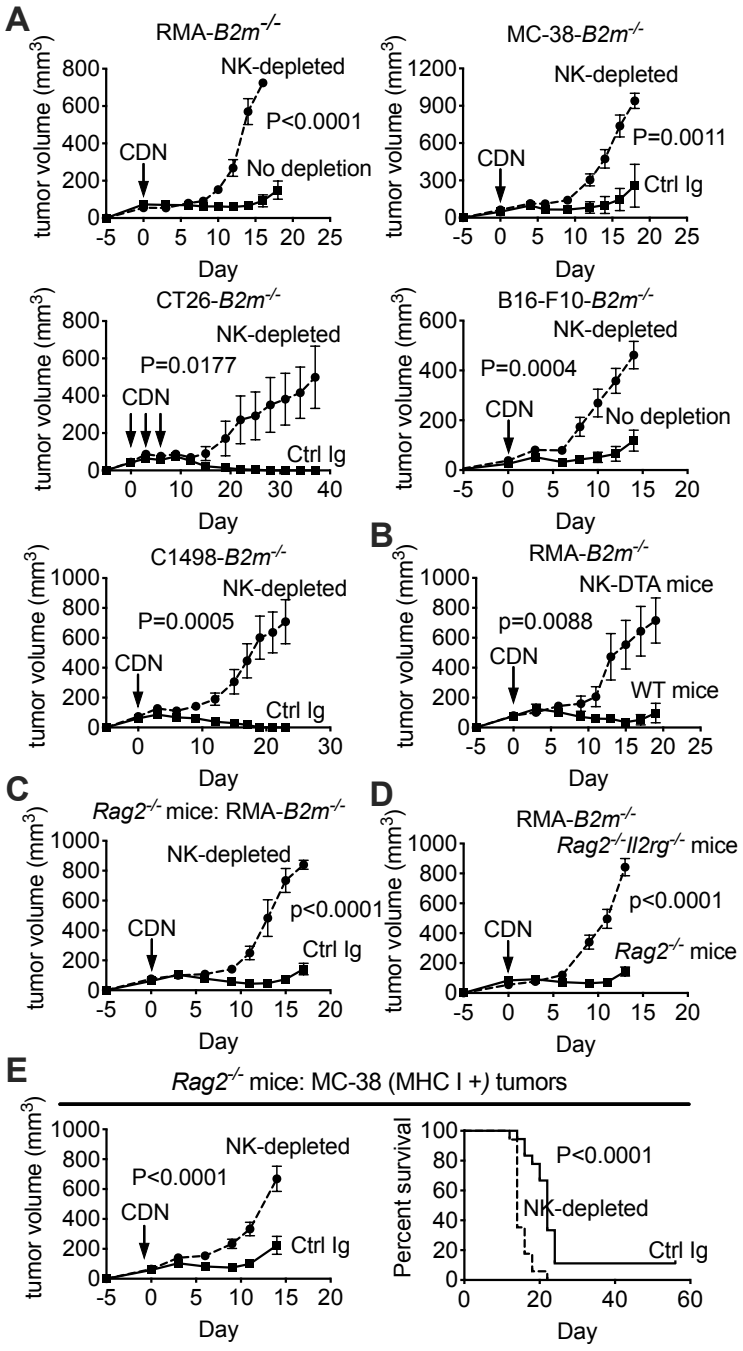

Fig. 4. NK-dependence of tumor rejection induced by CDNs. (**A**) C57BL/6J or BALB/c (CT26 and 4T1 tumors), (**B**) NK-DTA, (**C**-**D**) *Rag2*$^{-/-}$ or (**D**) *Rag2*$^{-/-}$*Il2rg*$^{-/-}$ mice were injected s.c. with tumor cells of the types indicated and tumors were allowed to establish for 5 days. In some experiments (**A**, **C**, **E**) mice were NK-depleted (see Methods). Tumors were treated and analyzed as described in Fig. 1B. (**E**) *B2m*$^{+/+}$ MC-38 tumors (MHC I^{+}) were established in *Rag2*$^{-/-}$ mice that were NK-depleted or not, CDN-treated, and analyzed as in Fig. 1B. For Fig. A-D, data representative of 2-3 independent experiments. n=5-9. For Fig. E, data was combined from 3 independent experiments. n=18.

NK cells are activated by i.t. CDN injections and accumulate within tumors.

To address the impact of CDN treatments on NK cells, we examined markers of NK cell activation among tumor-infiltrating, lymph node, and splenic NK cells one day after treatment, with no additional stimulation *ex vivo*. Compared to NK cells within PBS-treated tumors, NK cells within CDN-treated tumors had increased levels of IFN-γ, the degranulation marker CD107a, Granzyme B, and Sca-1 (Figure 5A and 6A), demonstrating an increased degree of NK activation. Furthermore, NK cells accumulated among $CD45^+$ cells within CDN-treated tumors (Figure 5B). The relative increase of NK cells within tumors coincided with an increase in Ki67 expression (Figure 5B and 6B), suggesting that CDNs promote NK cell proliferation in addition to activation.

CDN treatment also caused NK activation in the tumor-draining lymph node and even in the spleen (Figure 5A), suggesting that i.t. injection of CDNs resulted in systemic NK activation. Consistent with systemic activation, we found that splenocytes harvested from tumor-bearing CDN-treated mice, but not PBS-treated control mice, exhibited detectable cytotoxicity against RMA-*B2m*$^{-/-}$ tumor cells *ex vivo* (Figure 5C). Depleting NK cells after harvest abolished the killing.

Based on these observations, we tested whether systemic NK cell activation induced by CDN administered locally in one tumor would also trigger antitumor responses in an untreated distal tumor. We established C1498-*B2m*$^{-/-}$ tumors on both flanks of *Rag2*$^{-/-}$ mice and treated one tumor with PBS or CDN. As expected based on the results in Figure 1B, i.t. CDN treatment caused substantial tumor regression in the injected tumor (Figure 5D). Notably, there was also a significant growth delay in the untreated distal (contralateral) tumor compared to PBS, showing that i.t. CDN treatments induce systemic antitumor effects, independent of T and B cells. Similar results were obtained with a separate tumor model, B16-F10-*B2m*$^{-/-}$, in T cell-depleted WT mice (Figure 7). When mice with C1498-*B2m*$^{-/-}$ tumors were depleted of NK cells the antitumor effects at both the treated and distal tumor were severely abrogated. As these mice lack all T cells and B cells, the results demonstrate that the systemic, CDN-induced effects were mediated by NK cells independently of T cells (Fig 5D). In conclusion, i.t. CDN treatment induced NK activation within tumors and to some extent systemically, enhanced *ex vivo* NK killing capacity, and exerted antitumor effects on a distant tumor.

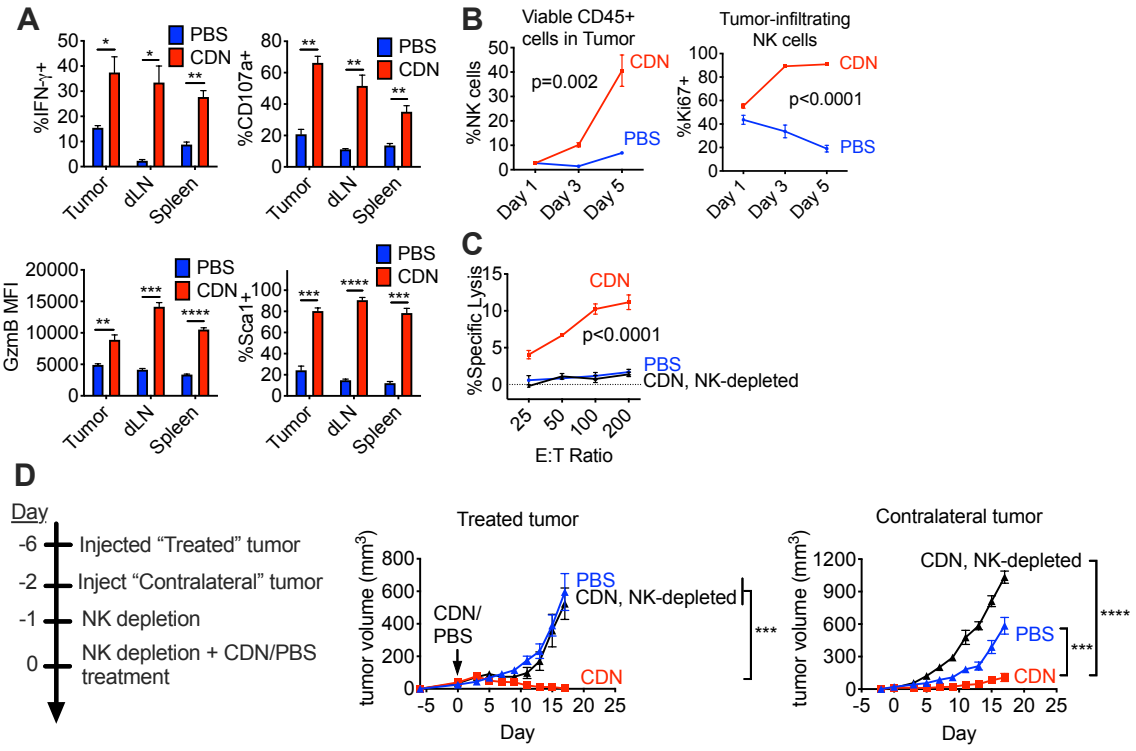

Fig. 5. Activation, proliferation and cytotoxicity of NK cells induced by CDN treatments of tumors. (**A**) RMA-*B2m*$^{-/-}$ tumors were established and treated as in Fig. 1B. 24 h later tumors, tumor-draining lymph nodes, and spleens were harvested and stained for flow cytometry. NK cells were gated as viable, CD45^{+}, CD3^{-}, CD19^{-}, F4/80^{-}, Ter119^{-}, NK1.1^{+}, NKp46^{+} cells. n=3. 2-tailed unpaired Student's t-tests with the Holm-Sidak method for multiple comparisons was used. *P<0.05; **P<0.01; ***P < 0.001, ****P<0.0001. Data are representative of 2 independent experiments. (**B**) RMA-*B2m*$^{-/-}$ tumors were established, treated, harvested, stained and analyzed on the days indicated. n=3. Data are representative of 2 independent experiments and analyzed with 2-way ANOVA. Error bars are shown but may be too small to see. (**C**) RMA-*B2m*$^{-/-}$ tumors were established and treated as in Fig. 1B. 24 h after treatment, splenocytes were harvested and identical groups were pooled. Some groups were NK-depleted (see Methods). Cytotoxicity against RMA-*B2m*$^{-/-}$ target cells was performed in technical triplicate and error bars are shown but are typically too small to see. Data (representative of two independent experiments) were analyzed by 2-way ANOVA. (**D**) Experimental schematic is shown. C1498-*B2m*$^{-/-}$ tumors were established in both flanks of *Rag2*$^{-/-}$ mice 4 days apart at a dose of 4x10^{6} cells each. One day after the second, "contralateral", tumor was injected, NK cells were depleted as in methods. NK cells were depleted again the next day and weekly thereafter. 6 days after the first, "Treated", tumor was injected it was treated with PBS or 50 μg CDN. Tumor growth at both sites was monitored and analyzed as described in Fig. 1B. Data (combined from two independent experiments) were analyzed by 2-way ANOVA. ***P < 0.001, ****P<0.0001. n=6-8.

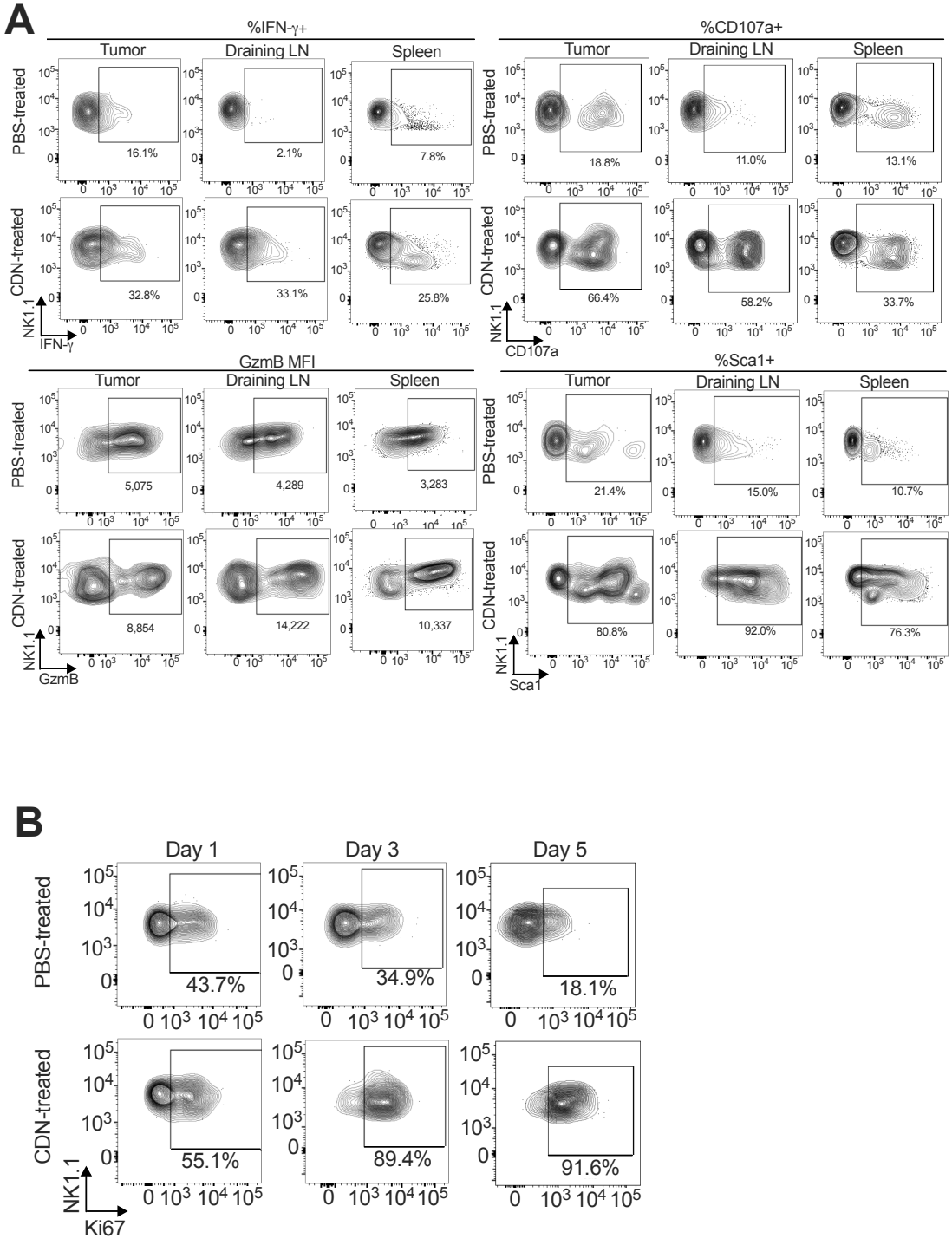

Fig. 6. (**A**) Representative flow plots for Figure 5A. (**B**) Representative flow plots for Figure 5B.

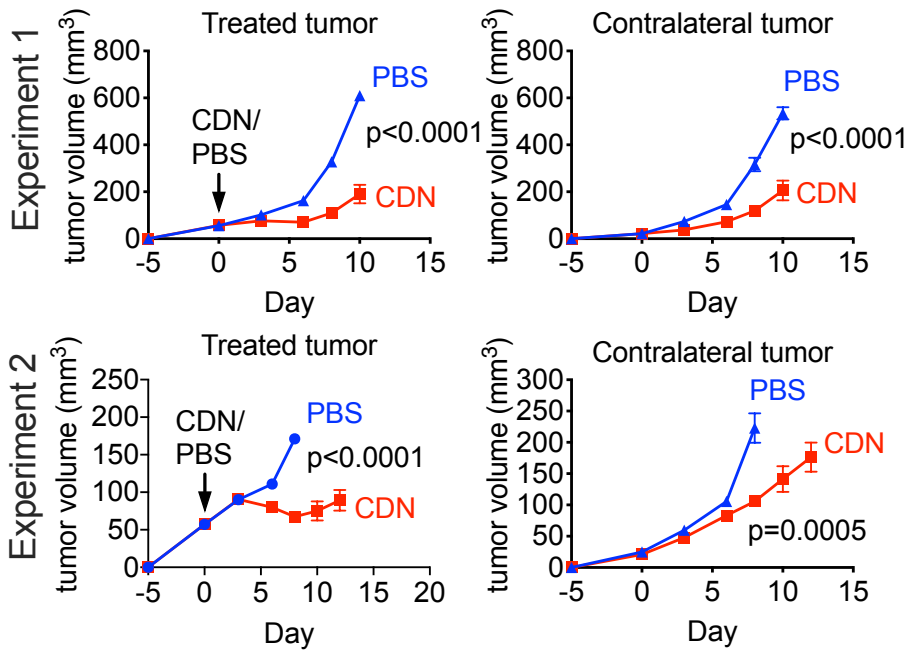

Fig. 7. Systemic T cell-independent antitumor effects of CDNs in B16-F10-*B2m*$^{-/-}$. Mice were CD4 and CD8-depleted and B16-F10-*B2m*$^{-/-}$ tumors were established in both flanks at different doses (4 x 10^6 for treated and 2 x 10^6 for distal). 5 days later one tumor was treated with PBS or 50 μg CDN and tumor growth at both sites was monitored and analyzed as described in Fig. 1B. (n=6 per group). Two individual experiments are shown.

NK cell activation and tumor rejection are dependent on type I interferon acting on host cells.

Consistent with the known role of STING activation in type I IFN production (Ishikawa et al., 2009), we observed a marked increase in *Ifnb1* transcripts within tumors 24 hours after CDN treatment compared to PBS-treated controls (Figure 8A). Serum of CDN-treated mice also contained high levels of IFNβ shortly after treatment (Figure 8B). These data are consistent with a recent study showing low but detectable circulating IFNβ in patients treated with CDNs combined with anti-PD-1 (Meric-Bernstam et al., 2019). The systemic anti-tumor effects reported in Figure 5 may be explained, at least in part, by the induction of significant levels of systemic IFNβ by local CDN treatments. NK cell activation was strongly dependent on type I IFN as CDN-treated *Ifnar1*$^{-/-}$ mice, which lack functional type I IFN receptors, did not display increases in IFN-γ, CD107a, Granzyme B, or Sca-1 in response to CDNs compared to WT controls (Figure 8C and 9). Similar results were obtained in the tumor-draining lymph nodes and spleens of WT mice injected with IFNAR1-blocking antibodies (Figure 10A and 10B). Furthermore, splenocytes from CDN-treated *Ifnar1*$^{-/-}$ mice, or WT mice given IFNAR1-blocking antibodies, were unable to kill RMA-*B2m*$^{-/-}$ tumor cells *ex vivo,* unlike splenocytes from CDN-treated WT mice (Figure 8D and 10C). Therefore, type I IFN action is essential for NK cell activation and deployment of effector functions after CDN injections.

In terms of tumor rejection, both MHC I-deficient tumor cell lines tested, RMA-*B2m*$^{-/-}$ and MC-38-*B2m*$^{-/-}$, were refractory to CDN therapy in *Ifnar1*$^{-/-}$ mice (Figure 8E). Knocking out *Ifnar1* in RMA-*B2m*$^{-/-}$ tumor cells had no effect on tumor rejection (Figure 10D), indicating that type I IFN action on host cells, rather than tumor cells, is necessary for the response. Importantly, IFNAR1 neutralization also abrogated the antitumor effects of CDN therapy for RMA-*B2m*$^{-/-}$ tumors (Figure 10E), suggesting that acute effects of CDN-induced type I IFN, rather than developmental or homeostatic effects, are key to the antitumor response. NK depletion combined with IFNAR1 blockade had no greater effect than either treatment alone in *Rag2*$^{-/-}$ mice (Figure 8F), supporting the conclusion that the NK-mediated antitumor activity is strongly dependent on type I IFN.

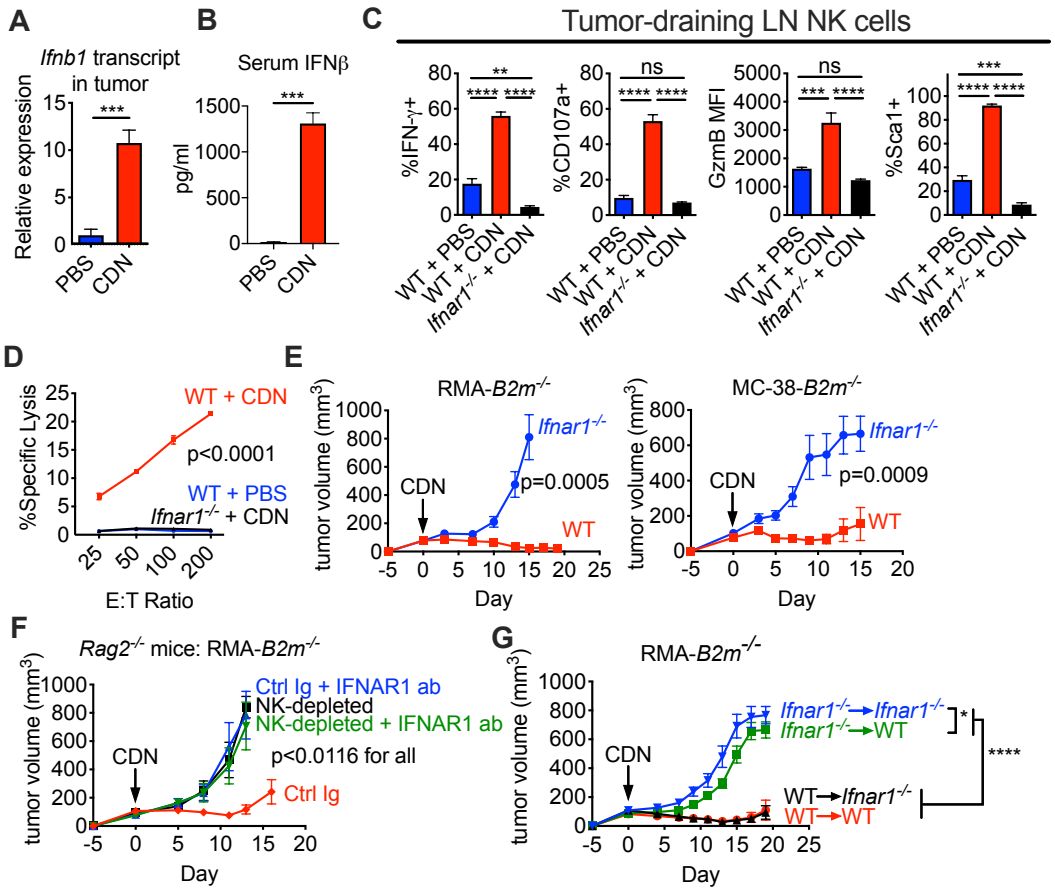

Fig. 8. Critical role for type I interferons in the NK-dependent tumor rejection response induced by CDNs. (**A**) RMA-*B2m*$^{-/-}$ tumors were established and treated as described in Fig. 1B. 24 hours later tumors were harvested, RNA extracted, and qRT-PCR performed to quantify *Ifnb1* transcripts. n=4. ***P < 0.001, as analyzed by 2-tailed unpaired Student's t-test. Data are representative of 2 independent experiments. (B) RMA-*B2m*$^{-/-}$ tumors were established and treated as described in Fig. 1B. 6 hours later serum was collected and IFNβ was quantified by ELISA. ***P<0.001. Data are combined from two independent experiments. n=8. (**C**) RMA-*B2m*$^{-/-}$ tumors were established and treated as described in Fig.1B. 24 h later tumor-draining lymph node cells were harvested for flow cytometry analysis as in Fig. 5A. n=5. **P<0.01; ***P < 0.001; ****P<0.0001, as analyzed by one-way ANOVA with Tukey's correction for multiple comparisons. Data are representative of 2 independent experiments. (**D**) Cytotoxicity of splenocytes from tumor-bearing, PBS or CDN-treated mice analyzed as in Fig. 5C. Data are representative of two independent experiments. Error bars are shown but are typically too small to see. (**E**) Tumors were established in C57BL/6J or *Ifnar1*$^{-/-}$ mice, treated, and analyzed as in Fig. 1B. n=5-6. Data are representative of two independent experiments. (**F**) RMA-*B2m*$^{-/-}$ tumors were established in *Rag2*$^{-/-}$ mice and treated and analyzed as in Fig. 1B. Some animals were depleted of NK cells and/or given IFNAR1 neutralizing antibody (see Methods). Data are representative of two independent experiments. **(G)** Bone marrow chimeras were established with the indicated donor → recipient combinations of C57BL/6J and *Ifnar1*$^{-/-}$ bone marrow (see Methods). Eight weeks later, RMA-*B2m*$^{-/-}$ tumors were established, treated, and analyzed as in Fig. 1B. n=8-12 per group.

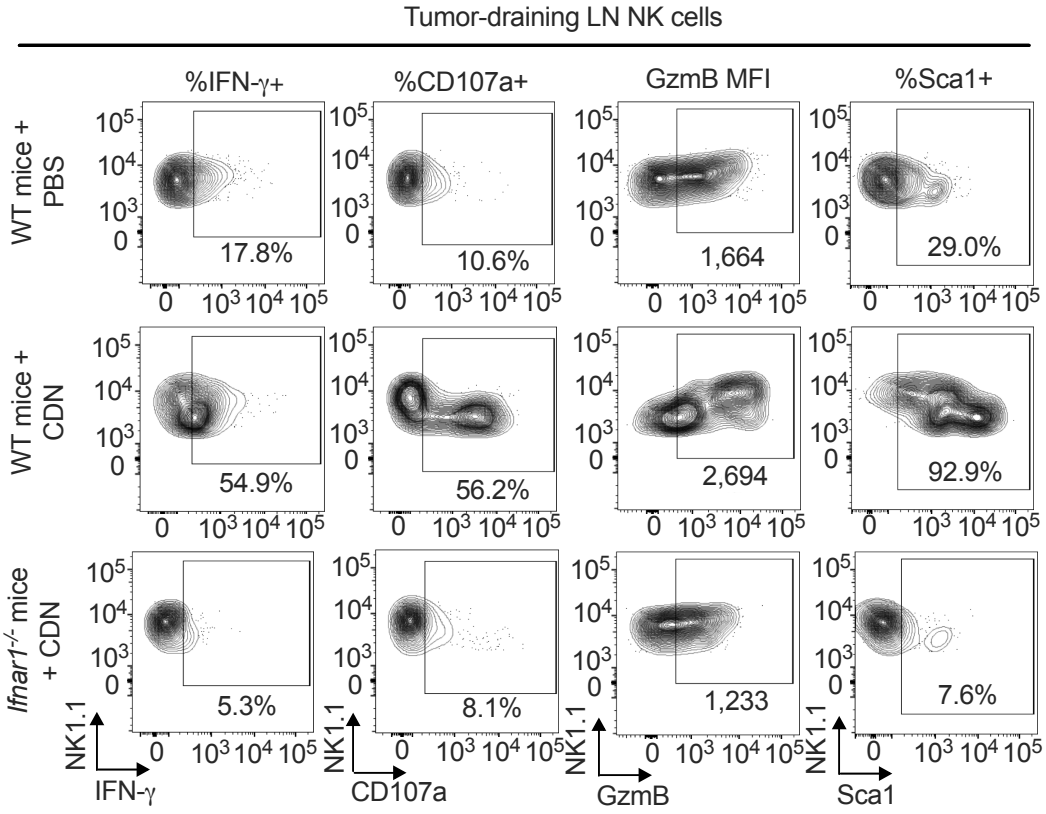

Fig. 9. Representative flow plots for Figure 8C.

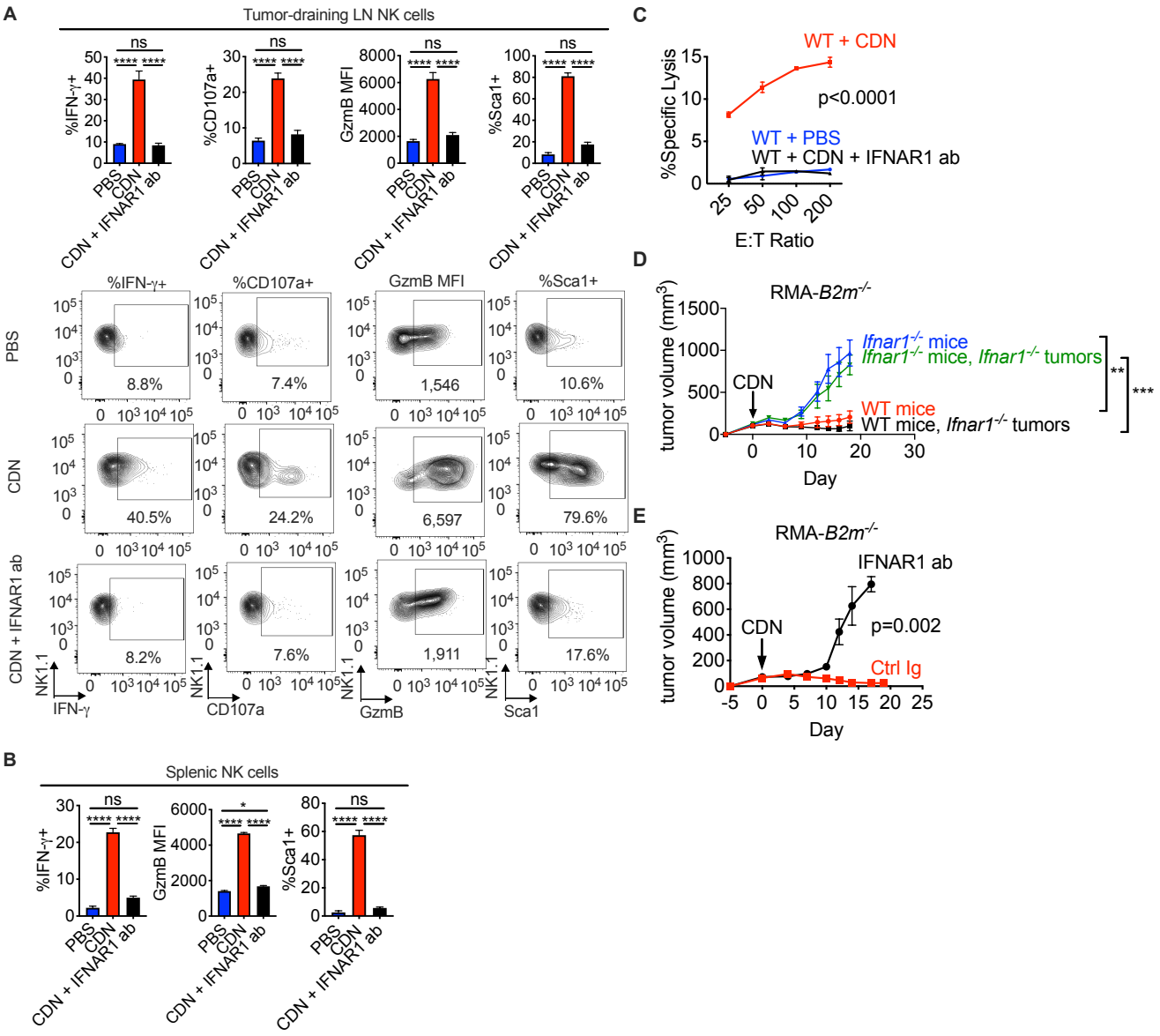

Fig. 10. IFNAR1-neutralization prevents CDN-induced NK cell activation, cytotoxicity, and tumor rejection. (A and B) IFNAR1-neutralization prevents CDN-induced NK cell activation. RMA-*B2m*$^{-/-}$ tumors were established and treated as described in Fig.1B. 24 h later tumor-draining lymph node cells (A), and spleens (B) were harvested for flow cytometry analysis as in Fig. 5A. One group received IFNAR1 neutralizing antibody or control Ig (see Methods). n=3-5. Data (representative of 2 independent experiments) analyzed by one-way ANOVA with Tukey's correction for multiple comparisons. *P < 0.05 ****P<0.0001. (C) IFNAR1-neutralization reduces CDN-induced cytotoxicity. Cytotoxicity of splenocytes from tumor-bearing PBS or CDN-treated mice analyzed as in Fig. 5C. Some mice injected with IFNAR1 neutralizing antibody (see Methods). Data shown are technical replicates and representative of two independent experiments. Error bars are shown but typically too small to see. (D) Host, and not tumor, IFNAR1 is necessary for the antitumor effects of CDNs. RMA-*B2m*$^{-/-}$ *Ifnar1*$^{-/-}$ tumor cells were generated using CRISPR-Cas9 and, along with RMA-*B2m*$^{-/-}$ tumors, were established, treated, and analyzed as in Fig. 1B. **P<0.01; ***P < 0.001. Data

combined from two independent experiments. n=10 (E) IFNAR1-neutralization prevents CDN-induced tumor rejection. RMA-*B2m*$^{-/-}$ tumors were established, treated, and analyzed as in Fig. 1B. Mice received IFNAR1 neutralizing antibody or control rat Ig. Data are representative of two independent experiments. n=4-5.

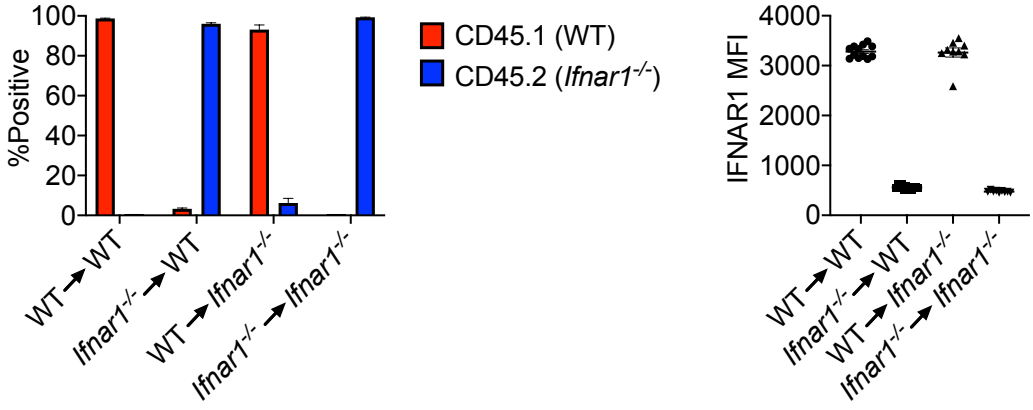

Fig. 11. Bone marrow chimera reconstitution efficiency for Figure 8G. Eight weeks after reconstitution, blood from bone marrow chimeras was collected, treated with ACK, and stained for flow cytometry. Percent of cells expressing either CD45.1 or CD45.2 are shown along with IFNAR1 MFI.

Type I IFN acts directly on NK cells to mediate the antitumor response.

We initially employed bone marrow chimeras between WT and *Ifnar1*$^{-/-}$ mice to address the cell types on which type I IFN acts to mediate NK-dependent antitumor responses. The chimeric mice, which showed near complete chimerism (Figure 11), were implanted with RMA-*B2m*$^{-/-}$ tumor cells, and the established tumors were subjected to CDN therapy i.t. Tumor rejection in *Ifnar1*$^{-/-}$ → *Ifnar1*$^{-/-}$ and *Ifnar1*$^{-/-}$ → WT chimeras was largely impaired compared to control chimeras, whereas WT → *Ifnar1*$^{-/-}$ chimeras behaved like WT → WT controls. These data argue that the action of type I IFN on hematopoietic cells is necessary and mostly sufficient for tumor rejection (Figure 8G). In this and another experiment, there were hints that type I IFN acting on radioresistant cells may play a minor role in the rejection response, such as the slight delay in tumor growth in *Ifnar1*$^{-/-}$ → WT chimeras compared to *Ifnar1*$^{-/-}$ → *Ifnar1*$^{-/-}$ chimeras in Figure 8G ($p=0.036$).

To examine if direct effects of type I IFN on NK cells were important for CDN-induced antitumor effects we employed *Ncr1-iCre, Ifnar1*$^{fl/fl}$ mice, in which *Ifnar1* expression is defective only in NK cells (Figure 12). *Ifnar1* deletion in NK cells was highly efficient (Figure 12). *In vivo*, *Ncr1-iCre, Ifnar1*$^{fl/fl}$ mice were unable to control tumor growth after CDN therapy and had reduced overall survival, indicating the importance of direct type I IFN action on NK cells for tumor rejection (Figure 13A). However, the defect in tumor control was not as substantial as in NK-depleted mice (Figure 13A) or as in *Ifnar1*$^{-/-}$ mice (Figure 13B), suggesting that type I IFN boosts NK-mediated tumor rejection in part by acting indirectly on non-NK cells. Furthermore, NK cells in the tumor-draining lymph nodes of CDN-treated *Ncr1-iCre, Ifnar1*$^{fl/fl}$ mice had decreased levels of IFN-γ, granzyme B, Sca-1, and CD107a (Figure 13C and 14), though they were not reduced to the control levels observed in *Ifnar1*$^{fl/fl}$ mice (no Cre) treated with PBS. We also observed that *Ifnar1* deletion specifically in NK cells resulted in a sharp reduction in CDN-induced cytotoxicity of splenocytes against RMA-*B2m*$^{-/-}$ tumor cells, though a very small amount of cytotoxicity may remain (Figure 13D). These data show that type I IFN acts directly on NK cells, but likely also acts on another cell type(s) to indirectly enhance NK cell activation.

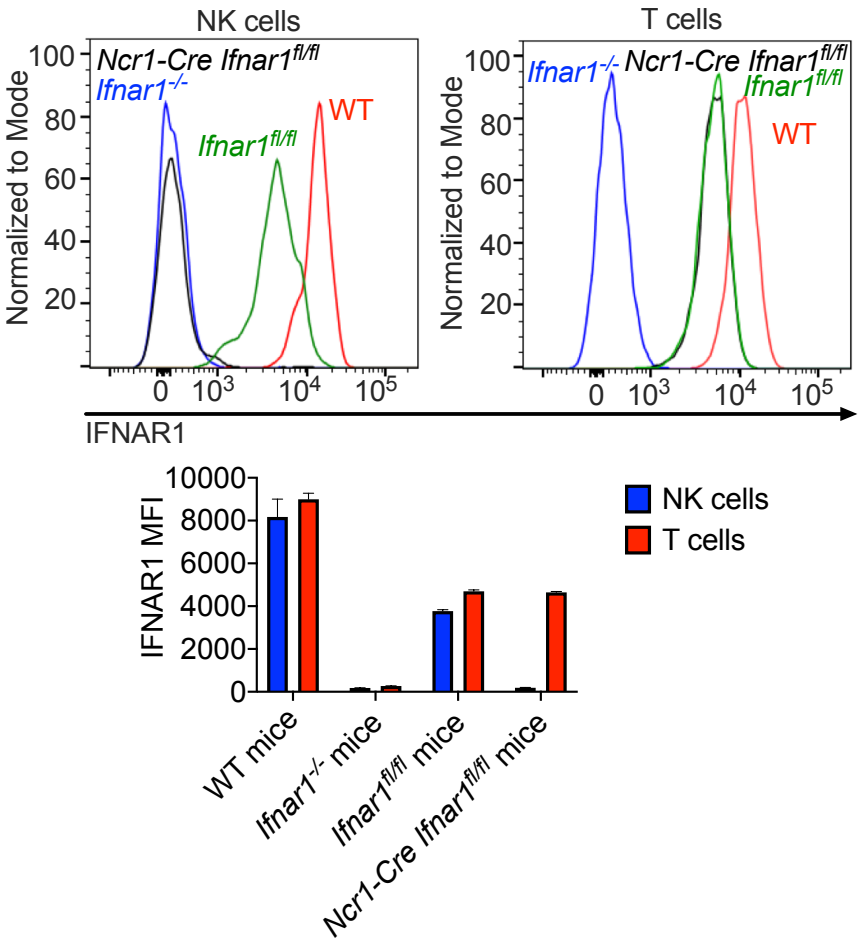

Fig. 12. NK cell and T cell IFNAR1 expression in *Ncr1-iCre, Ifnar1$^{fl/fl}$* mice. Representative histograms of IFNAR1 expression on NK cells and T cells are shown along with average MFI. Blood cells were ACK-treated. NK cells were gated as in Fig. 5A. T cells were gated as viable, CD19^{-}, NK1.1^{-}, CD3^{+} cells. n=6-7. Though IFNAR staining intensity was decreased on both NK cells and T cells from *Ifnar1$^{fl/fl}$* mice compared to WT mice, we observed no functional defects in antitumor responses in those mice.

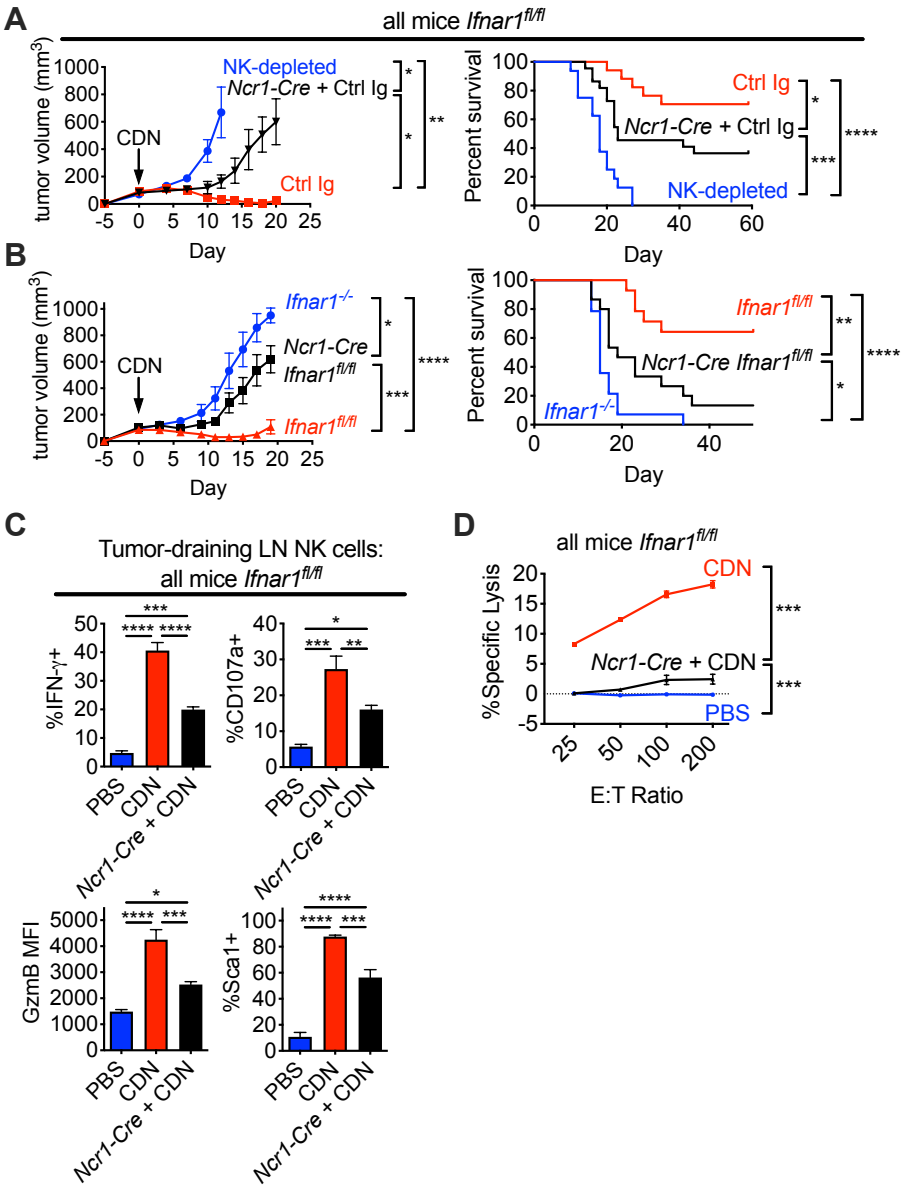

Fig. 13. Interferon acts directly on NK cells to mediate therapeutic effects of CDN treatments. (**A-B**) RMA-*B2m*$^{-/-}$ tumors were established in the indicated genotypes, treated, and analyzed as in Fig. 1B. NK-depletions were performed as in Methods. Data are representative of 2-3 independent experiments. n=4-8. Survival data is combined from 2-3 experiments (n=14-22 per group). (**C**) RMA-*B2m*$^{-/-}$ tumors were established in the indicated genotypes and treated as before. 24 h later tumor-draining lymph node cells were harvested for flow cytometry as in Fig. 5A. n=4-6. Data (representative of 2 independent experiments) were analyzed with one-way ANOVA with Tukey's correction for multiple comparisons. *P < 0.05; **P<0.01; ***P < 0.001; ****P<0.0001. (**D**) Cytotoxicity of splenocytes from tumor-bearing PBS or CDN-treated mice of the indicated genotypes analyzed as in Fig. 5C. Data are representative of two independent experiments. ***P < 0.001. Error bars are shown but are typically too small to see.

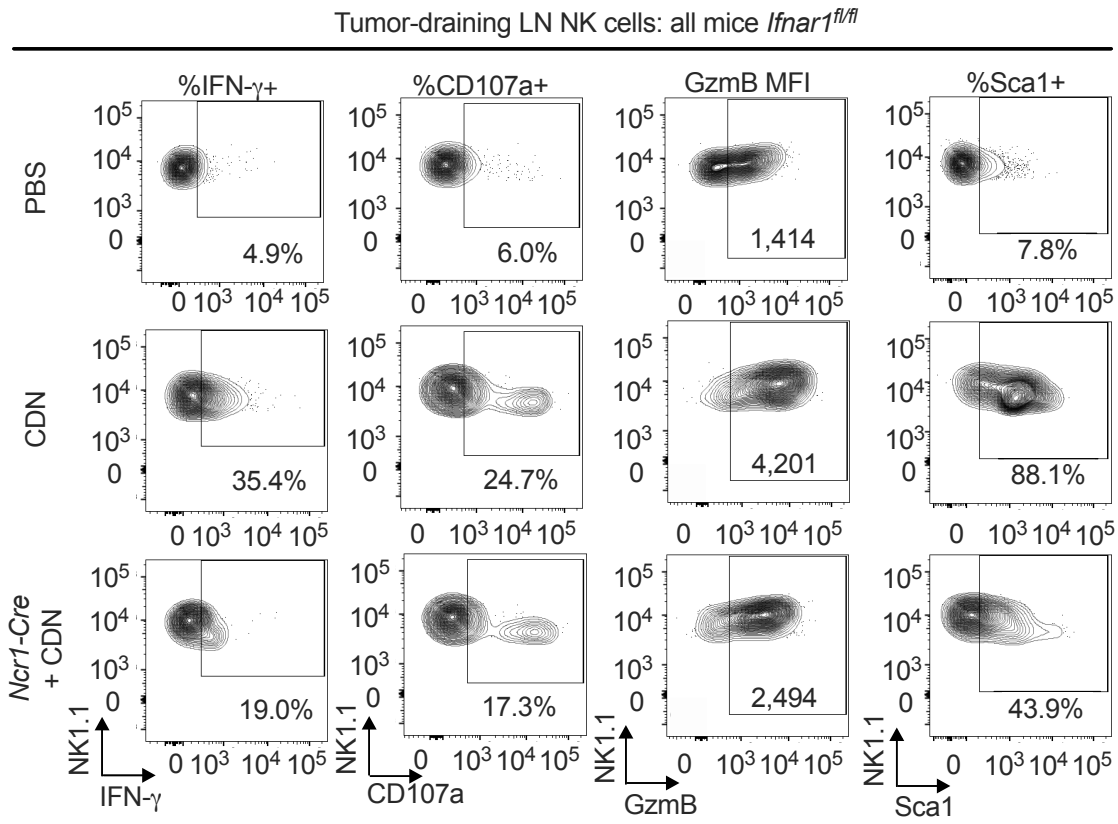

Fig. 14. Representative flow plots for Figure 13C.

CDN-induced type I IFN acts on DCs to boost NK cell activation and enhance antitumor effects.

Type I IFN is a key modulator of dendritic cell (DC) function, promoting maturation and immune stimulatory functions (Diamond et al., 2011; Montoya et al., 2002). We therefore hypothesized that CDN-induced type I IFN was acting in part on DCs, promoting NK cell effector function and enhanced tumor control. To determine if type I IFN-dependent DC activation was important for NK cell activation we employed *Cd11c-Cre, Ifnar1*$^{fl/fl}$ mice, in which *Ifnar1* undergoes deletion specifically in CD11c^{+} cells such as DCs (Figure 15). IFNAR1 expression was lost in most, but not all, CD11c^{+} MHC II^{+} cells in these mice (Figure 15). *Cd11c-Cre, Ifnar1*$^{fl/fl}$ mice exhibited a partial defect in tumor rejection compared to *Ifnar1*$^{fl/fl}$ (no Cre) control mice (Figure 16A), indicating a role for type I IFN acting on DCs. The defect was modest, however, in comparison to the defect in *Ifnar1*$^{-/-}$ mice or NK-depleted mice (Figure 16A), consistent with type I IFN action on other cells, such as NK cells as shown in Figure 13. Relative to NK cells in *Ifnar1*$^{fl/fl}$ (no Cre) control mice, NK cells in the tumor-draining lymph nodes of CDN-treated *Cd11c-Cre, Ifnar1*$^{fl/fl}$ mice had lower levels of IFN-γ, Granzyme B, and Sca-1 (Figure 16B and 17), indicating that type I IFN signaling on DCs is required for full NK cell activation. Again, however, the defect was only partial compared to PBS-treated control mice (Figure 16B). Degranulation (CD107a) levels were similar between the two groups, suggesting that for degranulation the direct action of type I IFN on NK cells may be more important than the indirect effects mediated by DCs. Splenocytes from CDN-treated *Cd11c-Cre, Ifnar1*$^{fl/fl}$ mice also showed a small but reproducible reduction in *ex vivo* cytotoxicity against RMA-*B2m*$^{-/-}$ tumor cells ($p=0.02$) (Figure 16C). Together, these data indicate that in CDN-treated tumors, type I IFN acts indirectly on DCs and directly on NK cells in promoting both NK cell activation and the rejection of tumors by NK cells.

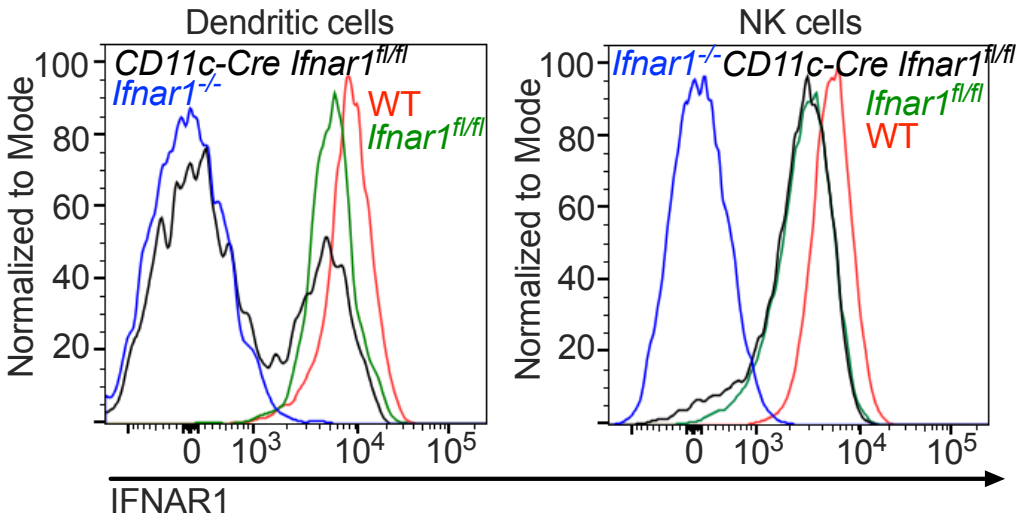

Fig. 15. IFNAR1 expression by DCs and NK cells in *CD11c-Cre, Ifnar1$^{fl/fl}$* mice. Representative histograms of IFNAR1 expression on DCs and NK cells. Splenocytes collected from the indicated genotypes and ACK-treated. DCs and NK cells gated as in Fig. 18B and Fig. 5A, respectively.

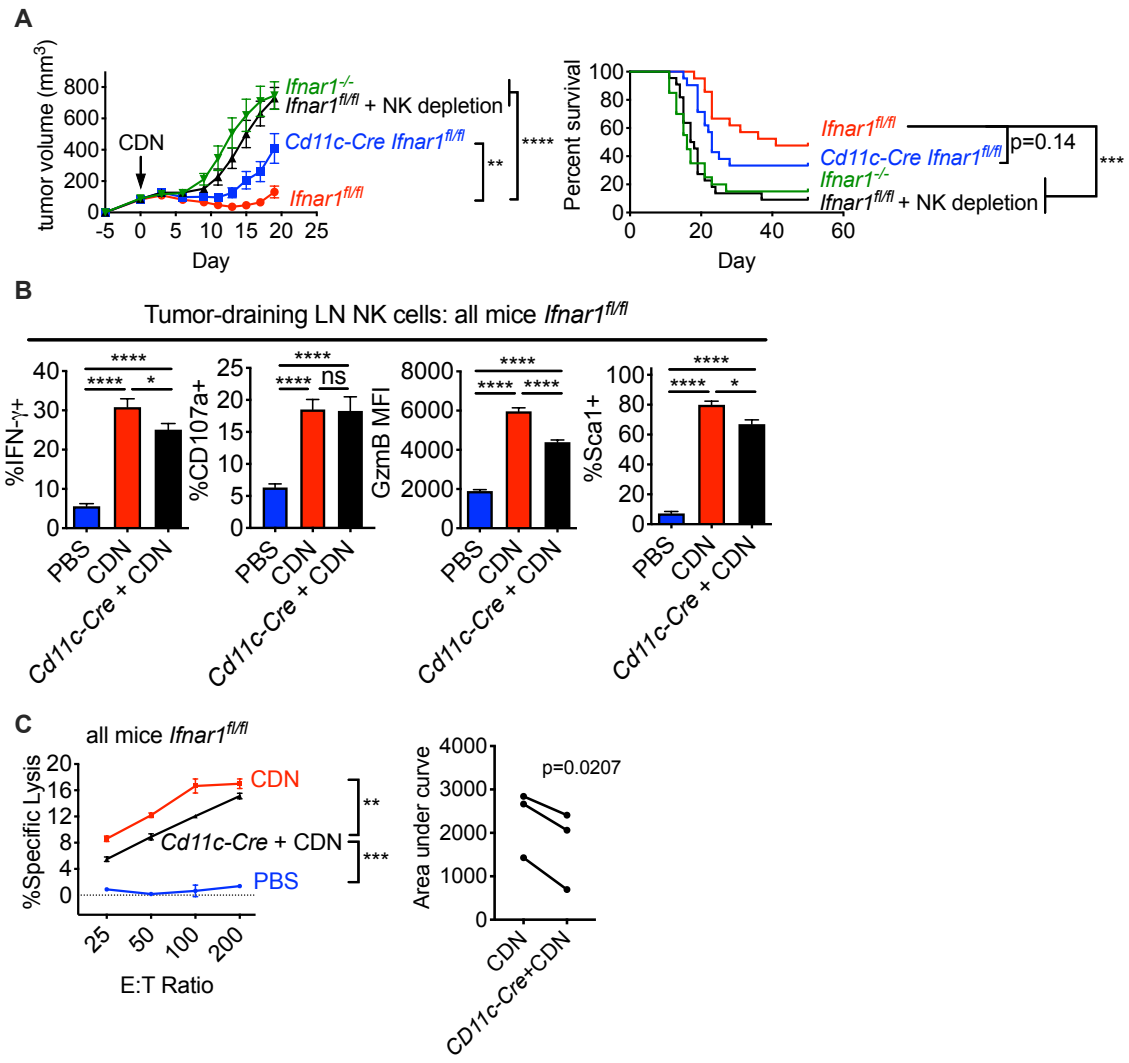

Fig. 16. Interferon acts on dendritic cells to enhance NK cell activation and tumor rejection induced by CDN therapy. (**A**) RMA-*B2m*$^{-/-}$ tumors were established in the indicated genotypes, treated, and analyzed as in Fig. 1B. NK-depletion was performed as in Methods. Tumor growth data are combined from 2 experiments (n=15-16 per group). Survival data are combined from 3 experiments (n=20-21 per group). **P<0.01; ***P < 0.001; ****P<0.0001. (**B**) RMA-*B2m*$^{-/-}$ tumors were established in the indicated genotypes and treated as before. 24 h later, flow cytometric analysis of tumor-draining LN NK cells was performed as in Fig. 5A. n=17-22. *P < 0.05; **P<0.01; ***P < 0.001; ****P<0.0001 as analyzed with one-way ANOVA tests with Tukey's correction for multiple comparisons or Kruskal-Wallis with Dunn's multiple comparisons test for nonparametric data. Data are combined from 4 independent experiments. (**C**) Cytotoxicity of splenocytes from tumor-bearing PBS or CDN-treated mice of the indicated genotypes were analyzed as in Fig. 5C. **P<0.01; ***P < 0.001. Error bars are shown but are typically too small to see. One experiment is shown in the left panel and the reduced killing from *Cd11c-Cre, Ifnar1*$^{fl/fl}$ splenocytes was confirmed in a total of 3 independent experiments where the areas under the cytotoxicity curves were compared using paired, 2-tailed Student's t-tests (right panel).

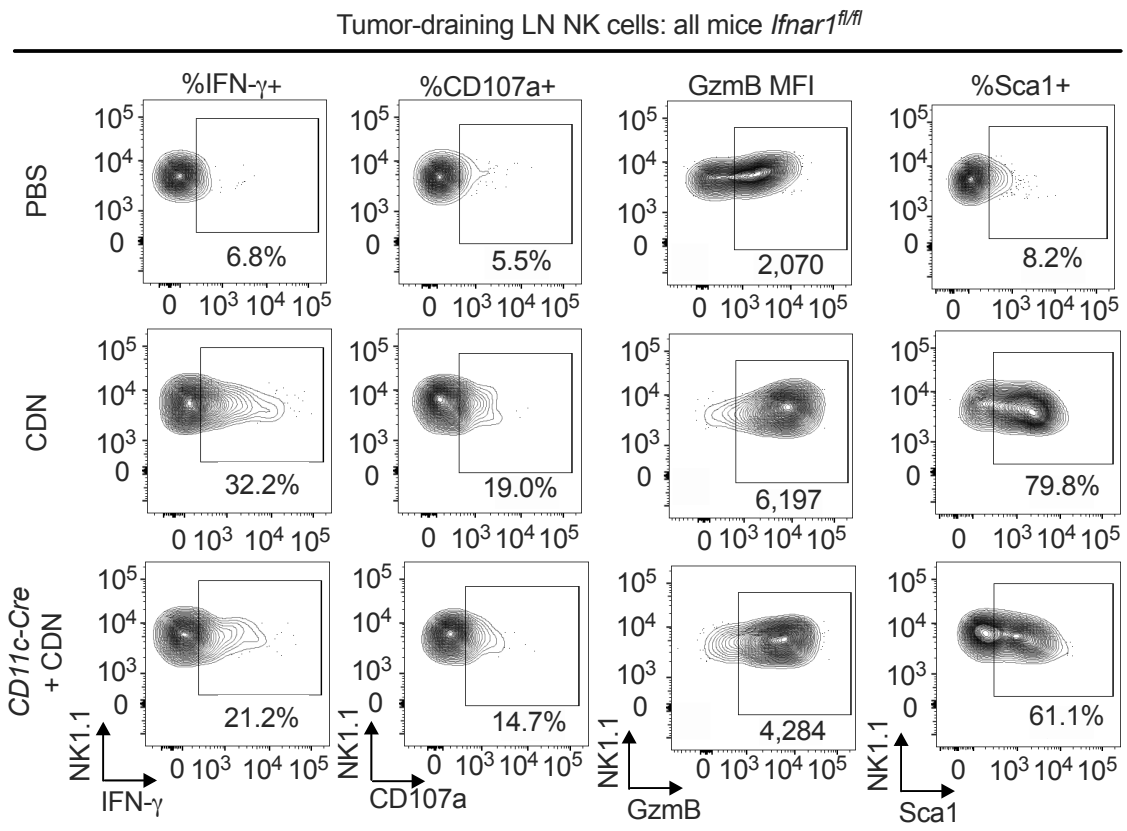

Fig. 17. Representative flow plots for Figure 16B.

IL-15 is induced by CDN injections, dependent on type I IFN, and is important for the antitumor response.

To address how type I IFN acts on DCs to enhance NK cell activation, we determined the impact of type I IFN on DC IL-15-IL-15Rα expression after CDN treatments. Unlike many cytokines, IL-15 is trans-presented to cells: it associates with the IL-15Rα chain during synthesis and the IL-15-IL-15Rα complex is presented to responding cells (Mortier et al., 2008), where it binds the IL-2/15Rβ chain leading to signaling by the common γ chain, γC . IL-15 signaling is especially important for NK cell biology as it enhances effector functions and promotes survival (Becknell and Caligiuri, 2005).

CDN-treated tumors had elevated levels of *Il15* and *Il15ra* transcripts relative to PBS-treated controls 24 hours after treatment (Figure 18A). In parallel, cell surface IL-15Rα expression was elevated in numerous cell types in the tumor-draining lymph node and spleen, including DCs, macrophages, monocytes, neutrophils, and interestingly, NK cells (Figure 18B and 19). IFNAR1 blockade during CDN treatment inhibited the induction of *Il15* and *Il15ra* transcripts in tumors, and cell surface IL-15Rα expression on the aforementioned cell types (Figures 18A, 7B, and 19). These data indicate that CDN treatment, mainly via the action of type I IFNs, induces IL-15/IL-15Rα expression on numerous cell types in the tumor microenvironment and systemically.

When IL-15 was neutralized during CDN treatment, NK cells in the tumor-draining lymph nodes had significantly reduced IFN-γ, CD107a, Granzyme B, and Sca-1 (Figure 18C and 20). In addition, neutralizing IL-15 caused a small but reproducible reduction in *ex vivo* cellular cytotoxicity ($p=0.03$) (Figure 18D). Finally, CDN-induced control of RMA-*B2m*$^{-/-}$ tumors was markedly diminished in mice given IL-15 neutralizing antibodies (Figure 18E). Overall, the data suggest that CDNs induce IL-15 production and presentation, potentially by multiple cell types, in a type I IFN-dependent manner. The IL-15 then acts to boost NK cell effector function and tumor killing capacity, leading to greater tumor control *in vivo*.

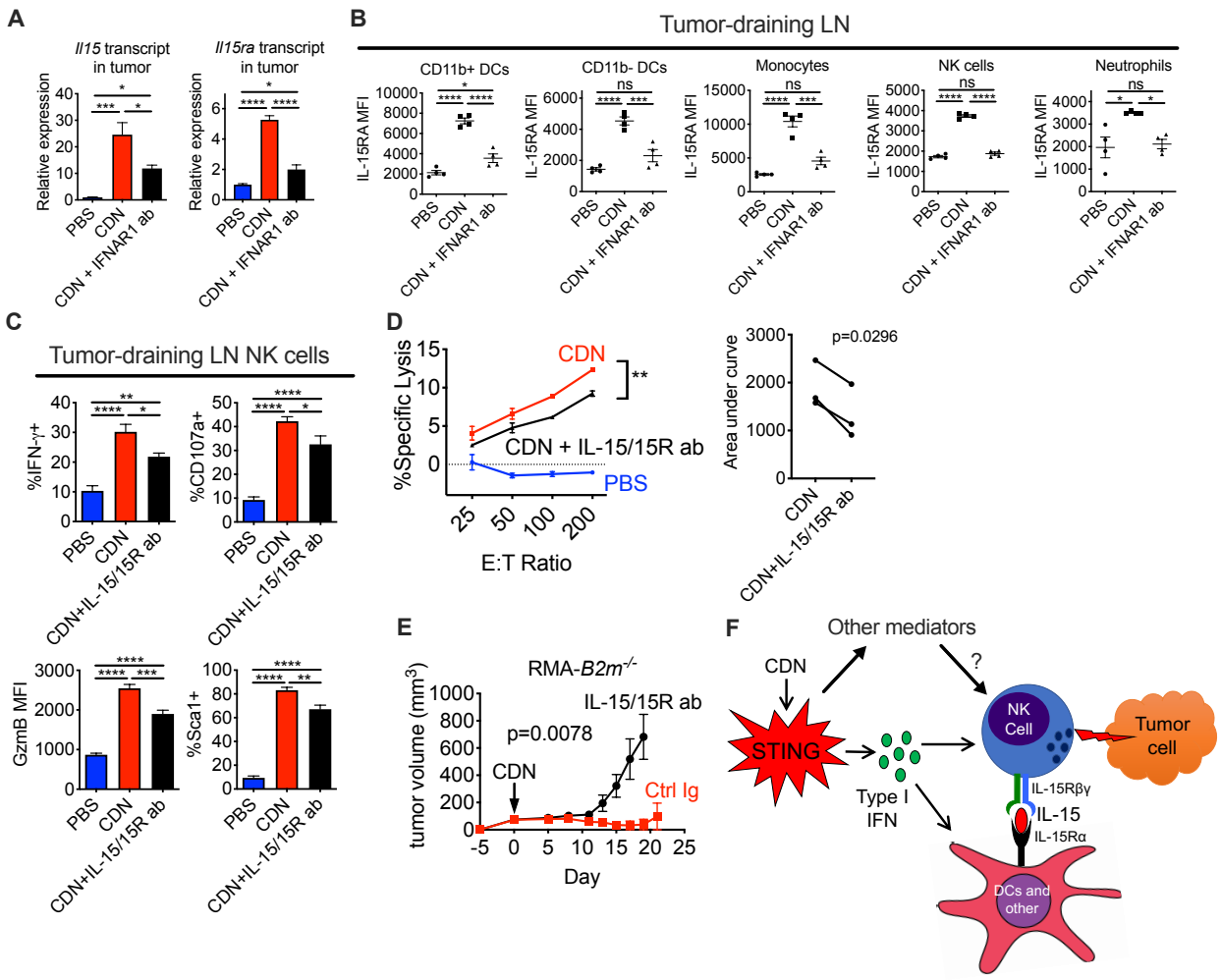

Fig. 18. IL-15/IL-15Rα expression is induced on DCs and other cells by interferons after CDN therapy and contributes significantly to optimal NK cell activation and tumor rejection.
(**A**) RMA-*B2m*$^{-/-}$ tumors were established, treated, RNA-extracted, and analyzed by qPCR for *Il15* or *Il15ra* transcripts as in Fig. 8A. Some mice received IFNAR1 neutralizing antibody (see Methods). n=4. Data (representative of 2 independent experiments) were analyzed with one-way ANOVA with Tukey's correction for multiple comparisons. (**B**) RMA-*B2m*$^{-/-}$ tumors were established and treated as before. 24 h later tumor-draining lymph node cells were harvested for flow cytometry as in Methods. The mean fluorescence intensity (MFI) of IL-15RA (BAF551) is displayed. Viable CD3^{-}, CD19^{-}, Ter119^{-} cells were further gated on DCs (NK1.1^{-}, Ly6G^{-}, CD11c^{high}, MHC-II^{high}), monocytes (NK1.1^{-}, Ly6G^{-}, CD11b^{high}, Ly6C^{high}), neutrophils (NK1.1^{-}, CD11b^{+}, Ly6G^{+}), NK cells (NK1.1^{+}), and macrophages (NK1.1^{-}, Ly6G^{-}, CD11b^{+}, F4/80^{+}). n=4. **P<0.01; ***P < 0.001; ****P<0.0001, as analyzed by one-way ANOVA with Tukey's correction for multiple comparisons. Data are representative of 2 independent experiments. (**C**) RMA-*B2m*$^{-/-}$ tumors were established, treated, and tumor-draining LN NKs were analyzed by flow cytometry as in Fig. 5A. Some mice received IL-15/IL-15R neutralizing antibody (see Methods). n=5. **P<0.01; ***P < 0.001; ****P<0.0001. Data (representative of 2 independent experiments) were analyzed with one-way ANOVA with Tukey's correction for multiple comparisons. (**D**) Cytotoxicity of splenocytes from tumor-bearing PBS or CDN-treated mice were analyzed as in Fig. 5C. Some mice received IL-15/IL-15R neutralizing antibody or control Ig (see Methods). **P<0.01. Error bars shown but typically too small to see. One experiment is shown in the left panel and the reduced killing from IL-15R neutralization was confirmed in a total of three independent experiments where the areas under the cytotoxicity curves were compare using paired, 2-tailed Student's t-tests (right panel). (**E**) RMA-*B2m*$^{-/-}$ tumors were established, treated, and

analyzed as in Fig. 1B. Mice received 5 μg IL-15/IL-15R antibody or control IgG (see Methods). n=5 per group. Data are representative of 2 independent experiments. (**F**) Model of CDN-induced NK cell activation. I.t. CDN treatment activates the STING pathway, resulting in production of type I IFN and other mediators including cytokines and chemokines, boosting NK cell effector functions and antitumor activities. Type I IFN elicits its effects on NK cells by direct action and indirectly via DCs, which upregulate IL-15/IL-15Rα complexes to enhance NK cell antitumor effects.

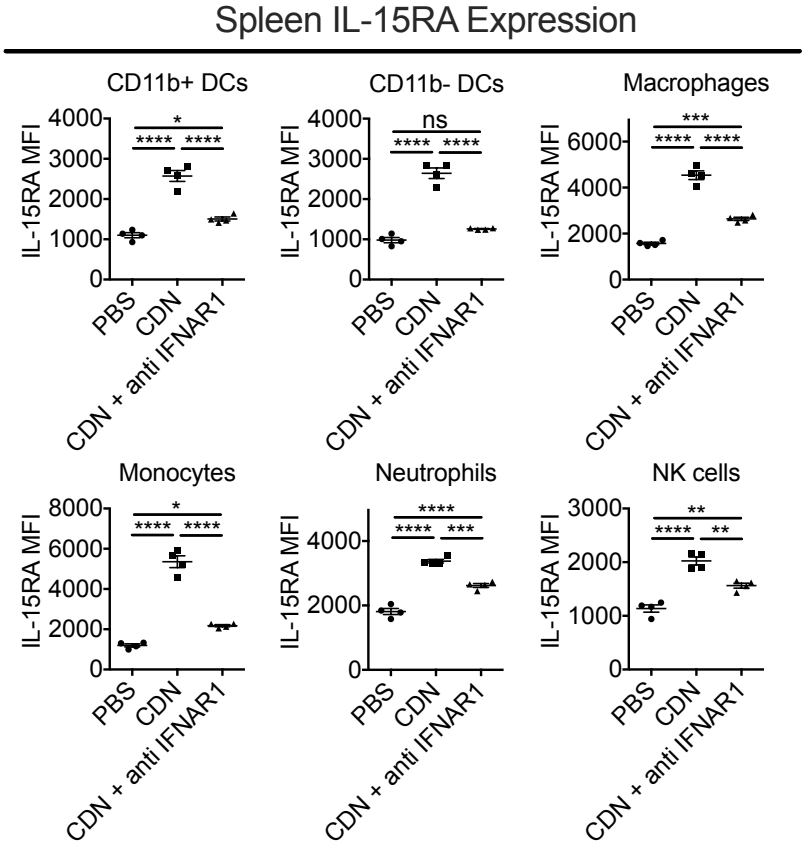

Fig. 19. IFNAR1-neutralization reduces CDN-induced IL-15RA expression in the spleen. RMA-*B2m*$^{-/-}$ tumors were established and treated as in Fig. 1B. One group of CDN-treated mice received IFNAR1 neutralizing antibody. 24 h later splenocytes were harvested, ACK-treated, and stained for flow cytometry as in Methods. The MFI is displayed. DCs, monocytes, neutrophils, NK cells, and macrophages were gated as in Fig. 18B. n=4. Data (representative of 2 independent experiments) were analyzed by one-way ANOVA with Tukey's correction for multiple comparisons. *P<0.05; **P<0.01; ***P < 0.001; ****P<0.0001.

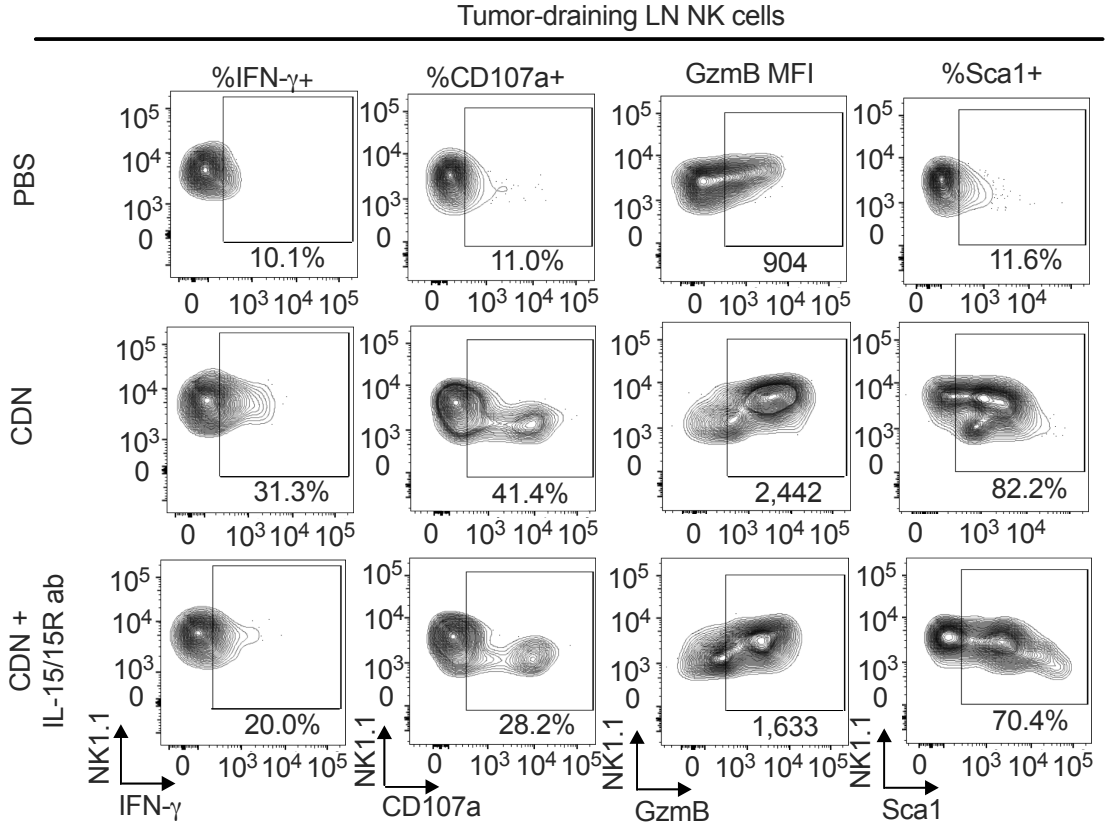

Fig. 20. Representative flow plots for Figure 18C.

NK cells promote their antitumor effects independently of perforin, Fas, IFN-γ, and TNF-α.

Up to this point, this study has mainly focused on the mechanisms of NK cell activation and NK cell-mediated clearance of MHC I-deficient tumors induced by CDN treatments. A remaining question is how do CDN-activated NK cells actually kill tumor cells? A major mechanism of NK cell cytotoxicity is through the release of granules containing perforin and a group of serine proteases, known as granzymes. Upon target recognition the granules are released into the intercellular space where perforin generates transmembrane pores that are necessary for granzymes to enter the target cell. Once inside, granzymes initiate cellular death mechanisms, such as apoptosis (Voskoboinik et al., 2006). Perforin is therefore crucial for granzyme-mediated killing. NK cells and T cells from perforin-deficient mice have severely impaired killing ability and these mice are unable to clear viral infections and have diminished antitumor responses (Kagi et al., 1994).

To test the role of perforin in NK-mediated, CDN-induced clearance of tumors, independently of T cells, we generated *Rag2*$^{-/-}$*Prf1*$^{-/-}$ double knockout mice. Interestingly, in a preliminary experiment, *Rag2*$^{-/-}$*Prf1*$^{-/-}$ mice showed no significant impairment in CDN-induced antitumor responses compared to *Rag2*$^{-/-}$ mice (Figure 21A). NK cell-depletion of *Rag2*$^{-/-}$*Prf1*$^{-/-}$ mice resulted in accelerated tumor growth comparable to the rate of tumor growth in *Rag2*$^{-/-}$ *Il2rg*$^{-/-}$ mice, which lack NK cells (Figure 21A). These data suggest that NK cells mediate most or all of their antitumor effects in the absence of perforin.

In addition to killing via perforin/granzyme exocytosis, activated NK cells produce IFN-γ which is known to have important antitumor functions (Ikeda et al., 2002), and the data in Figure 5 showed that CDN-treatments induced IFN-γ production by NK cells. To test the role of IFN-γ in CDN-induced, NK cell-mediated antitumor responses we injected IFN-γ neutralizing antibodies during CDN treatment in *Rag2*$^{-/-}$ mice. IFN-γ neutralizing produced a small, but insignificant, effect on tumor growth compared to control Ig-treated mice whereas NK-depletion had a much larger effect (Figure 21B). These data indicate that NK cell mediated antitumor functions occur largely independently of IFN-γ.

Activated NK cells can also kill tumors via upregulation of death receptor molecules, such as FASL and TRAIL (Smyth et al., 2005). RMA-*B2m*$^{-/-}$ tumor cells express the FAS death receptor but do not express detectable levels of TRAIL's ligand, DR5 (Figure 22A and 22B). MC-38 cells, which express DR5 (Haynes et al., 2010), were used as a staining control. To test the role of Fas, we generated *Fas*$^{-/-}$ RMA-*B2m*$^{-/-}$ tumor cells using CRISPR-Cas9 (Figure 22A). Knowing that there may be redundancy in killing mechanisms we compared RMA-*B2m*$^{-/-}$ and RMA-*B2m*$^{-/-}$*Fas*$^{-/-}$ tumor rejection in *Rag2*$^{-/-}$*Prf1*$^{-/-}$ mice. Interestingly, in a preliminary experiment, deficiency of FAS on the tumor cells only had a minor, insignificant, effect on CDN-induced antitumor responses (Figure 21C), suggesting that death receptors do not play a major role in tumor rejection in this model. Preliminarily, neutralization of IFN-γ during CDN-treatment of RMA-*B2m*$^{-/-}$*Fas*$^{-/-}$ tumors also had a small effect, which was significant when compared to RMA-*B2m*$^{-/-}$ tumors (Figure 21C), suggesting that Fas and IFN-γ may each make minor contributions to tumor rejection. However, tumor growth was still faster in *Rag2*$^{-/-}$*Il2rg*$^{-/-}$ mice (Figure 21C), suggesting that NK cells exert significant antitumor activity independent of perforin, Fas, and IFN-γ.

Activated NK cells also make TNF-α, which has long been known to have antitumor effects (Balkwill, 2009), and tumor-infiltrating NK cells in CDN-treated mice produce more TNF-α than in PBS-treated mice (Figure 21D). In a preliminary analysis, we first examined the role of TNF-α in tumor rejection using neutralizing antibodies against TNF-α in RMA-*B2m*$^{-/-}$ *Fas*$^{-/-}$ tumor-bearing *Rag2*$^{-/-}$*Prf1*$^{-/-}$ mice. TNF-α neutralization had a large impact on tumor rejection, causing tumors to grow out similarly to NK-deficient *Rag2*$^{-/-}$*Il2rg*$^{-/-}$ mice (Figure 21C). Furthermore, NK cells were less activated in CDN-treated TNFR1/2 dKO mice than in WT mice (Figure 21E), suggesting that TNF-α may mediate antitumor effects partly by promoting NK cell responses. Interestingly, NK cells in CDN-treated TNFR1/2 dKO mice had much higher expression of NKp46 compared to both PBS-treated and CDN-treated WT mice (Figure 21E). The reason for this is unclear. One hypothesis is that TNF-α acts directly on NK cells to limit NKp46 surface expression. Another hypothesis would be that a ligand for NKp46 is expressed in WT mice and not in TNFR1/2 dKO mice, and ligand engagement in WT mice causes NKp46 downregulation on NK cells. This would be analogous in some respects to what has been shown for NKG2D, where expression of NKG2D ligands on normal cells causes NKG2D downregulation (Thompson et al., 2017).

RMA-*B2m*$^{-/-}$ cells also express TNF receptors and even though a significant portion of the antitumor effects of TNF-α are due to action on host cells (Figure 2B and 2C), it remained possible that TNF-α also acts directly on tumors. In a preliminary study to examine the role of TNF-α on tumor cells we generated *Tnfrsf1a*$^{-/-}$*Tnfrsf1b*$^{-/-}$ (TNFR1/2 dKO) RMA-*B2m*$^{-/-}$ cells using CRISPR-Cas9 (Figure 22C). We assessed CDN-induced tumor clearance of TNFR1/2 dKO vs TNFR^{+} RMA-*B2m*$^{-/-}$ tumors in CD4+CD8-depleted TNFR1/2 dKO mice, so as to limit our observations to TNF-α's action on tumors and not host cells. Unexpectedly, TNFR1/2 dKO tumors were rejected better than the parental RMA-*B2m*$^{-/-}$ tumors (Figure 21F). Rejection was dependent on NK cells, as tumors in NK-depleted mice grew out much faster (Figure 21F). Furthermore, there was no difference between parental RMA-*B2m*$^{-/-}$ and TNFR1/2 dKO RMA-*B2m*$^{-/-}$ tumor growth in mice lacking CD4/CD8 T cells and NK cells (Figure 21F), indicating that loss of TNF receptors on tumors does not intrinsically affect tumor growth in the absence of these cells and that the difference in rejection is NK cell-dependent. Similar results were seen in *Rag2*$^{-/-}$*Prf1*$^{-/-}$ mice (Figure 21G), as loss of TNF receptors on tumors enhanced tumor rejection. These data show that TNF-α is produced by NK cells after CDN treatments and helps boost NK cell activation. However, TNF-α is not necessary for NK cell-mediated antitumor effects and interestingly, appears to actually promote tumor growth and/or survival, an effect that was completely abrogated upon NK cell depletion, suggesting that TNF-α acts on tumors to protect them from NK-mediated, perforin-independent killing.

Overall these data show that NK cells mediate significant antitumor responses independently of several "classic" NK cell antitumor effector functions, such as release of cytotoxic granules, death receptor expression, and secretion of IFN-γ and TNF-α.

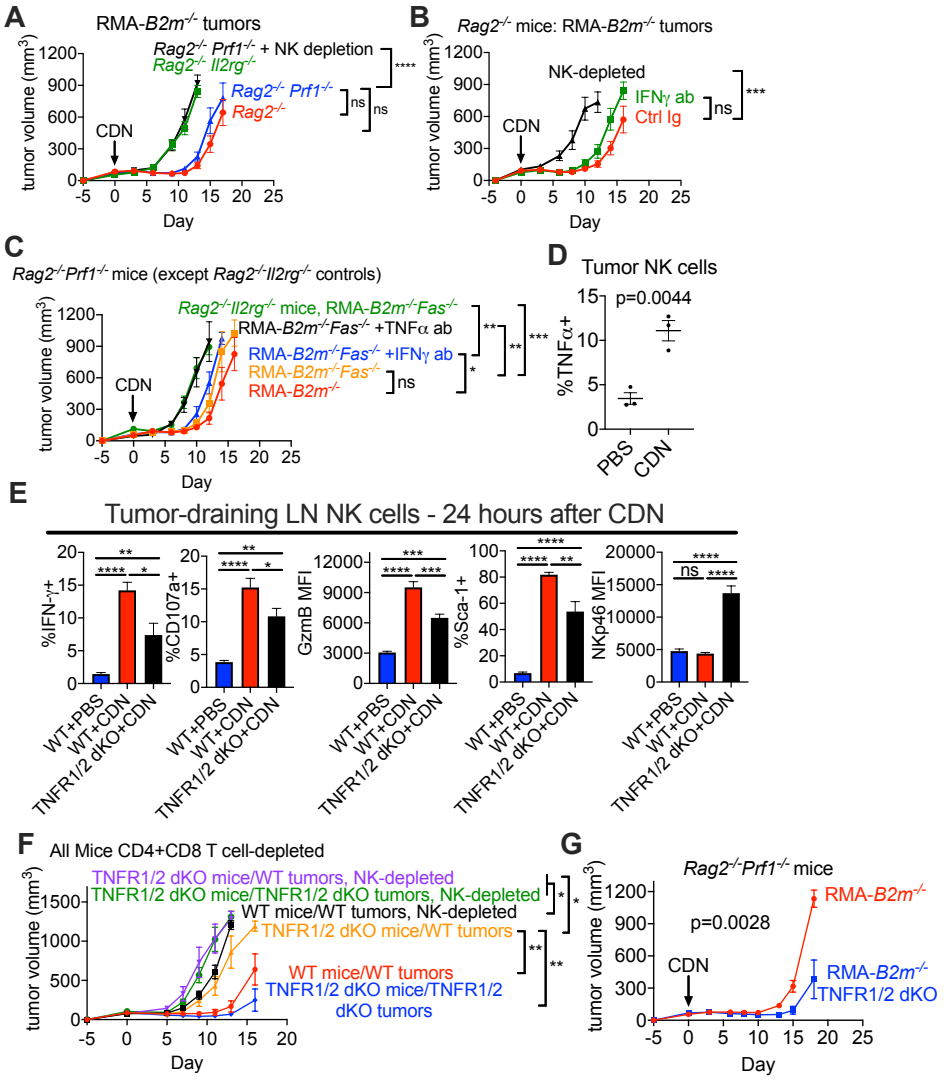

Fig. 21. NK cells elicit their antitumor effects independently of perforin, Fas signaling, IFN-γ, and TNF-α. (A-C) RMA-*B2m*$^{-/-}$ (A-C) or RMA-*B2m*$^{-/-}$*Fas*$^{-/-}$ (C) tumors were established in *Rag2*$^{-/-}$ (A and B), *Rag2*$^{-/-}$*Prf1*$^{-/-}$ (C), or *Rag2*$^{-/-}$*Il2rg*$^{-/-}$ (A and C) mice, treated, and analyzed as in Fig. 1B. For figure C, 2.5 x 10^6 cells were injected. For A and B, NK cells were depleted as in methods. Neutralizing antibodies for IFN-γ (B and C) or TNF-α (C) were used as described in methods. N=5-9 for all tumor growth experiments. **(D)** RMA-*B2m*$^{-/-}$ tumors were established and treated as is in Figure 21D. 72 hours later tumors were harvested, stained, and NK cells analyzed by flow cytometry as in Figure 5A. n=3. **(E)** RMA-*B2m*$^{-/-}$ tumors were established in WT or TNFR1/2 dKO mice and treated with PBS or CDN. 24 hours later tumor-draining LN NKs were analyzed by flow cytometry as in Figure 5A. n=5. **(F-G)** RMA-*B2m*$^{-/-}$ or RMA-*B2m*$^{-/-}$*Tnfrsf1a*$^{-/-}$*Tnfrsf1b*$^{-/-}$ tumors were established in WT (F), TNFR1/2 dKO (F), or *Rag2*$^{-/-}$*Prf1*$^{-/-}$ mice, treated, and analyzed as in Fig. 1B. In Figure F, all animals were depleted of CD4 and CD8 T cells as in methods. N=4-7 for F and n=5 for G. *P<0.05; **P<0.01; ***P < 0.001; ****P<0.0001. Panel B is representative of two independent experiments. Panels A and C-G are preliminary and have only been done once.

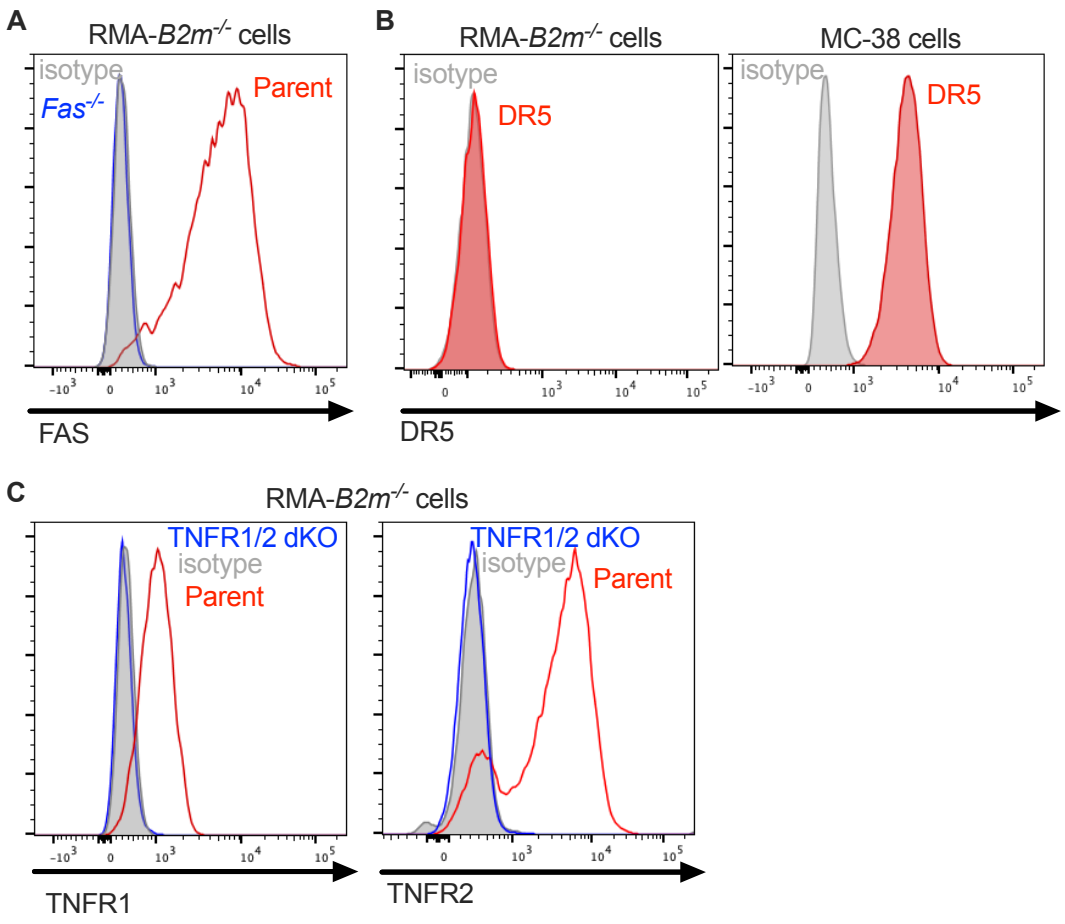

Fig. 22. Death receptor expression on RMA-*B2m*$^{-/-}$ tumor cells. RMA-*B2m*$^{-/-}$(A-C), RMA-*B2m*$^{-/-}$ *Fas*$^{-/-}$ (A), MC-38 (B), or TNFR1/2 dKO (*Tnfrsf1a*$^{-/-}$*Tnfrsf1b*$^{-/-}$) (C) cells were stained with anti-Fas (A), anti-DR5 (B), anti-TNFR1 (C), anti-TNFR2 (C), or isotype control (A-C), followed by flow cytometry.

Discussion

The immunotherapeutic potential of NK cells for cancer, including solid cancers, has not been fully established. Our data demonstrate therapy-induced NK cell-dependent long-term remissions of several types of transplanted MHC I-deficient, CD8 T cell-resistant, solid tumors. Importantly, the impressive impact of NK-dependent antitumor responses was not limited to MHC I-deficient tumors, but also occurred in MHC I-high MC-38 tumors in *Rag2*$^{-/-}$ mice, with some mice exhibiting long-term remissions. Like many tumor lines, MC-38 cells express abundant NKG2D ligands and these cells are killed efficiently by NK cells *in vitro* (Jamieson et al., 2002), despite the high MHC I expression. It is likely that the key attribute predicting favorable NK-dependent effects induced by CDNs or other NK-mobilizing therapeutics is not solely MHC I-deficiency but rather the overall sensitivity of the cells to NK cell killing, which reflects a balance of activating and inhibitory interactions (Raulet and Vance, 2006).

Considering that most tumor cells express NKG2D ligands (Diefenbach et al., 2000) or other ligands that activate NK cells (Moretta et al., 2001), and are sensitive to NK killing *in vitro*, therapies that amplify NK cell activity have the potential to show efficacy in a broad variety of cancers, including many that are resistant to destruction by T cells. We propose that such therapies will complement therapies that mobilize T cell responses, including checkpoint therapies, by eliminating variants with antigen presentation defects. Therapeutic mobilization of NK cells may be especially important for tumors that lack strong T cell epitopes or have lost MHC expression, as well as for combining with therapeutic antibodies that mediate antibody-dependent cellular cytotoxicity mediated by NK cells.

STING-agonists have shown dramatic efficacy in preclinical cancer models and are currently being tested in clinical trials. Most studies have focused on T cell-mediated responses induced by CDNs (Corrales et al., 2015; Demaria et al., 2015; Sivick et al., 2018). In the present study we demonstrated that intratumoral injection of CDNs triggered potent, NK-dependent, and CD8-independent rejection of several different NK-sensitive tumors originating from multiple tissue types. Notably, CDN injection triggered complete tumor rejection and long-term survival in a portion of the mice in most of the models tested.

Some of our studies utilized *B2m*$^{-/-}$ tumor cells, which lack MHC I, and are therefore more sensitive to NK cells because they fail to engage inhibitory KIR (or Ly49 in mice) (Karlhofer et al., 1992; Moretta et al., 1996). These models are potentially clinically relevant as many human tumors exhibit at least a partial loss of surface MHC I (Garrido et al., 2016; McGranahan et al., 2017; Roemer et al., 2016). Furthermore, resistance to checkpoint blockade correlates with absence of tumor MHC I expression, with *B2M* mutations found among the non-responding patient tumors (Rodig et al., 2018; Sade-Feldman et al., 2017; Zaretsky et al., 2016). Other cancers, such as classical Hodgkin's Lymphoma, generally have very low MHC I. The efficacy of PD-1 blockade in Hodgkin's lymphoma (Roemer et al., 2016) may possibly be due to the activity of NK cells, given that NK cells express functional PD-1 in mouse tumor models (Hsu et al., 2018).

Our results demonstrate that the CDN-induced, NK-mediated antitumor effects were dependent on type I IFN. A hallmark of STING activation is production of type I IFN and many

cell types, including both hematopoietic and nonhematopoietic cells, produce it in response to STING activation in tumors, including DCs, macrophages, monocytes, and endothelial cells. It has been shown that cells in each of these compartments can contribute to the antitumor effects of intratumoral CDN injection (Demaria et al., 2015; Francica et al., 2018; Sivick et al., 2018; Yang et al., 2019). Type I IFN enhances T cell responses (Diamond et al., 2011) and is important for cancer immunosurveillance and the efficacy of cancer immunotherapies (Dunn et al., 2006; Swann et al., 2007; Zitvogel et al., 2015). Type I IFN is also important for NK cell biology (Swann et al., 2007) and NK cells from *Ifnar1*$^{-/-}$ mice have greatly reduced cytotoxicity against tumor cell lines *in vitro* (Swann et al., 2007). Less clear is how type I IFN exerts its effects on NK cells, with reports of both direct and indirect action. Consistent with direct action, mice lacking type I IFN signaling specifically in NK cells had reduced *in vitro* cytotoxicity against tumor cell lines (Mizutani et al., 2012). However, that study failed to find a survival difference between *Ncr1-iCre, Ifnar1*$^{fl/fl}$ and *Ifnar1*$^{fl/fl}$ control mice after exposure to oncogenic Abelson murine leukemia virus, leaving it unclear whether type I IFN acts directly on NK cells in the antitumor response.

Other reports have highlighted the importance of indirect action of type I IFN on NK cells, particularly cells of the myeloid lineage. DCs regulate NK cells both through direct interactions and the release of cytokines, such as IL-12, IL-15, and IL-18 (Degli-Esposti and Smyth, 2005). IL-15 is especially important for NK cell survival and homeostasis, and is known to promote NK cell proliferation and effector activity (Koka et al., 2004; Mortier et al., 2008). Mice lacking IL-15 presentation in either LysM or CD11c-expressing cells exhibited significant defects in NK cell homeostasis and activation (Mortier et al., 2009). Type I IFN induces IL-15 production and presentation by DCs (Degli-Esposti and Smyth, 2005; Lucas et al., 2007) and it has been observed that IL-15 trans-presenting-DCs are required for type I IFN-dependent "priming" of NK cells *in vivo* by TLR agonists or infections for enhanced *ex vivo* stimulation assays (Lucas et al., 2007).

While informative, these studies conflicted in how type I IFN stimulates NK cells, and the role of type I IFN for NK cell-mediated tumor control *in vivo* remained unclear. Our findings provide clarity by indicating that both direct action of type I IFN and indirect action, via IL-15, are important for maximum NK cell antitumor activity *in vivo*. Our studies suggest that DCs are significant contributors to indirect NK activation by type I IFN *in vivo*, but do not rule out a role for other myeloid cell populations. In fact, we observed that other cell types upregulated IL-15R after CDN treatments, including monocytes, macrophages, and even NK cells, suggesting that these other cell types may play some role in amplifying NK activity. We cannot test definitively whether the response depends on IL-15 from DCs with available tools, because studies show that mice lacking IL-15 expression specifically in DCs (as well as those lacking IL-15 expression in macrophages) exhibit steady-state defects in NK cell numbers and functionality (Mortier et al., 2009), making it impossible to attribute any phenotypes we might observe to events occurring after establishing tumors and injecting CDNs. It has also been reported that tumors from patients with colorectal cancer have mutations in IL-15 and other cytokines and that this correlates with higher risk of tumor recurrence and decreased survival, suggesting that tumors may also be relevant sources of NK-activating cytokines (Mlecnik et al., 2014). Our study found that type I IFN action on host cells, and not the tumor, was crucial for the antitumor effect in our model, but it remains possible that IFN induces IL-15 production by tumor cells in other cancers or models.

Furthermore, we cannot rule out the importance of other CDN-induced, IFN-independent tumor-derived molecules. Finally, we note that in addition to effects of CDNs on IL-15 (via IFN), CDNs are known to induce numerous other cytokines, chemokines and cell surface receptors, and it is highly likely that some of those other induced molecules also play important roles in the antitumor NK response.

CDN-treatment led to systemic activation of NK cells and delayed the growth of distal tumors. Intratumoral injections of CDN led to increased levels of IFNβ in the serum and it is likely that the systemic type I IFN response promoted the systemic NK cell activation and antitumor effects. There are, however, other potential mechanisms of systemic NK cell activation that may play some role. When very high doses of CDNs are injected in mice with two tumors, some leakage from the injected tumor occurs and low amounts of CDNs can be detected in distal tumors (Sivick et al., 2018). While we used much lower doses of CDN than in that study, it remains possible that CDN leakage from the tumors into the circulation contributed to the systemic activation we observed. The possibility that large numbers of NK cells that were initially activated locally near the tumor recirculated to the spleen and to distal tumors appears less likely given that such a large percentage of splenic NK cells were activated shortly after local CDN administration. Regardless of the exact mechanism, our data makes clear that i.t. CDN treatment alone is capable of promoting antitumor effects on distal tumors independently of T cells.

NK cells are thought to kill primarily through the release of cytotoxic granules containing perforin and granzymes and through FasL and TRAIL death receptors (Voskoboinik et al., 2006). NK cells can also secrete cytokines with antitumor functions, such as IFN-γ and TNF-α (Balkwill, 2009; Ikeda et al., 2002). Somewhat surprisingly, mice lacking perforin, in which cytotoxic cells are unable to kill by the granule exocytosis pathway, still mobilized substantial NK cell-dependent antitumor responses after CDN treatments. Furthermore, perforin-deficient mice still had NK-mediated antitumor effects on tumors lacking Fas and DR5 death receptors and when IFN-γ was neutralized. In fact, the only treatment that resulted in significant abrogation of the antitumor response was TNF-α neutralization.

The role of TNF-α in our model is quite complicated, however. Consistent with previous studies (Zhao et al., 2002), we found that TNF-α action on host cells has potent antitumor effects in the absence of lymphocytes, possibly by acting on the host vasculature. We also found that NK cells in TNFR1/2 dKO mice were less activated by CDNs supporting the conclusion that TNFα acts directly or indirectly to activate NK cells. Nevertheless, NK cells could still mediate significant antitumor effects in the complete absence of TNF receptors on host cells or tumor cells. Hence, while TNF is necessary for effective anti-tumor NK responses in one context, TNFR signaling is not necessary for NK-mediated tumor clearance in another context. Interestingly, our data suggest that TNF-α has a tumor-protective role when acting on the tumor cells themselves, as TNFR1/2 dKO tumors were rejected better than the parental tumors. This effect was completely dependent on NK cells, and TNFR1/2 dKO tumors grew similarly to parental tumors in the absence of CD4/CD8 T cells and NK cells. A model of the action of TNF-α after CDN treatments is depicted below (Figure 23). One interpretation of this data is that TNF-α acts on tumors to block susceptibility to NK cell-mediated killing, although the mechanism of this remains unclear. TNFR2 is often expressed on tumor cells and has been

reported to promote tumor growth (Sheng et al., 2018) suggesting that these effects are mediated by TNFR2. Future experiments are needed to address how TNF-α protects tumors from NK cell-mediated killing and these experiments may ultimately reveal how NK cells exert their antitumor effects.

Cancer immunotherapy, especially checkpoint blockade, has led to major improvements in cancer treatment (Ribas and Wolchok, 2018; Sharma and Allison, 2015a), and while substantial numbers of long term remissions have been achieved in several cancers, many patients do not respond. Combining checkpoint therapy with CDN therapy may be beneficial not only because CDNs amplify T cell responses (Demaria et al., 2015; Sivick et al., 2018), but because tumor cells in patients treated with checkpoint inhibitors are sometimes selected for loss of MHC I (Rodig et al., 2018; Sade-Feldman et al., 2017; Zaretsky et al., 2016), and CDN-activated NK cells may eliminate those cells. Furthermore, NK cells in tumors express checkpoint receptors such as PD-1 and TIGIT (Hsu et al., 2018; Zhang et al., 2018), suggesting that checkpoint therapy could enhance the function of CDN-activated NK cells. Combinations of CDNs with NK-activating inflammatory cytokines such as IL-15, IL-12 and IL-18 may also provide added benefit (Ardolino et al., 2014; Meazza et al., 2011). Finally, blocking endogenous interactions that lead to NK cell desensitization (Deng et al., 2015; Thompson et al., 2017) or providing CDNs in combination with antibodies that mediate NK-dependent antibody-dependent cellular cytotoxicity of cancer cells may also be impactful.

In conclusion, our results show that CD8 T cell-resistant tumors can be effectively treated using CDNs. The antitumor effects were mediated by NK cells and dependent on type I IFN, which boosts NK cell antitumor responses *in vivo.* Mechanistically, type I IFN boosts NK cell responses by both direct action and indirect action via DCs, which induce IL-15 to further promote NK activation and tumor destruction (Figure 18F). These findings support the view that NK cells could be a cornerstone of next-generation cancer immunotherapies.

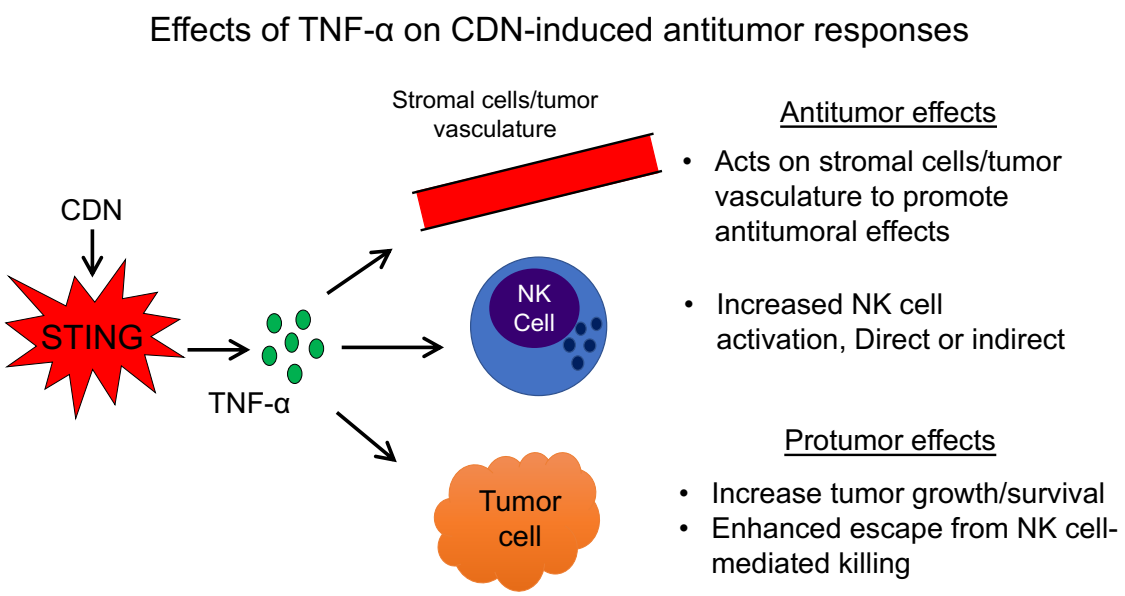

Fig. 23. Effects of TNF-α on CDN-induced antitumor responses. Model depicting action of TNF-α. TNF-α is produced by numerous cell types after CDN treatments, including NK cells. TNF-α also acts on numerous cell types to illicit both pro- and antitumoral effects. Action of TNF-α on non-hematopoietic stromal and/or vasculature cells promotes antitumoral effects. TNF-α also promotes full NK cell activation after CDN treatments, by acting either directly or indirectly on NK cells. Finally, TNF-α acts on tumor cells to promote NK-mediated tumor escape.

Chapter 4
STING agonists trigger CD4 T cell-dependent clearance of CD8 T cell-resistant tumors

Abstract

Immunotherapeutic drugs have revolutionized modern cancer treatment, greatly increasing patient survival and leading to remission in a significant number of people. These groundbreaking drugs enhance antitumor CD8 T cell responses to promote tumor destruction. However, tumors may evade such therapies via loss of MHC molecules. Hence, novel approaches mobilizing distinct types of immune cells to kill CD8 T cell-resistant tumors are needed. In the previous chapter I detailed potent NK cell activation and tumor clearance induced by CDNs. NK cell activation was found to be dependent on type I IFN, acting both directly on NK cells, but also indirectly via induction of IL-15/IL-15R complexes on DCs. Here we show that in response to CDN therapy, CD4 T cells also mediate potent antitumor responses in some tumor models, independently of CD8 T cells and, in the primary response, independently of NK cells, B cells, and γδ T cells. CDN treatments led to increased tumor-specific CD4 T cell priming and enhanced effector functions. Tumor-specific CD4 T cells in tumors treated with CDNs had a less exhausted, Th1-like phenotype, with increased production of IFN-γ, which was necessary for the antitumor response. Mice that cleared their primary tumors exhibited a long-lasting antitumor memory response, which was dependent on CD4 T cells, IFN-γ and partially dependent on B cells, myeloid cells and possibly NK cells. Interestingly, the antitumor response did not rely on MHC II expression by the tumor cells, suggesting that CD4 T cells either initiate antitumor effects indirectly, without direct recognition of the tumor cell by CD4 T cells, or engage ligands other than conventional MHC II (and MHC I) on tumor cells. These data shed light on novel mechanisms of immune-mediated tumor clearance which will be important for the design of next-generation immunotherapies.

Introduction

In the previous chapter I showed that i.t. CDN treatments induce potent antitumor effects against MHC I-deficient, CD8 T cell-resistant tumors and that these effects are mediated by NK cells. CDNs activate NK cells primarily through the induction of type I IFN, which acts both directly on NK cells, but also indirectly via the induction of IL-15/15R complexes. NK cells are important antitumor effector cells but CDNs have been shown to promote the activation of numerous cell types and it is likely that other cells and mechanisms contribute to MHC I-independent tumor clearance. It is well documented that i.t. injection of STING-agonists induce priming and activation of CD8 T cells, and most of the antitumor effects of STING agonists to date have been attributed to CD8 T cells (Corrales et al., 2015; Demaria et al., 2015; Sivick et al., 2018). While there is no role for CD8 T cells in the clearance of MHC I-deficient tumors in our models, it is possible that CDNs activate CD4 T cells and that these contribute to the CDN-induced tumor regression.

CD4 T cells recognize peptide antigens presented on MHC class II (MHC II) molecules. Unlike MHC I, MHC II is typically restricted to antigen presenting cells, although its expression can be induced in certain other cell types by IFN-γ (Boehm et al., 1997), a phenomenon that is more prevalent in humans than in mice. Once activated, CD4 T cells differentiate to give rise to a variety of differentiated $CD4^+$ effector cells, including Th1, Th2, Th17 and T regulatory (Treg) cells, each with unique functions. Th1 cells are characterized by production of IFN-γ and TNF-α and are important for protection against intracellular pathogens. Th2 cells produce IL-4, IL-13

and IL-5 and help mediate defense against extracellular parasites. Th17 cells produce IL-17, IL-22 and IL-21 and are important for protection against extracellular bacteria. Tregs are important for limiting immune responses in order to maintain self-tolerance and are important for limiting autoimmunity. CD4 T cells, through the various cytokines that they produce, have numerous cellular functions, such as activation and recruitment of myeloid cells, triggering B cell differentiation and antibody production and maturation, and enhancing effector functions of CD8 T cells (Zhu and Paul, 2008).

As discussed previously, CD8 T cells are highly cytotoxic cells and are traditionally thought to be the main drivers of antitumor immunity. However, CD4 T cells have also been implicated in tumor rejection, independent of their CD8 T cell-helper abilities (Greenberg et al., 1985), although the mechanisms of tumor destruction remain poorly defined. As mentioned above, IFN-γ can induce expression of MHC II molecules on several cell types, including tumor cells (Mach et al., 1996) and this may render them susceptible to direct recognition and killing by cytotoxic CD4 T cells. This has been shown using adoptively transferred TCR transgenic CD4 T cells into B16 melanoma-bearing mice. Upon transfer, the CD4 T cells acquired a cytotoxic Th1-like phenotype, expressing IFN-γ, perforin, and granzyme B. IFN-γ, produced by the transferred transgenic CD4 T cells, induced MHC II expression on the B16 tumor cells *in vivo*, ultimately leading to tumor MHC II-dependent tumor clearance (Quezada et al., 2010; Xie et al., 2010). Notably, however, even in those studies it was not proven that MHC II expression by the tumor cells was necessary for tumor rejection.

Many tumors, however, do not express MHC II, even when stimulated by IFN-γ, and there is evidence that CD4 T cells can have antitumor effects independent of direct recognition of tumor MHC II. Although the exact mechanisms are unclear, several studies have found that IFN-γ is critical for the indirect antitumor response (Corthay et al., 2005; Hung et al., 1998; Mumberg et al., 1999; Qin and Blankenstein, 2000). In these scenarios it is most often hypothesized that macrophages, which are activated by IFN-γ, mediate the antitumor responses (Corthay et al., 2005; Hung et al., 1998). In addition, one study found that IFN-γ can act on non-hematopoietic cells within the tumor, inhibiting tumor-induced angiogenesis, and limiting tumor growth (Qin and Blankenstein, 2000). Besides IFN-γ, IL-5 was reportedly important for CD4 T cell-mediated control of MHC II-deficient tumors in one instance, with the proposed mechanism involving the activation of tumor-killing eosinophils (Hung et al., 1998).

In this chapter I will detail my findings showing STING-induced activation and antitumor effects mediated by CD4 T cells, independently of NK cells, against CD8 T cell-resistant, MHC I-deficient tumors. Although the potential for CD4 T cell-mediated tumor rejection was first suggested over 30 years ago (Greenberg et al., 1985), there has been limited focus on developing approaches to mobilize direct CD4 T cell responses against tumors, possibly due to the lack of understanding of the mechanisms of tumor cell killing mediated by these cells. A better understanding of this phenomenon will likely marshal a greater effort to develop new therapies to mobilize these cells for treating CD8 T cell-resistant tumors.

Results

CDNs promote CD4 T cell-mediated antitumor responses that act independently of CD8 T cells, NK cells, and B cells, and γδ T cells, but may depend on perforin.

In the previous chapter I showed that i.t. injection of STING-agonizing CDNs could successfully treat MHC I-deficient RMA-*B2m*$^{-/-}$ tumors, and that this was highly dependent on NK cells. Furthermore, we showed that the antitumor effects were independent of CD8 T cells but did not address the role of cell types other than NK cells. Interestingly, although NK cells in *Rag2*$^{-/-}$ mice exerted partial rejection responses against RMA-*B2m*$^{-/-}$ tumors after CDN therapy (Fig. 4C), they were nevertheless substantially deficient in rejecting RMA-*B2m*$^{-/-}$ tumors compared to WT mice (Figure 24A). These data suggested that in addition to mobilizing NK responses, CDNs also induce strong antitumor adaptive immune responses against RMA-*B2m*$^{-/-}$ tumors. Because we found no role for CD8 T cells in chapter 3, we hypothesized that CD4 T cells were mediating these antitumor effects. To test the role of CD4 T cells, we injected mice with either CD4 or CD8-depleting antibodies or control Ig prior to CDN treatments. Consistent with our hypothesis, depleting CD4 T cells, but not CD8 T cells, severely diminished the antitumor effects of CDN treatments (Figure 24B). Furthermore, CDN-induced rejection was also deficient in MHC II KO mice (Figure 24C), which lack CD4 T cells due to an inability to positively select these cells during development in the thymus. These data argue that CD4 T cells play a significant role in rejecting MHC I-deficient RMA-*B2m*$^{-/-}$ tumors after CDN therapy.

We also examined several other *B2m*$^{-/-}$ tumors for CD4 T cell-mediated tumor clearance. For B16-F10-*B2m*$^{-/-}$, although CD4-depletion in WT mice caused tumors to grow out somewhat faster in one experiment (Figure 25A) it did not in two repeat experiments (Figure 25B, and not shown). Furthermore, CDN-induced rejection of B16-F10-*B2m*$^{-/-}$ tumors in *Rag2-/-* mice was only slightly (and non-significantly) faster than in WT mice (Figure 25C), suggesting that CD4 T cells do not play a major or consistent role in rejecting B16-*B2m-/-* tumors. CD4-depletion also had small effects in MC-38-*B2m*$^{-/-}$ (Figure 25D) and CT26-*B2m*$^{-/-}$ (Figure 25E) tumors, but these again were not significant. There was no effect on C1498-*B2m*$^{-/-}$ tumor rejection upon CD4 depletion in the primary CDN-induced response and most of the tumors were completely rejected (Figure 25F). Therefore, CD4 T cells play a significant role in CDN-induced tumor rejection in some tumor models but not in others.

CD4 T cells are known to provide important signals necessary for antibody production and B cell maturation, raising the possibility that CD4 T cells mediate antitumor effects via antitumor antibodies produced by B cells. To address the role of B cells we used *Ighm*$^{-/-}$ mice which lack the B cell receptor and as a result lack mature B cells (Kitamura et al., 1991). Interestingly, B cell-deficient mice still exhibited substantial CDN-induced antitumor effects which were abrogated upon CD4 T cell depletion (Figure 24D), suggesting that CD4 T cells mediate their antitumor effects independently of B cells. CD4 T cells can also promote NK cell activation (Gasteiger and Rudensky, 2014; Kerdiles et al., 2013) raising the possibility that CD4 T cells mediate their effects by enhancing NK cell mediated antitumor responses. To test the role for NK cells, we depleted CD4 T cells in NK cell-deficient NK-DTA mice, which are highly selective in lacking NK cells. Even in the absence of NK cells, CD4 T cells exhibited CDN-induced antitumor activity against RMA-*B2m*$^{-/-}$ tumors (Figure 24E). Similar results were

obtained in NK cell-depleted WT mice that were further depleted of CD4 T cells (Figure 24F), indicating that CD4 T cells also work independently of NK cells. Overall these data suggested that CD4 T cells mediate powerful responses against RMA-*B2m*$^{-/-}$ tumors, independently of CD8 T cells, B cells, and NK cells.

Even though NK or B cell-deficiency did not individually affect the antitumor CD4 T cell response, it was possible that both of these cell types were activated by CD4 T cells and inhibited tumor growth in a somewhat redundant fashion. To address if CD4 T cells promote antitumor responses in the absence of both NK cells and B cells, we used NK cell-depleted *Ighm*$^{-/-}$ mice and then depleted CD4 T cells or not. CD4 depletion caused the tumors to grow out faster under these conditions (Figure 24G), suggesting that CD4 T cell antitumor responses are present even in the combined absence of NK cells and B cells. Similar results were obtained when using *Tcrd*$^{-/-}$ mice, which lack γδ T cells. NK-depleted *Tcrd*$^{-/-}$ mice still exhibited antitumor effects when compared to *Tcrd*$^{-/-}$ mice depleted of both NK cells and CD4 T cells (Figure 24H), indicating that CD4 T cells mediate antitumor effects in the combined absence of NK cells and γδ T cells.

Notably, when doing a similar depletion experiment in *Prf1*$^{-/-}$ mice (preliminary data), the CD4-mediated antitumor effect was significantly blunted and there was not a large difference between NK-depleted *Prf1*$^{-/-}$ mice and NK+CD4-depleted *Prf1*$^{-/-}$ mice (Figure 24I). These data suggested that perforin may be an important mediator of the antitumor effects of CD4 T cells, whether it be expressed by CD4 T cells themselves or on another cell population. Interestingly, this result contrasts with the findings in Chapter 3 that host perforin plays little to no role in the NK cell-mediated antitumor response (Figure 21A).

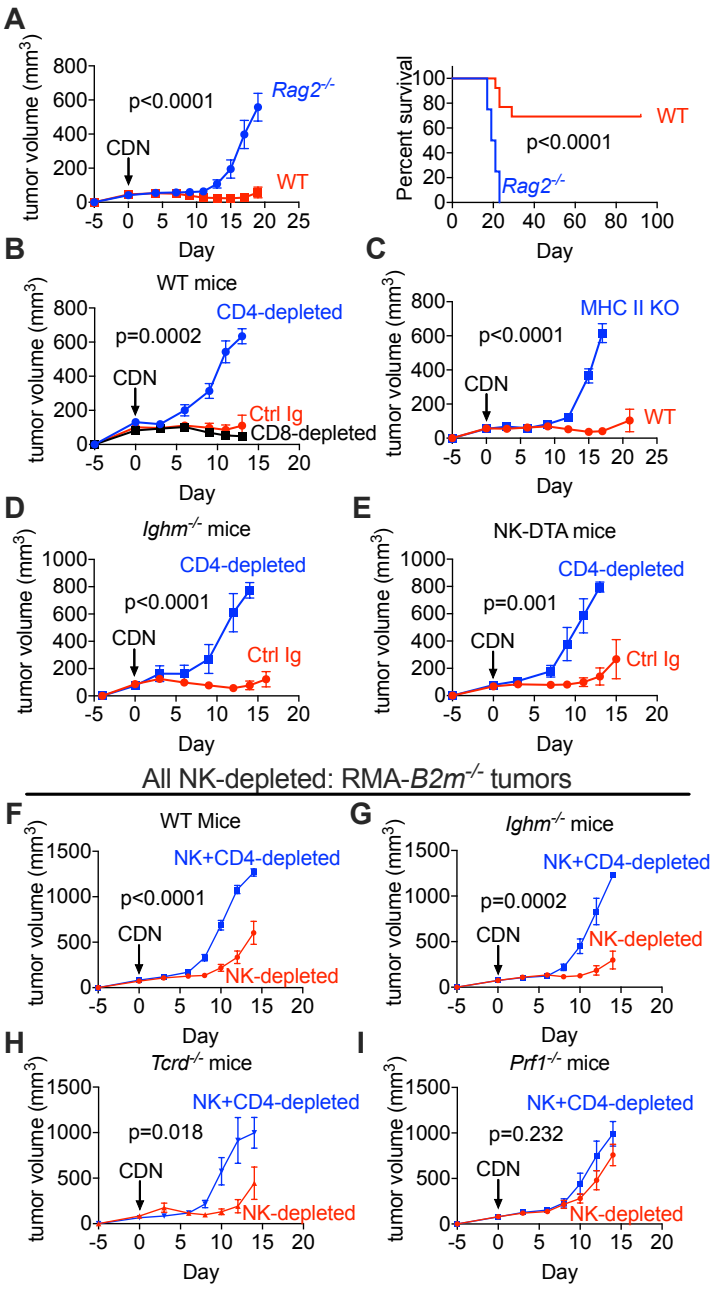

Fig. 24: CDNs promote CD4 T cell-mediated antitumor responses that act independently of CD8 T cells, NK cells, and B cells, and γδ T cells, but may depend on perforin. (A-E) RMA-*B2m*$^{-/-}$ tumors were established in WT (A-C), *Rag2*$^{-/-}$ (A), MHC II KO (C), *Ighm*$^{-/-}$ (D), or NK-DTA (E) mice, treated i.t. with 50μg CDN, and growth was monitored. **(F-I)** RMA-*B2m*$^{-/-}$ were established in NK cell-depleted WT (F), *Ighm*$^{-/-}$ (G), *Tcrd*$^{-/-}$ (H), or *Prf1*$^{-/-}$ (I) mice, treated with CDNs, and growth was measured as described previously. In some experiments, mice were also depleted of CD4 or CD8 T cells or injected with control Ig as described in methods. Figures A-D representative 2 independent experiments. Figure E is representative of 5 independent experiments. N=4-13 for A-E. Figure F is combined data from 4 independent experiments (N=20-21). Figure G and H have only been done once, n=4-6. Figure I is combined from two independent experiments (n=10). Statistics done using 2-way ANOVA for all.

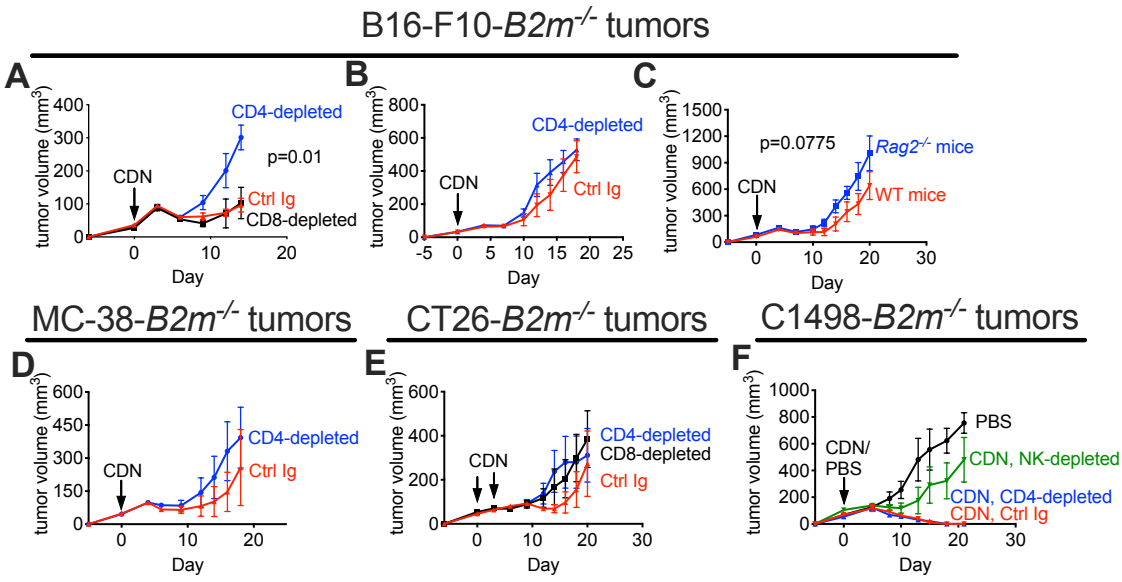

Fig. 25: CD4 T cells play less of a role in the clearance of B16-F10-*B2m*$^{-/-}$, MC-38-*B2m*$^{-/-}$, CT26-*B2m*$^{-/-}$, and C1498-*B2m*$^{-/-}$ tumors in the primary response but CD4 T cells do promote antitumor memory responses against C1498-*B2m*$^{-/-}$ tumors. (A-F) B16-F10-*B2m*$^{-/-}$ (A-C), MC-38-*B2m*$^{-/-}$ (D), CT26-*B2m*$^{-/-}$ (E), or C1498-*B2m*$^{-/-}$ (F) tumors were established in WT (A,B,D-F) or *Rag2*$^{-/-}$ (C) mice, treated i.t. with 50μg CDN, and growth was monitored. In some experiments mice were depleted of CD4 or CD8 T cells or injected with control Ig as in methods. In some experiments, mice were depleted of CD4 T cells as described in methods. N=6 for A, n=8 for B, n=5-6 for C, n=5-6 for D, n=7-8 for E, n=3-5 for F, n=3-6 for G, and n=3-4 for H. A and B are repeats but CD8 depletion has only been done once. C-E and G have only been done once. F is representative of two independent experiments. H is representative of two independent experiments. **P<0.01.

CDNs promote CD4 T cell-mediated antitumor memory responses that works independently of CD8 T cells but are partially dependent on NK cells and B cells.

A hallmark of adaptive immunity is the capacity for immunological memory. In the RMA-*B2m*$^{-/-}$ tumor model, a large fraction of CDN-treated mice completely cleared their tumors and exhibited no sign of tumor recurrence (Figure 24A). To assess if these mice developed a long-term antitumor memory response, we rechallenged CDN-treated survivor mice with subcutaneous RMA-*B2m*$^{-/-}$ tumors >60 days after they had cleared their primary tumors, without providing any therapeutic agents during rechallenge. Consistent with a memory response, tumor growth was severely diminished in rechallenged mice compared to naïve controls (Ctrl Ig group, Figure 26A). As expected, depleting CD8 T cells had no effect on the antitumor memory response (Figure 26A). Notably, the rechallenge response appeared to be highly dependent on CD4 T cells, as shown using CD4 T cell-depleting antibodies (Figure 26A, B). Depleting NK cells had a small, albeit significant, effect on the rechallenge response (Figure 26B). Interestingly, NK cell-depletion had no additional effect in CD4-depleted animals (Figure 26B), suggesting that CD4 cells play by far the greatest role in the memory response. Since CD4-depletion had a much greater effect than NK depletion, it appears that the major anti-tumor effects of the CD4 cells are mediated independently of NK cells. The data are consistent with the possibility that a small part of the CD4 T cell recall response is mediated via mobilization of NK cells, but do not allow a definitive conclusion on that point. The experiments also do not address whether the NK response observed is greater than would occur with NK cells from unprimed animals. Therefore we cannot be sure whether the NK cells in the rechallenge experiment are exhibiting the properties of "memory-like" NK cells (Cooper et al., 2009; Ni et al., 2012).

The impact of CD4 T cells on rechallenge was also observed in a second tumor model, C1498-*B2m*$^{-/-}$ cells. Primary challenges of those tumors were uniformly rejected in WT mice (Figure 1B), in an NK-dependent fashion (Figure 4A). When the mice were rechallenged >60 days post tumor clearance with subcutaneous C1498-*B2m*$^{-/-}$ cells, tumor growth was greatly delayed compared to tumor growth in naïve mice, whereas tumors grew rapidly when CD4 T cells were depleted (Figure 26C). Unlike the RMA-B2m$^{-/-}$ model, primary rejection of C1498-*B2m*$^{-/-}$ cells did not require CD4 T cells (Figure 25F). However, if CD4 T cells were depleted during the primary response, the memory response was abrogated (Figure 26D).

CD4 T cells also promote antibody production and affinity maturation and it was therefore possible that tumor-specific antibodies mediate some of the antitumor memory responses seen in rechallenged mice, even if B cells do not play a major role in the rejection of tumors in the primary response (Figure 24D). We examined this possibility in mice exposed to RMA-*B2m*$^{-/-}$ tumors. Interestingly, upon rechallenge, *Ighm*$^{-/-}$ mice exhibited a defect in tumor rejection that was partial compared to the impact of CD4 depletion in WT mice (compare Figure 26E with Figures 26A and 26B), raising the possibility that B cells and/or their antibody products play a partial role in the CD4 T cell-dependent memory response.

In light of the possible role of B cells, we examined serum for tumor specific antibodies. Serum collected from rechallenged survivor mice stained tumor cells *in vitro*, even when diluted 1:900, whereas serum from tumor-bearing naïve mice had much less staining activity (Figure 26F). These data indicate that the rechallenged animals had generated substantial titers of

antitumor antibodies. Furthermore, when samples of pooled serum from several rechallenged mice were injected into naïve WT mice, the growth of fresh RMA-*B2m*$^{-/-}$ tumors was modestly delayed, albeit the difference was not statistically significant (Figure 26G). Overall these data show that CDNs promote a CD4 T cell-dependent antitumor response that results in long-term immunological memory. The memory response is independent of CD8 T cells but partially dependent on B cells and possibly NK cells. However, the majority of the antitumor memory response is still present in mice lacking B cells or NK cells individually, and future experiments should address whether mice lacking both NK cells and B cells are capable of mounting a CD4 T cell-dependent memory response.

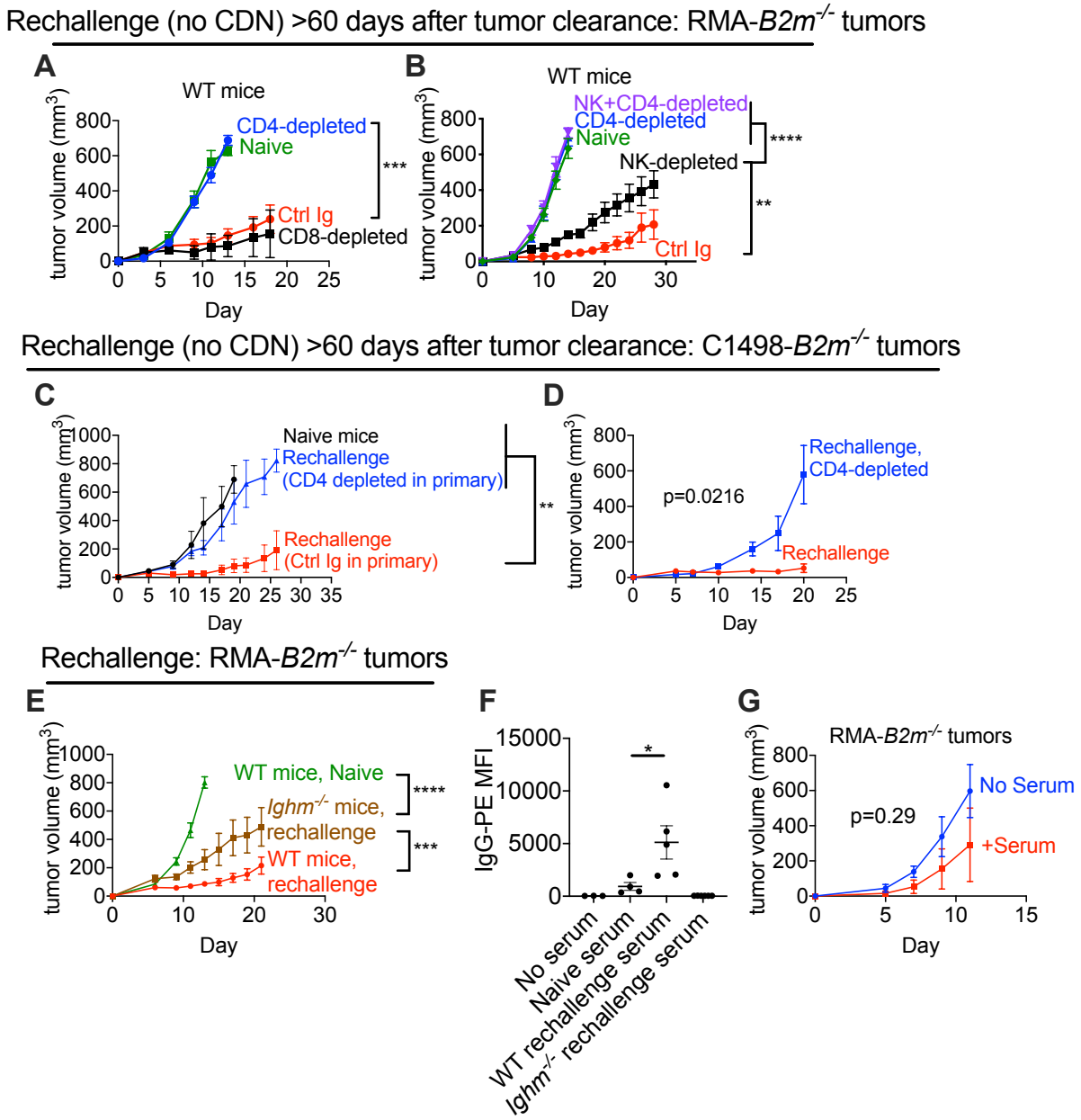

Fig. 26: CDNs promote CD4 T cell-mediated antitumor memory responses that works independently of CD8 T cells but are partially dependent on NK cells and B cells.
(A-E) 60 days after CDN-induced tumor clearance, WT mice (A-E) or *Ighm*$^{-/-}$ mice (E) were rechallenged with 2 x 10^6 RMA-*B2m*$^{-/-}$ cells (A-B and E) or C1498-*B2m*$^{-/-}$ cells and measured as described previously. In some experiments, mice were depleted of NK, CD4, or CD8 T cells or injected with control Ig as described in methods. **(F)** Animals from panel E were bled at day 14 and serum was collected and used to stain RMA-*B2m*$^{-/-}$ cells *in vitro* (1:900 dilution), followed by anti IgG-PE staining and flow cytometry. **(G)** Serum was collected and pooled from several CDN-survivor mice after RMA-*B2m*$^{-/-}$ rechallenge. Naïve WT mice were injected with 1 x 10^6 RMA-*B2m*$^{-/-}$ cells followed by injection of undiluted serum IP (200 μl) every 2 days (total of 4 doses). Growth was monitored as in previous experiments. In panel A, CD8-depletion is preliminary and has only been done once (CD4 depletion has been done 4 times). In panel B, NK depletion has been done twice while NK+CD4 depletion has only been done once. Panel E is combined data from two independent experiments. Panels F and G are preliminary and have only been done once. N=5-16 for C-E, n=5 for F, and n=3 for G. Figure C-E and G analyzed by 2-way ANOVA. Figure F analyzed by 2-tailed unpaired Student's t-test. *P<0.05; **P<0.01; ***P < 0.001; ****P<0.0001.

CDNs promote tumor-specific CD4 T cell responses with a Th1-like, less-exhausted, phenotype.

Previous studies have shown that CDNs promote tumor-specific CD8 T cell priming and antitumor effector functions (Corrales et al., 2015; Demaria et al., 2015; Sivick et al., 2018), but very few studies have characterized the effect of CDNs on CD4 T cells. To examine tumor-specific CD4 T cell priming in our model we used a tetrameric MHC class II (A^b) / epitope complex, in which the epitope is a defined MHC II epitope in RMA cells, from the gp70 envelope protein of Murine Leukemia virus (MuLV) (Shimizu et al., 1994). RMA cells were derived from the RBL-5 cell line, which was originally transformed by infection with Rauscher MuLV (Chesebro et al., 1976; van Hall et al., 2000) and we hypothesized that this antigen would be present on RMA-*B2m*$^{-/-}$ cells. Consistent with this hypothesis, CD4 T cells harvested from the spleens of tumor-bearing mice 6 days after CDN or PBS treatment stained positive with the gp70 tetramer while cells from naïve, nontumor-bearing control mice did not (Figure 27A). The presence of tumor alone, without CDN therapy, was sufficient to prime some tumor-specific CD4 T cells, as evidenced by positive tetramer staining in the PBS-treated group (Figure 27A). Consistent with previous findings for CD8 T cells, CDN therapy led to an expansion (approximately 2-fold) of tumor specific CD4 T cells in the spleen (Figure 27A). These data show that CDNs trigger priming of tumor-specific CD4 T cells.

To examine functionality of the tumor-specific CD4 T cells we stimulated splenocytes from treated mice with a peptide of the same epitope as the tetramer and analyzed cytokine production by CD4 T cells using flow cytometry. CD4 T cells from splenocytes of CDN-treated mice exhibited substantial increases in IFN-γ, IL-2, and TNF-α production compared to PBS-treated control mice (Figure 25B and 28A), indicating that CDNs enhance CD4 T cell antitumor responses. We did not see any expression of IL-17 or IL-4 in peptide stimulated splenocytes (data not shown). The expression of IFN-γ and TNF-α suggested that the tumor-specific CD4 T cells were of the Th1 subtype. Transcription factor staining confirmed that a large fraction of tetramer$^+$ cells expressed Tbet (Figure 27C) but there was not a significant difference between PBS and CDN-treated mice. The transcription factor Eomesodermin (Eomes) has also been implicated in CD4 T cell-mediated antitumor immunity (Curran et al., 2013), but we were unable to detect Eomes in the tetramer$^+$ cells (Figure 28B). Interestingly we were able to detect a small population of FoxP3$^+$ tetramer$^+$ cells, and these were less frequent in CDN-treated mice compared to PBS-treated controls (Figure 28B). We have not established what role, if any, these cells play in our model. These data suggest that CDN treatment enhances tumor-specific Tbet$^+$ Th1 CD4 T cell effector functions.

Comparisons of Figures 27A and 27B suggested that a larger percentage of tetramer$^+$ CD4 T cells in CDN-treated mice than in PBS-treated mice produced cytokines. Detection of IFNγ-costained tetramer+ cells after stimulation was not possible, because TCR levels were reduced as a consequence of stimulation, but the ratio of IFNγ+ cells after peptide stimulation to tetramer+ cells before stimulation was higher in CDN-treated mice (0.13/0.3=0.43) than in PBS-treated mice (0.03/0.17=0.18). These data suggested that many of the CD4 T cells in PBS-treated tumor-bearing mice were dysfunctional, and that CDN treatments were associated with greater functionality of the tumor-specific T cells. This possibility was supported by analysis of expression of the transcription factor TOX, which was recently identified as a key driver of CD8 T cell exhaustion following chronic antigen stimulation in both viral infections and cancer (Khan

et al., 2019; Scott et al., 2019; Seo et al., 2019). Although a role for TOX in dysfunction of CD4 T cells has not been independently reported, we found that the increased dysfunction of CD4 T cells in PBS treated mice compared to CDN-treated mice was associated with a higher percentage of TOX+ cells in the PBS-treated mice (Figure 27C). For CD8 T cells, TOX is necessary for the exhaustion program and *Tox*$^{-/-}$ cells fail to upregulate inhibitory ("checkpoint") receptors within tumors (Khan et al., 2019; Scott et al., 2019; Seo et al., 2019). Consistent with a loss of TOX expression and decreased exhaustion in the tetramer^{+} CD4 T cells after CDN treatments, we found that CDN treatments resulted in lower percentages of PD-1^{+}, Tim3^{+}, Lag-3^{+} and TIGIT^{+} T cells among tetramer^{+} cells (Figure 27D). Overall these data show that CDNs promote the expansion and enhancement of effector activity of tumor-specific CD4 T cells and may prevent or reverse exhaustion. The tumor-specific CD4 T cells exhibit a Th1-like phenotype and have reduced expression of the exhaustion transcription factor TOX and inhibitory receptors PD-1, Tim-3, Lag-3, and TIGIT.

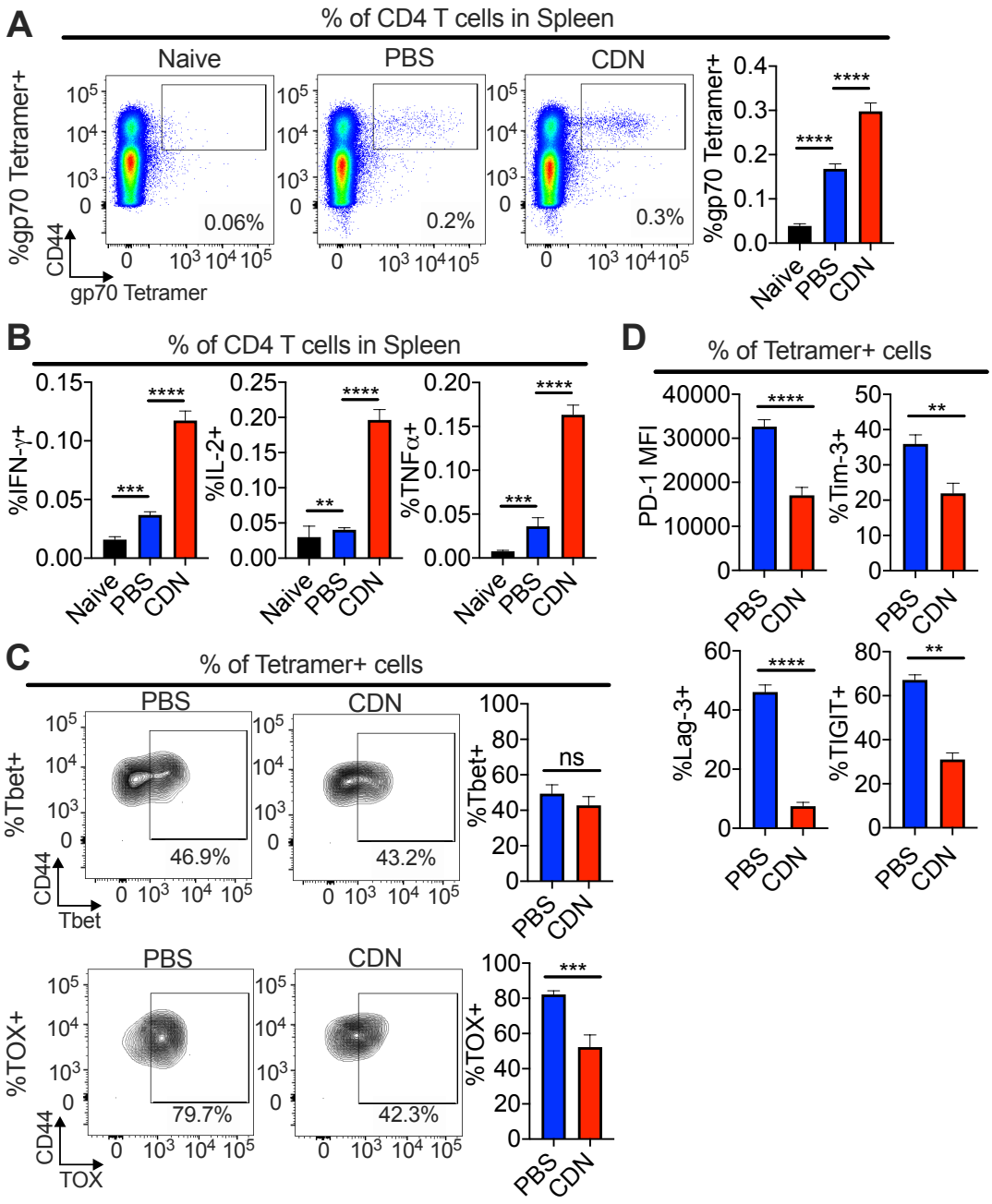

Fig. 27: CDNs promote tumor-specific CD4 T cell responses with a Th1-like, less-exhausted, phenotype. (A and B) RMA-*B2m*$^{-/-}$ were established or not and treated with PBS or CDN as in Fig. 1B. 6 days after treatment single cell suspensions of spleens were either stained with gp70 tetramer (A) or stimulated with gp70 peptide for 4 hours (B) followed by staining for flow cytometry. CD4 T cells were gated as viable, CD45^{+}, NK1.1^{-}, CD19^{-}, F4/80^{-}, Ter119^{-}, CD3^{+}, CD4^{+} cells. Data are combined from 9 independent experiments. n=30-48. Kruskal-Wallis test with Dunn's test for multiple comparisons was used. **(C and D)** Tumors were treated and stained with gp70 tetramer as in A. Tetramer^{+} CD4 T cells were then co-stained for transcription factors (C) or surface inhibitory receptors (D). n= 9 (C) and n=6 (D). Data combined from 2 independent experiments (C) or representative of 4 independent experiments (D). Analyzed by 2-tailed unpaired Student's t-test. **P<0.01; ***P < 0.001, ****P<0.0001 for all data.

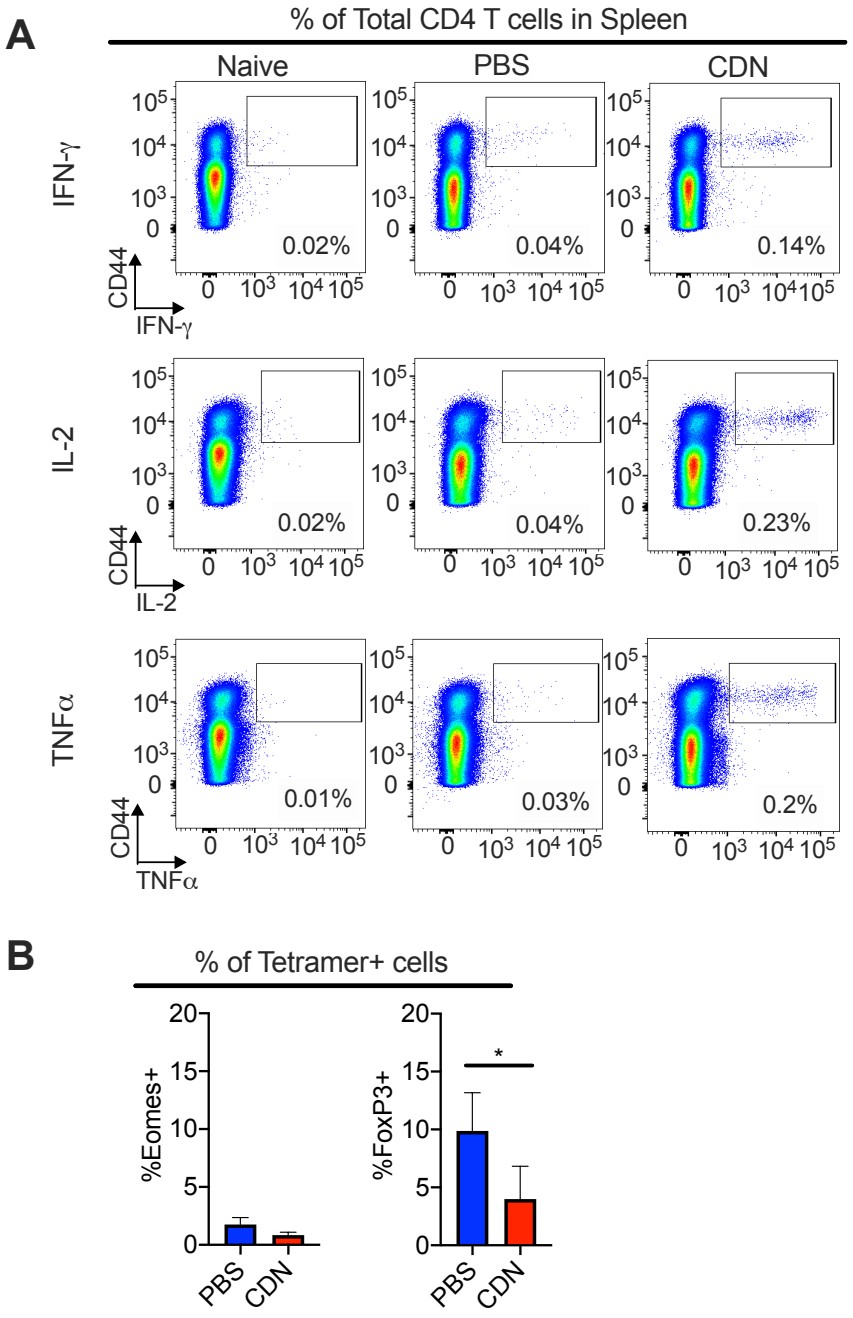

Fig. 28. (A) Representative flow plots for Fig. 27B. (B) Expression of Eomes and FoxP3 on gp70 Tetramer^{+} cells. Tumor-bearing mice were treated and splenocytes harvested and stained as in Figure 3C. n=6. Experiment is preliminary and has only been done once. Analyzed by 2-tailed unpaired Student's t-test. *P<0.05.

Type I IFN is required for promoting fully functional CD4 T cells and for the antitumor response.

STING activation results in the production of type I IFN (Ishikawa and Barber, 2008) and in Chapter 3 we showed that type I IFN is indispensable for CDN-induced NK cell activation and tumor clearance. Previous studies have also shown that type I IFN is necessary for CD8 T cell effector function and tumor clearance in response to i.t. injection of STING agonists (Corrales et al., 2015; Curran et al., 2016; Demaria et al., 2015), but it remains unknown whether type I IFN is necessary for CD4 T cell priming and antitumor effector functions. To examine the role of type I IFN on CDN-induced tumor-specific CD4 T cell priming, activation, and antitumor responses we used *Ifnar1*$^{-/-}$ mice. Unexpectedly, tumor-bearing, CDN-treated *Ifnar1*$^{-/-}$ mice had slightly more, not fewer, gp70 tetramer^{+} cells in their spleens compared to WT mice (Figure 29A). Furthermore, the IL-2 and TNF-α responses of the CD4 T cells to gp70 peptide after CDN treatments were of similar magnitude in *Ifnar1*$^{-/-}$ mice as in WT mice (Figure 29A), and the reduced expression of checkpoint receptors associated with CDN treatments was also not IFNAR1-dependent (Figure 29B). Hence, type I IFN action via IFNAR1 was not necessary for priming the T cells, for imparting a similar capacity to produce IL-2 and TNF-α, or for dampening checkpoint receptor expression. There was, however, a consistent partial reduction in the frequency of IFN-γ producing cells in *Ifnar1*$^{-/-}$ mice (Figure 29A), indicating that type I IFN may be important for establishing the full functional Th1 activity of the CD4 T cells. Overall, these data showed that type I IFN signaling is dispensable for CDN-induced CD4 T cell priming and decreased inhibitory receptor expression. Furthermore, type I IFN does not seem to be necessary for some aspects of CD4 T cell effector function, such as production of IL-2 and TNF-α, but may be important for promoting fully functional Th1 CD4 T cell responses, as evidenced by reduced levels of IFN-γ.

To address the role of type I IFN in CD4 T cell-mediated tumor clearance we used IFNAR1-blocking antibodies and NK-deficient NK-DTA mice to focus the antitumor response on the CD4-mediated component. Blocking IFNAR1 in RMA-*B2m*$^{-/-}$ tumor-bearing NK-DTA mice resulted in more rapid tumor growth than was observed in control Ig-treated mice (Figure 29C), indicating that type I IFN is important for the NK-independent antitumor effects, which we know are predominantly mediated by CD4 T cells (Fig. 24E). In contrast, a preliminary experiment showed that blocking IFNAR1 in lymphocyte-deficient *Rag2*$^{-/-}$*Il2rg*$^{-/-}$ mice had no effect (Figure 29D), suggesting that all of the antitumor effects induced by type I IFN are mediated by lymphocytes. These data, combined with the observations in Figure 24, suggest that type I IFN is important for the antitumor CD4 T cell response. A future study to advance this analysis could utilize CD4-depleting antibodies in combination with IFNAR1 blockade to determine how much of the CD4 T cell-mediated response is type I IFN-dependent.

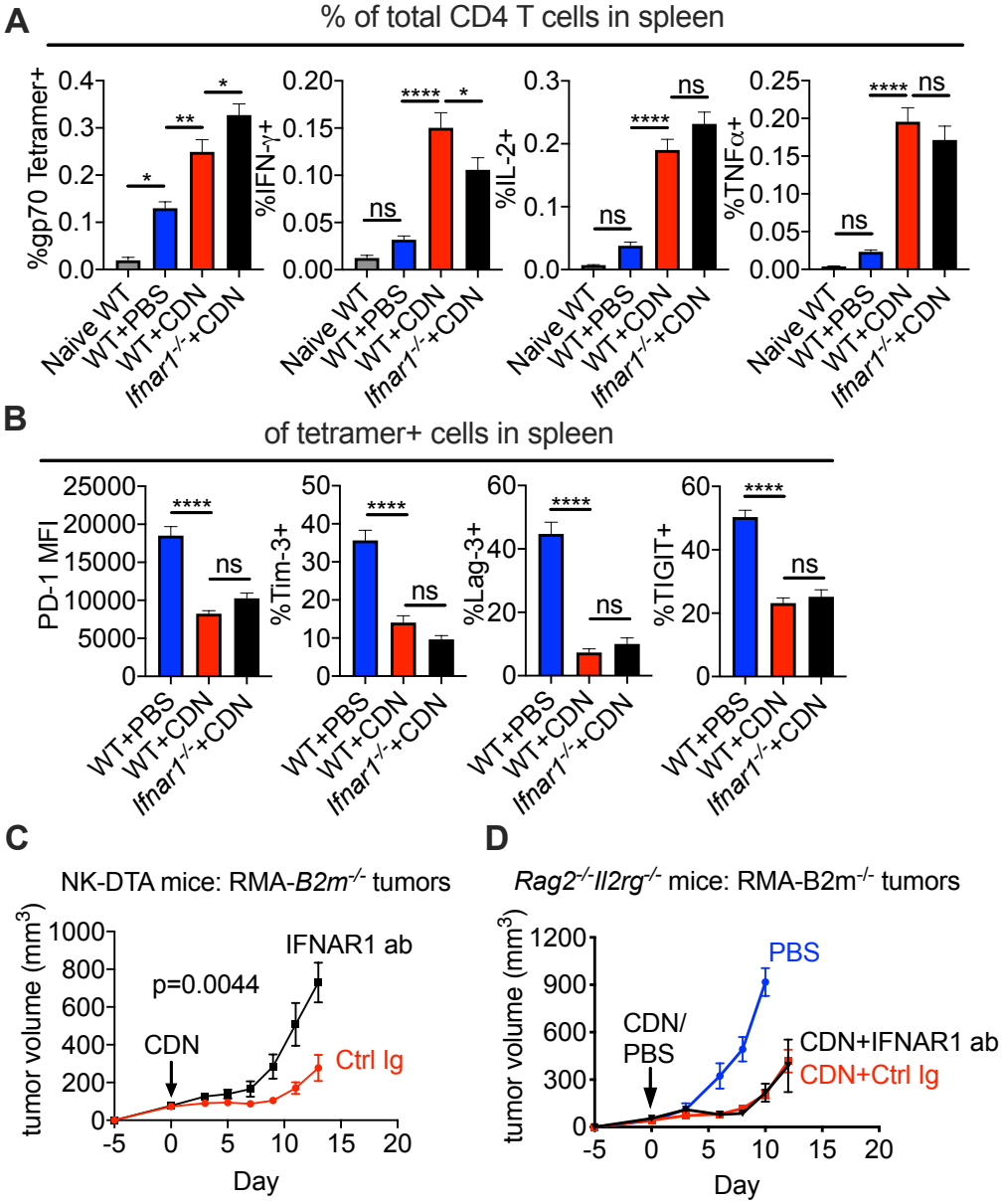

Fig. 29. Type I IFN is important for promoting fully functional CD4 T cells and for the antitumor response. (A and B) RMA-*B2m*$^{-/-}$ tumors were established or not in WT or *Ifnar1*$^{-/-}$ mice and treated with PBS or CDN as in Fig. 1B. Six days after treatment, spleen cells were either stained with gp70 tetramer (A and B) or stimulated with gp70 peptide for 4 hours followed by staining for flow cytometry (B). CD4 T cells were gated as in Figure 27. Data were combined from 3 (A) or 2 (B) independent experiments; n=9-18 for A and n=9-12 for B. **(C and D)** RMA-*B2m*$^{-/-}$ tumors were established in NK-DTA (C) or *Rag2*$^{-/-}$*Il2rg*$^{-/-}$ (D) mice, treated, and analyzed as in Fig. 1B. In some experiments, mice were treated with anti-IFNAR1 or control Ig as described in methods. C (n=10) is combined from two independent experiments and D (n=3-4) has only been done once. Kruskal-Wallis test with Dunn's for multiple comparisons was used for A and B. 2-way ANOVA was used for C and D. *P<0.05; **P<0.01; ***P < 0.001; ****P<0.0001.

TNF-α neutralization in WT mice does not inhibit the antitumor response and TNF-α signaling may negatively regulate CDN-induced CD4 T cell responses.

Besides type I IFN, STING activation also leads to production of TNF-α. In Chapter 3 we showed that CDN-induced TNF-α is important for the modest antitumor effects seen in CDN-treated *Rag2*$^{-/-}$*Il2rg*$^{-/-}$ (Figure 2B) and T cell-depleted (Figure 21F) mice and it appeared that TNF-α primarily mediates its antitumor effects by acting on host cells (Figure 2C and 21F). In contrast, in T cell-sufficient WT mice, TNF-α neutralization did not prevent tumor rejection or accelerate tumor growth, but instead caused a slight reduction in tumor volume 3 days post CDN treatment, followed by tumor rejection similar to that of WT mice (Figure 30A). In line with this finding, tumor volumes were smaller in TNFR 1/2 dKO mice after CDN treatment than in WT mice (Figure 30B). The latter data also indicated that TNF-α mediates this effect by acting on host cells, rather than on tumor cells. Finally, neutralizing TNF-α during tumor rechallenge of CDN-treated survivor mice did not diminish tumor rejection (Figure 5C), indicating that TNF-α does not play a major role in the CD4 T cell-mediated antitumor memory response.

Interestingly, CDN-treated mice lacking TNF receptors had substantial increases in CD4 T cells specific for tumor antigen as well as increased frequencies of T cells producing IFN-γ, IL-2, and TNF-α after peptide stimulation (Figure 30D), suggesting that the CD4 T cell response is restrained by CDN-induced TNF-α. gp70 tetramer^{+} cells in CDN-treated TNFR1/2-deficient mice also had lower expression of PD-1, Tim-3, Lag-3, and TIGIT checkpoint receptors compared to CDN-treated WT mice (Figure 30E). Overall, these data suggest that TNF-α restrains the magnitude of the T cell response and is associated with increased expression of checkpoint receptors by these T cells, and therefore appears to negatively impact antitumor CD4 T cell responses.

With available data it is not clear whether these effects actually impact the tumor rejection process. In WT mice, complete rejection occurs even without TNF blockade, so these are not the appropriate conditions to evaluate whether TNF blockade improves tumor rejection. The tumors were slightly smaller at day 3 when TNF action was blocked (with antibody or due to TNF receptor deficiency), which may possibly reflect a more potent early T cell response, but could also simply reflect the absence of TNF-induced inflammation at the tumor site. It will be important to repeat these experiments in mice that lack NK cells, where tumors generally eventually grow out despite an ongoing CD4 T cell response, to evaluate whether TNF blockade increases the efficacy of CDN-induced tumor rejection by CD4 T cells.

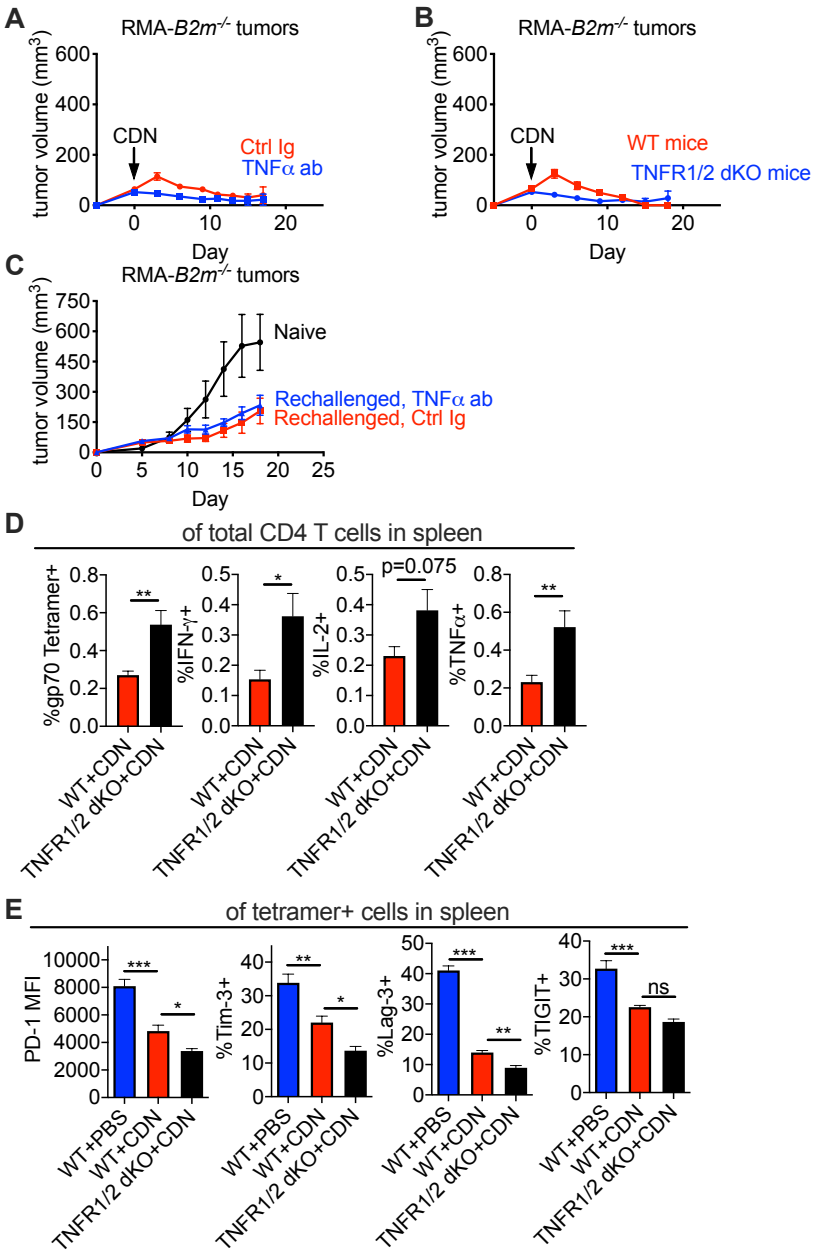

Fig. 30. TNF-α-neutralization in WT mice does not inhibit the antitumor response and TNF-α signaling may negatively regulate CDN-induced CD4 T cell responses. (A and B) RMA-*B2m*$^{-/-}$ were established or not in WT (A and B) or TNFR 1/2 dKO (B) mice and treated with PBS or CDN as in Fig. 1B. In (A) mice were treated with anti-TNF-α or control Ig as in methods. **(C)** 60 days after CDN-induced tumor clearance, mice were rechallenged with 2 x 10^6 RMA-*B2m*$^{-/-}$ cells and analyzed as before. One group received anti-TNF-α or control Ig every 3 days for the entirety of the experiment. **(D and E)** RMA-*B2m*$^{-/-}$ were established or not in WT or *Ifnar1*$^{-/-}$ mice and treated with PBS or CDN as in Fig. 1B. 6 days after treatment single cell suspensions of spleens were either stained with gp70 tetramer (D and E) or stimulated with gp70 peptide for 4 hours followed by staining for flow cytometry (D). CD4 T cells were gated as in Figure 27. Data for figure D is combined from 3 independent experiment. Data in figure A, B, C, and E are preliminary and have only been done once. N=4-7 for A-C, n=14-15 for D, and n=5-6 for E. *P<0.05; **P<0.01; ***P < 0.001.

IFN-γ, produced by CD4 T cells, is important for the antitumor response and acts on both tumor and host cells.

In Figure 27, we showed that CDN treatment induces IFN-γ-producing antitumor CD4 T cells and in Figure 29 we observed that neutralizing type I IFN led to decreases in IFN-γ production by CD4 T cells and inhibited antitumor responses. Several previous studies reported that IFN-γ is important for mediating antitumor CD4 T cell responses (Corthay et al., 2005; Hung et al., 1998; Mumberg et al., 1999; Qin and Blankenstein, 2000) and we hypothesized that IFN-γ would also be key to the CD4 T cell-mediated antitumor effects induced by CDNs. Consistent with this hypothesis, tumors eventually grew out in *Ifng*$^{-/-}$ mice after CDN treatments (Figure 31A). Furthermore, neutralizing IFN-γ in NK cell-deficient NK-DTA mice produced similar results (Figure 31B), suggesting that IFN-γ is important for promoting the CD4 T cell-mediated antitumor response.

IFN-γ-neutralization also inhibited the antitumor memory response observed in CDN-survivor mice after tumor rechallenge (Figure 31C) and caused tumors to grow out at a similar pace as observed in naïve control animals. These data indicated that IFN-γ is necessary for the antitumor effects mediated by CDNs.

Interestingly, splenocytes from CDN-treated *Ifng*$^{-/-}$ mice showed a modest increase in gp70 tetramer^{+} cells compared to the frequency in WT mice, and generated IL-2 and TNF responses similar to those from WT mice after peptide stimulation (Figure 31D). These data suggested that IFN-γ was not necessary for tumor-specific T cell expansion and at least some of the functional activities of the CD4 T cells.

We next addressed whether the necessary IFN-γ is produced by T cells. We generated *Rag2*$^{-/-}$ + *Ifng*$^{-/-}$ → B6 CD45.1 and WT + *Ifng*$^{-/-}$ → B6 CD45.1 mixed (50:50) bone marrow chimera mice. After reconstitution, most of the peripheral blood cells were >95% donor type, but two were 50-70% donor type (Figure 32A). After reconstitution, the T cells (and B cells) from *Rag2*$^{-/-}$ + *Ifng*$^{-/-}$ → B6 CD45.1 chimeras should all arise from *Ifng*$^{-/-}$ cells whereas half of most other hematopoietic cells are expected to be *Ifng*$^{+/+}$. Comparing these chimeras to the control chimeras allows us to test the role of IFNγ produced by the T cells.

We confirmed that the T cells from *Rag2*$^{-/-}$ + *Ifng*$^{-/-}$ chimeric mice lacked IFN-γ production upon stimulation with PMA + Ionomycin (Figure 32B). As a control we also examined IFN-γ production by NK cells in these mice. Interestingly, NK cells from *Rag2*$^{-/-}$ + *Ifng*$^{-/-}$ chimeras produced less IFN-γ than NK cells from WT + *Ifng*$^{-/-}$ chimeras. It is unclear why there might be less IFN-γ production by NK cells in these mice. A previous report suggested that *Rag2*-deficiency may have some cell-intrinsic consequences on NK cell development (Karo et al., 2014); alternatively the difference may simply reflect slight variations in the donor bone marrow mixes.

After tumor implantation and CDN therapy, the *Rag2*$^{-/-}$ + *Ifng*$^{-/-}$ → B6 CD45.1 chimeras proved to be as defective in tumor rejection as control *Ifng*$^{-/-}$ → B6 CD45.1 chimeric mice. The control WT + *Ifng*$^{-/-}$ → B6 CD45.1 chimeras resisted the tumors more effectively (Figure 31E).

These data suggested that IFN-γ produced by T cells is necessary for anti-tumor effects, rather than the alternative possibility that IFN-γ is necessary for T cell priming or activation.

RMA-*B2m*$^{-/-}$ cells express the receptor for IFN-γ (Figure 31F) and IFN-γ has been reported to act directly on certain tumor cells to induce apoptosis and to inhibit proliferation (Castro et al., 2018). To address the role of IFN-γ acting directly on the tumor cells we used CRISPR-Cas9 to knock out *Ifngr1* in RMA-*B2m*$^{-/-}$ tumor cells (Figure 31F). To validate the RMA-*B2m*$^{-/-}$*Ifngr1*$^{-/-}$ cell line we incubated the cells in IFN-γ overnight and measured induction of *Irf1* mRNA transcripts. *Ifngr1*$^{-/-}$ cells stimulated with IFN-γ failed to induce *Irf1*, unlike the parental line (Figure 31F), indicating that the cells lost the ability to respond to IFN-γ.

We then established RMA-*B2m*$^{-/-}$ or RMA-*B2m*$^{-/-}$*Ifngr1*$^{-/-}$ tumors in WT and *Ifngr1*$^{-/-}$ mice and treated the tumors with CDNs. Remarkably, CDN-induced antitumor effects were diminished only when IFNγ receptors were absent both on the host cells and the tumor cells. That is, RMA-*B2m*$^{-/-}$*Ifngr1*$^{-/-}$ tumors grew rapidly in *Ifngr1*$^{-/-}$ mice but were strongly resisted in WT mice; and *Ifngr*$^{+/+}$ tumors were strongly resisted in *Ifngr1*$^{-/-}$ mice, as they were in WT mice (Figure 31G). These results suggest that IFN-γ can act on either host or tumor cells to mediate its antitumor effects. Overall, these data argue that IFN-γ is produced by CD4 T cells and is important for mediating their antitumor effects and that IFN-γ can act on either the host or tumor to limit tumor growth.

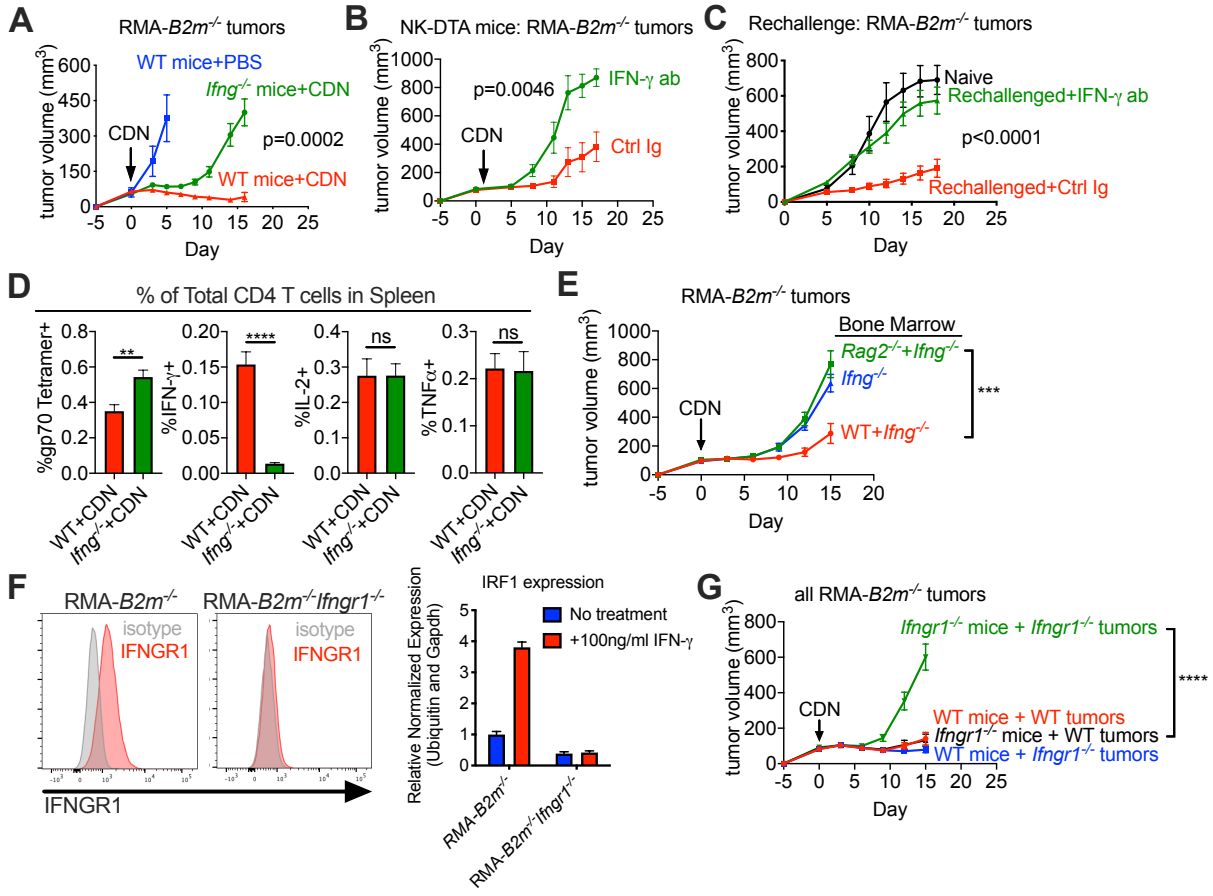

Fig. 31. IFN-γ, produced by CD4 T cells, is important for the antitumor response and acts on both tumor and host cells. (A and B) RMA-*B2m*$^{-/-}$ tumors were established or not in WT (A) or NK-DTA (B) mice and treated with PBS or CDN as in Fig. 1B. In (B) mice were treated with anti-IFN-γ or control Ig as in methods. For (A), N=3 for PBS-treated group and n=9-16 for CDN-treated groups. For (B) n=5-6. Data representative of two independent experiments for (A) and (B). **(C)** 60 days after CDN-induced tumor clearance, mice were rechallenged with 2 x 10^6 RMA-*B2m*$^{-/-}$ cells and analyzed as before. Mice received anti-IFN-γ or control Ig every 3 days for the entirety of the experiment. N=9-12. Data combined from two independent experiments. **(D)** RMA-*B2m*$^{-/-}$ tumors were established or not in WT or *Ifng*$^{-/-}$ mice and treated with PBS or CDN as in Fig. 1B. 6 days after treatment single cell suspensions of spleens were either stained with gp70 tetramer or stimulated with gp70 peptide for 4 hours followed by staining for flow cytometry. CD4 T cells were gated as in Figure 27. N=11-12. Data combined from 2 independent experiments. **(E)** Bone marrow chimeras were established with the indicated mixes of donor bone marrow into CD45.1 recipients (see Methods). Eight weeks later, RMA-*B2m*$^{-/-}$ tumors were established, treated, and analyzed as in Fig. 1B. n=12-20 per group. Data combined from two independent experiments. **(F)** The indicated cell lines were stained with anti-IFNGR1 or isotype control antibodies followed by flow cytometry. For the right panel analysis, the indicated cell lines were incubated with 100 ng/ml recombinant IFN-γ *in vitro* overnight, RNA was extracted and qRT-PCR performed to quantify *Irf1* transcripts. n=3 (technical triplicate). Data representative of two independent experiments. **(G)** RMA-*B2m*$^{-/-}$ or RMA-*B2m*$^{-/-}$*Ifngr1*$^{-/-}$ tumors were established in WT or *Ifngr1*$^{-/-}$ mice and treated with CDN as in Fig. 1B. Data pooled from 6 experiments. N=21-46. *P<0.05; **P<0.01; ***P < 0.001; ****P<0.0001.

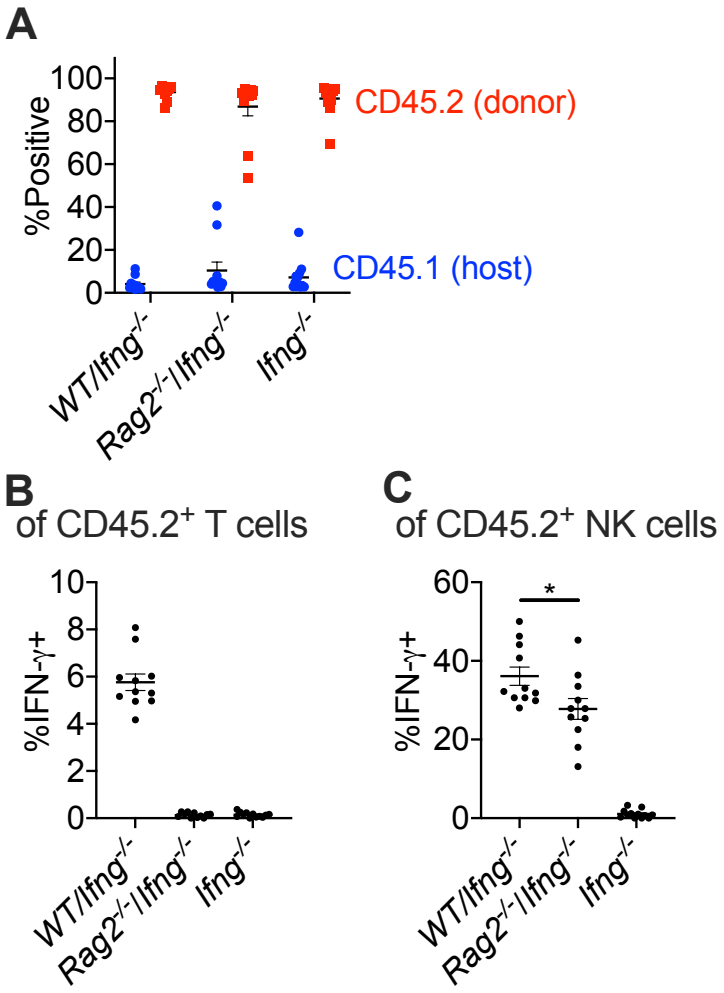

Fig. 32. IFN-γ Bone Marrow chimera verification. (A) Eight weeks after reconstitution, blood from bone marrow chimeras was collected, treated with ACK, and stained for flow cytometry. Percent of cells expressing either CD45.1 or CD45.2 are shown. **(B-C)** Samples in A were stimulated with PMA+Ionomycin in the presence of Brefeldin A and Monensin for 4 hours followed by surface staining and intracellular staining for IFN-γ. T cells were gated as Viable, $CD45.2^+$, $CD19^-$, $Ter119^-$, $NK1.1^-$, $CD3^+$ cells. NK cells were gated as Viable, $CD45.2^+$, $CD19^-$, $Ter119^-$, $CD3^-$, $NK1.1^+$ cells. N=11-12 for all.

CD4 T cells mediate their antitumor effects independently of tumor MHC II and Fas.

We have shown that CD4 T cells mediate their antitumor effects, independently of CD8 T cells, NK cells, and B cells, and that IFN-γ is necessary for this process. IFN-γ is known to induce MHC II expression on some tumor cells and a potential antitumor mechanism may involve IFN-γ-dependent induction of MHC II on tumors leading to direct recognition and killing by cytotoxic CD4 T cells. To test the role of direct recognition of MHC II on tumor cells we used CRISPR-Cas9 to disrupt the *Ab1* gene, followed by a selection protocol, so as to generate MHC II KO tumor cells, specifically RMA-*B2m*$^{-/-}$*Ab1*$^{-/-}$ cells (Figure 33A). These cells were not cloned, but employed as a population of targeted cells. To ensure that the cells indeed lacked MHC II expression, we transduced RMA-*B2m*$^{-/-}$*Ab1*$^{-/-}$ cells with a vector expressing CIITA, a transcription factor that drives MHC II expression (Mach et al., 1996). Unlike parental RMA-*B2m*$^{-/-}$ cells, RMA-*B2m*$^{-/-}$*Ab1*$^{-/-}$ cells failed to upregulate MHC II upon CIITA overexpression (Figure 33A), confirming loss of MHC II in these cells.

We then established RMA-*B2m*$^{-/-}$ or RMA-*B2m*$^{-/-}$*Ab1*$^{-/-}$ tumors in NK cell-deficient NK-DTA mice, some of which were depleted of CD4 T cells, and treated the tumors with CDNs. As shown in Figure 33B, CD4-depletion caused RMA-*B2m*$^{-/-}$ tumors to grow out faster than in non-depleted animals. Interestingly, similar results were obtained in mice with RMA-*B2m*$^{-/-}$*Ab1*$^{-/-}$ tumors (Figure 33C), indicating that CD4 T cells resist the tumors similarly even when tumor cells lack MHC II expression.

We tested whether tumor MHC II recognition was important in the rechallenge model as well. In this case, mice that had rejected RMA-*B2m*$^{-/-}$ tumors weeks before were rechallenged with either RMA-*B2m*$^{-/-}$ or RMA-*B2m*$^{-/-}$*Ab1*$^{-/-}$ tumors and no additional therapy. The MHC II-deficient tumor cells were rejected as effectively as the tumor cells with wildtype MHC II genes, and CD4 T cell-depletion completely abrogated rejection (Figure 33D). Therefore, rejection in the rechallenge model, like primary rejection, does not require MHC II to be expressed by the tumor cells.

IFN-γ has also been shown to induce FAS death receptor expression on target cells (Maciejewski et al., 1995) and it was possible that FAS may play a role in the CD4 T cell-mediated antitumor response. To examine the role of FAS, we used the RMA-*B2m*$^{-/-}$*Fas*$^{-/-}$ tumor cells generated in Chapter 3 and employed in Figure 21C. RMA-*B2m*$^{-/-}$*Fas*$^{-/-}$ tumors were rejected similarly to RMA-*B2m*$^{-/-}$ tumors in CDN-treated NK-DTA mice (Figure 33E) as well as in the rechallenge setting (Figure 33F), suggesting FAS does not play an appreciable role in CD4 T cell-mediated tumor clearance.

Finally, we considered the possible role of the death receptor-engaging TRAIL receptor, which NK cells can also express. However, we failed to observe expression by RMA-*B2m*$^{-/-}$ cells of DR5, the ligand for TRAIL, even after IFN-γ treatment (Figure 33G). The same antibody stained DR5^{+} MC-38 cells in a separate experiment (Figure 22). Therefore, it is unlikely that TRAIL plays a role in rejection of these tumor cells.

Overall these data show that CD4 T cells mediated their antitumor effects independently of tumor MHC II and FAS or DR5 death receptors, suggesting that CD4 T cells mediate their effects through other mechanisms that remain to be defined.

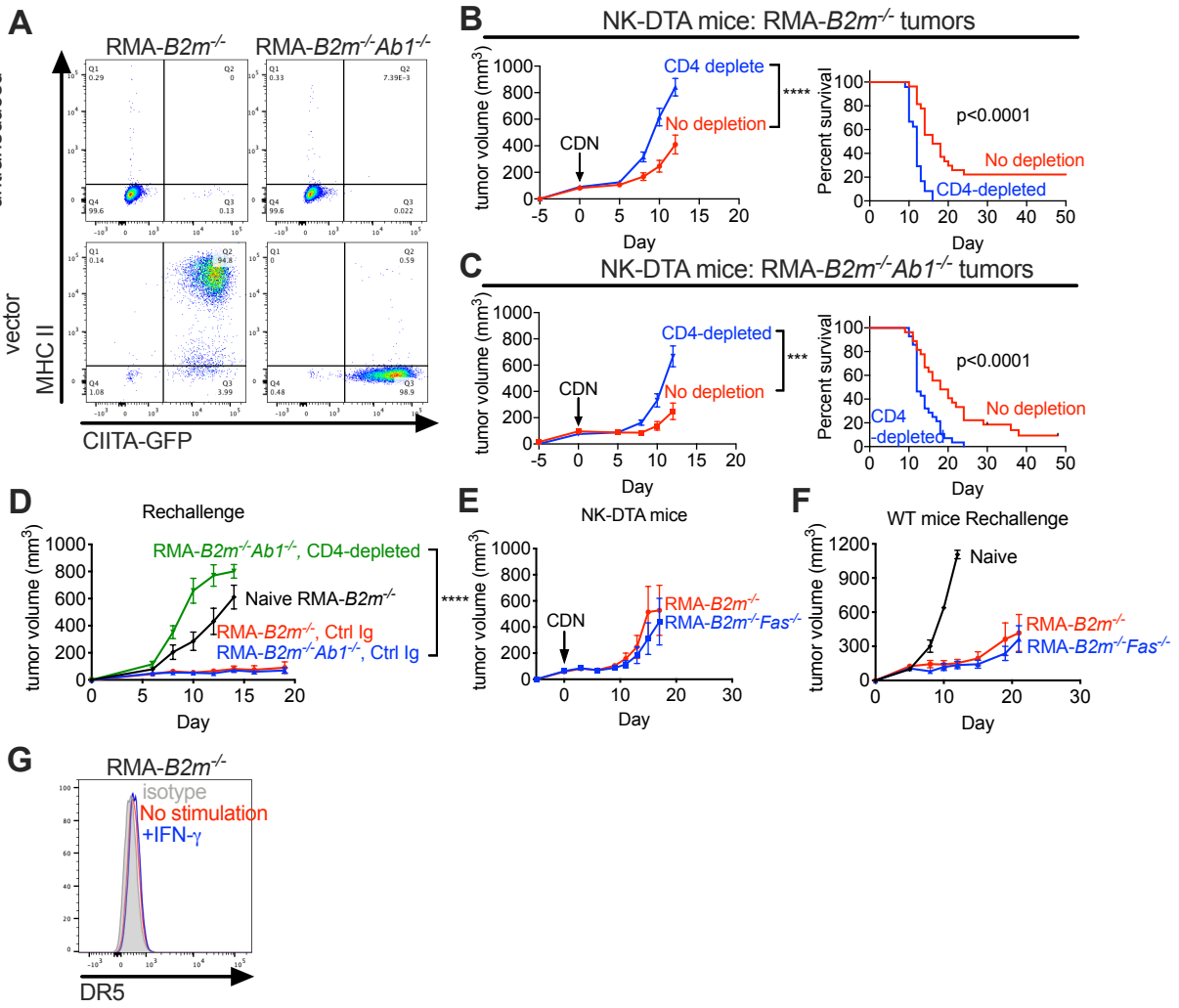

Fig. 33. CD4 T cells mediated their antitumor effects independently of tumor MHC II and Fas. **(A)** For testing MHC II expression, CIITA fused to GFP (CIITA-GFP) was expressed or not in samples of the indicated cell lines via retroviral transduction (see Methods). The cells were then stained with MHC II followed by flow cytometry. **(B and C)** RMA-*B2m*$^{-/-}$ (B) or RMA-*B2m*$^{-/-}$*Ab1*$^{-/-}$ (C) tumor cells, lacking CIITA transduction, were established in NK-DTA mice and treated with CDNs as described in Fig. 1B. Some of the mice were depleted of CD4 T cells as described in Methods. **(D)** CDN-survivor mice, at least 60 days after clearing RMA-*B2m*$^{-/-}$ tumors, were rechallenged with 2 x 10^6 RMA-*B2m*$^{-/-}$ or RMA-*B2m*$^{-/-}$*Ab1*$^{-/-}$ cells and tumor growth was monitored. Some groups were injected with CD4-depleting antibodies or control Ig as in Methods. **(E)** RMA-*B2m*$^{-/-}$ or RMA-*B2m*$^{-/-}$*Fas*$^{-/-}$ tumors were established in NK-DTA mice and treated with CDN as in Fig. 1B. **(F)** CDN-survivor mice (at least 60 days after clearing RMA-*B2m*$^{-/-}$ tumors) or naïve mice were rechallenged with 2 x 10^6 RMA-*B2m*$^{-/-}$ or RMA-*B2m*$^{-/-}$*Fas*$^{-/-}$ cells and growth was monitored. **(G)** RMA-*B2m*$^{-/-}$ cells were stimulated *in vitro* with 100 ng/ml recombinant IFN-γ overnight, followed by staining with anti-DR5 and flow cytometric analysis. For B and C, N=20-23 and data are combined

from 3 independent experiments. For D, n=4-6, for E, n=5, and for F, n=4-5. For D-G data is preliminary and has only been done once. Significance calculated with 2-way ANOVA for all. ***P < 0.001; ****P<0.0001.

Myeloid cells, such as macrophages, monocytes, and neutrophils, may be important for the CD4 T cell-mediated antitumor response.

Our data show that CD4 T cells mediate potent antitumor effects independently of tumor MHC expression, suggesting that CD4 T cells promote tumor destruction indirectly, through the activation of other cells. We also show in Figure 24 that these effects appear to be, at least partially, independent of other lymphocytes, such as NK cells, B cells, CD8 T cells, and γδ T cells. Tumor-specific CD4 T cells produce IFN-γ (Figure 27B) and IFN-γ is crucial for the CDN-induced antitumor response (Figure 31). IFN-γ is known to act on myeloid cells, especially macrophages, to induce numerous effector functions, such as production of reactive oxygen species which are necessary to limit certain bacterial infections (Boehm et al., 1997). Furthermore, macrophages isolated from tumors containing tumor-specific IFN-γ-producing CD4 T cells could kill tumor cells *in vitro* while macrophages isolated from T cell-deficient SCID mice could not (Corthay et al., 2005). This raises the possibility that tumor-specific CD4 T cells may promote tumor destruction via IFN-γ-activated myeloid cells. To test the role of myeloid cells, independently of NK cells, we depleted NK-DTA mice of various myeloid subsets before treating the tumors with CDNs. In these experiments we used the GR-1 antibody, which binds to both Ly6G and Ly6C, to deplete neutrophils and monocytes, the anti-Ly6G clone 1A8 to deplete neutrophils only, anti-IL-5 for depleting eosinophils, and Clodronate liposomes for depleting phagocytic cells, such as macrophages and dendritic cells. Depletion outcomes for GR-1 antibody and clodronate liposomes are shown in Figure 34.

Interestingly, injection of anti-GR-1 or clodronate caused tumors to grow out modestly faster than in untreated NK-DTA mice, although this was only significant for anti-GR-1 (Figure 35A). A similar outcome was observed when comparing overall survival, with mice treated with clodronate or anti-GR-1 showing reduced survival compared to untreated mice, although this was only significant for clodronate treatment (Figure 35E). Smaller differences were observed in mice treated with anti-IL-5 or anti-Ly6G, clone 1A8, but these differences were not statistically significant (Figure 35A). It is worth noting, however, that none of the animals treated with myeloid-depleting antibodies survived (Figure 35A), whereas approximately 20% of the untreated control mice survived. Notably, GR-1 antibody depletion had no effect on tumor growth in *Rag2*$^{-/-}$*Il2rg*$^{-/-}$ mice (Figure 35B), suggesting that CD4 T cells were necessary for the antitumor effects mediated by GR-1^{+} cells.

Finally, depleting various myeloid cell subsets in the rechallenge setting caused a modest reduction in the antitumor memory response (Figure 35C), but none of these effects were statistically significant, and none came close to restoring tumor growth to the rates seen in naïve mice (Figure 35C). These data suggested that some of the CD4 T cell-mediated antitumor effects may be mediated through the activation of antitumor myeloid cells, but significant antitumor mechanisms are still present. It therefore appears likely that CD4 T cells activate numerous cells or mechanisms, and that each play a part in the overall antitumor response.

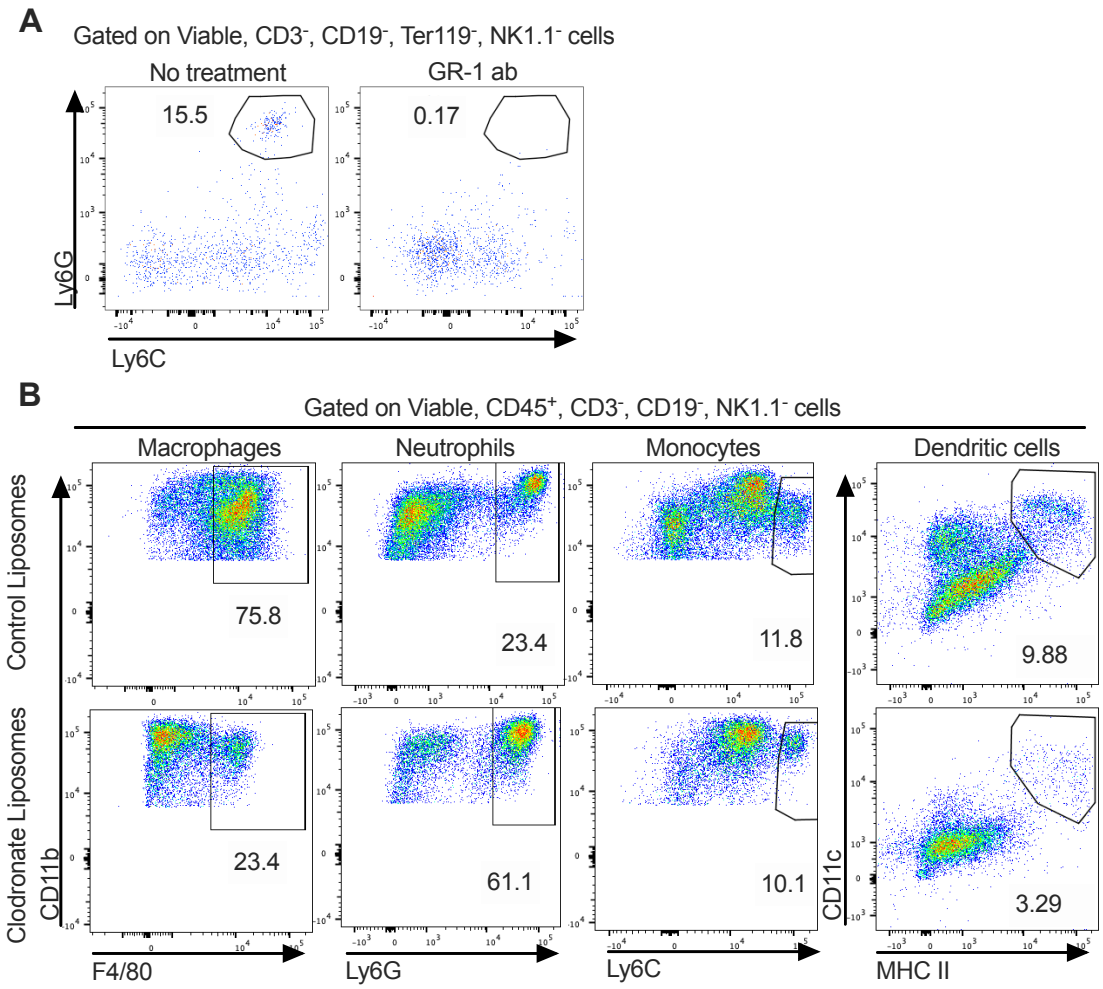

Fig. 34. Depletion outcomes using anti-GR-1 and Clodronate liposomes. (A-B) B6 mice were injected IP with 100 µg anti-GR-1 (A), 200 µl clodronate liposomes (B), or 200 µl control liposomes (B) on days -2 and -1. On day 0 blood (A) or spleens (B) were collected and single cell suspensions were stained for flow cytometry. Gating and cell percentages are shown.

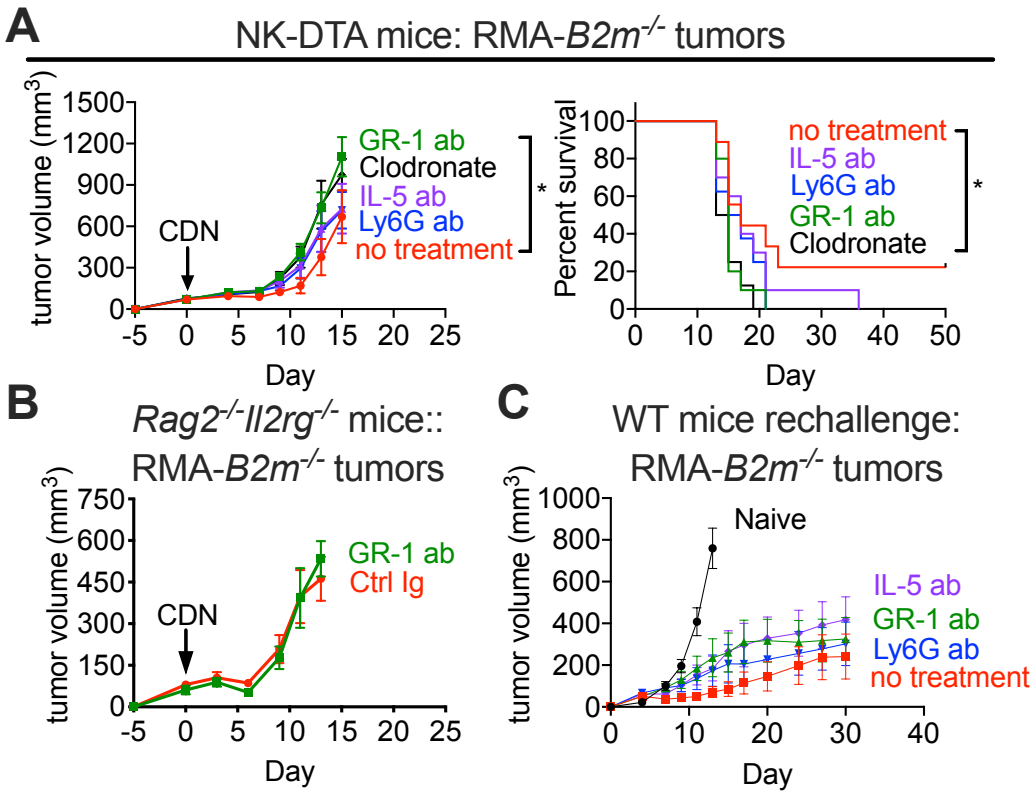

Fig. 35. Myeloid cells, such as macrophages, monocytes, and neutrophils, may be important for the CD4 T cell-mediated antitumor response. (A-B) RMA-*B2m*$^{-/-}$ were established in NK-DTA (A) or *Rag2*$^{-/-}$*Il2rg*$^{-/-}$ (B) mice, followed by depletions of various myeloid populations, and treatment of the tumors with CDNs. Tumor growth and/or survival was measured as described previously. GR1 antibody depletes neutrophils and some monocytes, Ly6G antibody depletes neutrophils, IL-5 antibody depletes eosinophils, and Clodronate treatments deplete phagocytic cells, including macrophages and dendritic cells. **(C)** WT CDN-survivor mice (at least 60 days after tumor clearance) were depleted as in A, and rechallenged with 2 x 10^6 RMA-*B2m*$^{-/-}$ cells. Naïve mice were implanted in parallel and tumor growth was monitored. Panels A and C are each combined from two independent experiment, n=7-10. The experiment in panel B has been done only once, n=5-6. *P<0.05.

Discussion

The data presented in this chapter show that CD4 T cells mediate powerful antitumor immune responses, independent of CD8 T cells, against MHC-deficient RMA-*B2m*$^{-/-}$ tumors induced by CDNs. CD4 T cells promoted antitumor effects independently of other lymphocytes, including NK cells, B cells, and γδ T cells. Interestingly tumor killing was independent of tumor MHC II and FAS death receptor expression, indicating that direct tumor recognition may not be necessary, and that CD4 T cells may act by inducing other cell(s) in the tumor microenvironment to promote tumor destruction or via soluble mediators.

CDNs were shown to prime tumor-specific CD4 T cells with a Th1-like phenotype, expressing Tbet, IFN-γ, IL-2, and TNF-α. Furthermore, CDN treatments enhanced effector functions and reduced the expression of inhibitory and checkpoint molecules such as, TOX, PD-1, Tim-3, Lag-3, and TIGIT on tumor-specific CD4 T cells, indicating that CDN treatments promoted a more functional and less exhausted pool of antitumor CD4 T cells. A key factor for the antitumor response was IFN-γ, although its mechanism of action remains unclear as it appeared to be able to act both on the tumor cells directly or on the host to mediate the response. One role for IFN-γ in the CDN-induced response may be to promote activation of tumor-killing myeloid cells, as the antitumor response was partially reduced upon depletion of various myeloid subsets. Overall the results documented in this chapter make clear that CD4 T cells mediate potent antitumor effects independently of classic cytotoxic cells, such as CD8 T cells and NK cells.

CD4 T cells are an interesting, but often overlooked, target for immunotherapy. CD4 T cells have been shown to promote fully functional antitumor CD8 T cell responses (Borst et al., 2018; Ossendorp et al., 1998) and MHC II-restricted tumor neoantigens are important for promoting effective antitumor immunity (Alspach et al., 2019; Kreiter et al., 2015). Furthermore, in human melanoma patients receiving anti-PD-1 or anti-PD-L1 therapy, tumor MHC II expression was associated with increased infiltration of CD4 and CD8 T cells into tumors and enhanced overall survival (Johnson et al., 2016). CD4 T cells have also been shown to promote antitumor effects independently of CD8 T cells (Greenberg et al., 1985). It was concluded in one set of studies that antitumor effects were mediated through direct recognition and killing via tumor-expressed MHC II (Quezada et al., 2010; Xie et al., 2010) though this was not definitively established. In other cases it was concluded that CD4 T cells acted indirectly, most often via IFN-γ acting on other immune cells (Corthay et al., 2005; Hung et al., 1998; Mumberg et al., 1999; Qin and Blankenstein, 2000).

Most cancer immunotherapies focus on activating CD8 T cell responses, but tumors may evade CD8 T cells by extinguishing expression of MHC I molecules. In the case of CD4 T cells, evasion through loss of MHC may be more difficult, especially given that CD4 T cells can mediate potent antitumor effects independently of tumor MHC II expression. CD4 T cells are also known to orchestrate the effector functions of many different cell types. Tumors may evolve to escape one response, but escaping several different antitumor effectors becomes increasingly unlikely. A better mechanistic understanding of the antitumor effects of CD4 T cells will likely enable the development of new therapies targeting these T cell responses.

Recently there has been increased interest in STING agonists in cancer immunotherapies. The antitumor effects of STING agonists have primarily been attributed to CD8 T cells (Curran et al., 2016; Demaria et al., 2015; Sivick et al., 2018) with less focus being given to their impact on CD4 T cell responses. In this chapter, we showed that, similar to CD8 T cells, CDNs promote the priming of antitumor CD4 T cells as well as enhancing their effector functions. CDNs seemed to promote Th1-like CD4 T cells capable of producing IFN-γ, which previous studies have shown to be important for antitumor responses (Corthay et al., 2005; Hung et al., 1998; Mumberg et al., 1999; Qin and Blankenstein, 2000). We also showed that tumor-specific CD4 T cells in CDN-treated mice exhibit a less exhausted phenotype, with decreased expression of TOX, PD-1, Tim-3, Lag-3, and TIGIT, a finding that, to our knowledge, has not been previously reported for either CD4 or CD8 T cells.

A major mediator of the antitumor effects of STING activation are type I IFNs and in Chapter 3 we showed that type I IFN is crucial for CDN-induced NK cell activation and NK-mediated tumor clearance. In this chapter we showed that blocking type I IFN signaling caused tumors in NK cell-deficient NK-DTA mice to grow out faster, suggesting that type I IFN is also important for CD4 T cell-mediated responses. Multiple studies have shown that type I IFN is important for the priming of tumor-specific CD8 T cells (Demaria et al., 2015; Sivick et al., 2018) but we found, surprisingly, that CD4 T cell priming was not reduced in mice deficient for type I IFN signaling, and there were actually more tumor-specific CD4 T cells in CDN-treated *Ifnar1*$^{-/-}$ mice than in WT mice. While the reason for this increase remains unclear, type I IFN is known to have antiproliferative and pro-apoptotic effects in certain contexts (Bekisz et al., 2010) and it is possible that this explains the reduction in tumor-specific CD4 T cells in IFNAR1-sufficient WT mice. We also found that splenocytes from *Ifnar1*$^{-/-}$ mice produced similar amounts of IL-2 and TNF-α compared to WT mice, indicating type I IFN is unnecessary for acquisition of these effector functions. Interestingly splenocytes from *Ifnar1*$^{-/-}$ mice showed a significant decrease in their ability to produce IFN-γ after tumor peptide stimulation. This finding is consistent with previous studies showing that the presence of type I IFN during CD4 T cell priming promotes the development of IFN-γ-producing CD4 T cells (Brinkmann et al., 1993). Type I IFN has also been shown to suppress Th2 and Th17 developmental programs (Harrington et al., 2005; Huber et al., 2010), further biasing the development of Th1 CD4 T cells. Overall these data suggest that type I IFN is important for the CD4 T cell-mediated antitumor response because it helps drive the development of tumor-specific Th1 CD4 T cells capable of producing IFN-γ.

Similar to previous studies (Corthay et al., 2005; Hung et al., 1998; Mumberg et al., 1999; Qin and Blankenstein, 2000), IFN-γ was found to be a major mediator of the antitumor response and mice lacking IFN-γ were unable to clear their primary tumors. IFN-γ was also essential for the antitumor memory response. Mixed bone marrow chimera experiments suggested that the relevant source of IFN-γ was from *Rag2*-dependent cells and peptide stimulation experiments showed that tumor-specific CD4 T cells produce IFN-γ. These data support the hypothesis that CD4 T cells are the relevant source of IFN-γ driving MHC I-deficient antitumor immunity.

Interestingly our data suggest that IFN-γ can act on either tumor cells or host cells to mediate its effects. One potential explanation is that IFN-γ induces the production of a common

antitumor effector molecule(s) by both tumor and host cells, and that either can supply it for productive antitumor responses; according to this hypothesis, the putative effector molecule either destroys cancer cells directly or elicits other immune cells to do so. Alternatively, IFN-γ may elicit distinct antitumor mechanisms when it acts on tumor cells versus host cells, which act somewhat redundantly to mediate the antitumor response. For example, IFN-γ may act partly by promoting the activation of host antitumor myeloid cells (discussed below) and also partly by inducing MHC II on tumors, thus allowing direct recognition by CD4 T cells. One way to test this hypothesis would be to examine CDN-induced antitumor effects in *Ifngr1*$^{-/-}$ mice with MHC II KO tumors. If CDN-induced tumor rejection were impaired in this scenario, it would suggest that IFN-γ acts partly by inducing MHC II on tumor cells to enable direct CD4 T cell recognition and partly on host cells to mediate a distinct antitumor mechanism.

IFN-γ is an extremely pleiotropic cytokine, having a wide range of effects on numerous cell types. One potential effect of IFN-γ is the activation of antitumor myeloid cells and several groups have claimed roles for antitumor myeloid cells, especially macrophages, in CD4 T cell-mediated antitumor responses (Corthay et al., 2005; Hung et al., 1998; Mumberg et al., 1999). In support of a role for myeloid cells, we documented modest decreases in tumor rejection upon depletion of phagocytes with clodronate liposomes or after treatments with anti-GR-1 Ab, effects that were lost in *Rag2*$^{-/-}$*Il2rg*$^{-/-}$ mice, suggesting that CD4 T cells were necessary for the antitumor effects of these cells. However, depletion only caused minor differences in growth, suggesting other mechanisms exist. Clearly IFN-γ is a key driver of the antitumor response mediated by CD4 T cells in CDN-treated mice, but we lack a complete mechanistic understanding of how it mediates tumor cell destruction. Therefore, further research will be necessary to define the relevant antitumor mechanisms mediated by IFN-γ in the CD4 T cell-mediated antitumor response.

CD4 T cells were able to promote tumor destruction independently of tumor MHC II expression, indicating that they mediated their antitumor effects indirectly, likely via IFN-γ. CD4 T cells have long been known to enhance the effector functions of other cells, such as B cells and NK cells. We did see a partial defect in the tumor rechallenge response in B cell-deficient *Ighm*$^{-/-}$ mice, suggesting B cells may mediate some antitumor effects. These could be due to loss of tumor-specific antibodies or because B cells can act as antigen presenting cells to T cells. Consistent with a role for antibodies, serum from rechallenged mice was capable of providing small amounts of protection against RMA-*B2m*$^{-/-}$ tumors. Interestingly, there were still significant antitumor effects in the absence of NK cells, B cells, and γδ T cells, suggesting that other cell types play larger roles. A potential clue is that the response was defective in perforin-deficient mice, although the identity of the cells that must express perforin for the antitumor response remains unclear. Perforin is not thought to be expressed by myeloid cells (Pipkin et al., 2010; Voskoboinik et al., 2006) and the antitumor effects in our model were independent of NK cells, CD8 T cells, and γδ T cells. NKT cells can also kill via perforin-mediated cytotoxicity (Pipkin et al., 2010; Voskoboinik et al., 2006). We did not directly address the role of these cells in our study.

Overall this chapter details the antitumor responses mediated by CD4 T cells independently of NK cells, B cells, and γδ T cells. Type I IFN was important for the antitumor effects and was necessary to promote full antitumor effector functions of tumor-specific CD4 T

cells, especially production of IFN-γ. CD4 T cells appeared to mediate their antitumor effects independently of tumor MHC II, suggesting indirect mechanisms, likely via secretion of IFN-γ, although the exact mechanisms of tumor killing in our model remain unknown. CD4 T cells are capable of promoting the activation of numerous cell types and it is likely that multiple cell types and effector molecules play a role in the antitumor response. The results are important for understanding how CD4 T cells mediate antitumor responses against MHC-deficient tumors. Our findings argue that more attention should be paid to these cells when designing future immunotherapies.

Chapter 5
A screen to identify novel ligands for NK cell-activating receptors

Abstract

NK cells are innate lymphocytes capable of killing virus-infected cells and tumor cells. NK cell activation is triggered upon ligand recognition by an assortment of germline-encoded activating receptors. Generally, NK activating ligands are not usually expressed on normal, healthy cells, but can be induced under conditions of cellular stress, often occurring during tumorigenesis and viral infections. NK cells express numerous activating receptors, but the cellular ligands for several of these receptors remain undefined. In this Chapter I will detail multiple screens employing chimeric antigen receptor (CAR) T cells expressing NK cell activating receptors as selecting agents, with the goal of identifying novel cellular ligands for these receptors. We successfully generated multiple NK receptor CAR T cells and performed several screens using the NKp44 and NKp46 CAR T cells. These screens resulted in lists of genes, that when mutated, were found to be enriched in the surviving cellular population. Future work will be needed to validate the hits from these screens and perform additional screens if necessary.

Introduction

In the previous chapters we detailed powerful CDN-induced antitumor effects against CD8 T cell-resistant, MHC-deficient tumors mediated by NK cells and CD4 T cells. CDNs are powerful immune stimulating agents, capable of greatly increasing antitumor effector functions of many different cells. In addition to enhancing antitumor immune cell activation, if an immunotherapy is to be successful it is crucial that the activated cells are capable of recognizing the tumor cells to promote tumor destruction. In this chapter I will discuss screens aimed at identifying novel NK cell activating ligands, expressed by tumor cells, necessary for NK cell recognition and killing.

As discussed in the introduction, NK cells are innate immune lymphocytes capable of killing virus infected and tumor cells (Vivier et al., 2011). Unlike T and B cells, which have a single rearranging antigen receptor with the potential to recognize a near limitless number of antigens, NK cells utilize a variety of germline-encoded activating receptors to engage targets. The most widely studied NK cell activating receptor is NKG2D and NKG2D ligands are well characterized, consisting of MULT1 and the RAE-1 and H60 families in mice, and MICA, MICB, and the ULBP family in humans (Raulet et al., 2013). These molecules are not normally expressed at appreciable levels on normal, healthy cells, but can be induced by cellular stress associated with viral infections and tumorigenesis (Marcus et al., 2014).

In addition to NKG2D, NK cells possess several other activating receptors. One group of activating receptors includes the so-called natural cytotoxicity receptors (NCRs), NKp30, NKp44 and NKp46. Like NKG2D, when engaged, the NCRs trigger NK cell activation and target cell lysis (Kruse et al., 2014). Human NK cells express all three NCRs (Marcus et al., 2014), although NKp44 is only induced upon activation (Vitale et al., 1998). In contrast NKp46 is the only of these three NCRs that is expressed in the mouse. The NCRs were originally named for their ability to mediate lysis of numerous tumor cell lines *in vitro* (Pende et al., 1999; Sivori et al., 1999; Vitale et al., 1998). However, the identity of the ligands they recognize on tumor cells remains an area of active research. B7-H6 and BAT3 are proposed ligands for NKp30 (Brandt et

al., 2009; Pogge von Strandmann et al., 2007), while an isoform variant of MLL5 and a secreted protein, PDGF-DD, have been reported to be ligands for NKp44 (Barrow et al., 2017; Baychelier et al., 2013). These ligand identifications have not been confirmed by other investigators, however. Furthermore, the cellular ligand(s) for NKp46 remain unclear. One recent report claimed that compliment factor P (CFP) is a ligand for NKp46 (Narni-Mancinelli et al., 2017), but this study only examined one cell line and it remains unclear how relevant CFP is for NKp46-mediated killing of other tumor cell lines.

Here we detail the design and implementation of screens aimed at identifying novel cellular ligands for NK cell activating receptors. Specifically, we have employed chimeric antigen receptor T cells expressing CARs that incorporate NK cell activating receptors (NK CAR T cells) as selecting agents against human tumor cell lines mutagenized with a retroviral gene-trap or stably expressing CRISPR-Cas9 and a genome-wide guide library. Our hypothesis is that the NK CAR will direct T cell-mediated killing of tumor cells expressing the ligand(s) for the chosen NK cell receptor. Tumor cells lacking the ligand(s) genes, should the ligand be a protein, and/or cells lacking genes encoding enzymes involved in production or expression of the ligands, should confer enhanced survival, thus expanding their relative abundance within the population. After multiple rounds of selection, the surviving cells can be deep-sequenced, and mutated genes enriched in the surviving population can be validated individually on the basis of whether gene disruptions or knockdowns in the tumor cells confer resistance to killing and/or decreased NK CAR T cell cytokine responses in cocultures.

NK cells are important for cancer immunosurveillance (Guerra et al., 2008) but a major roadblock in the understanding of NK cell biology is that the ligands for several important NK activating receptors remain unknown. This Chapter outlines a method that may be useful for detecting ligands, without bias, whether they are protein monomers, dimers, or non-proteinaceous molecules. Identification of natural killer cell ligands will provide a deeper understanding of the role of NK cells in the immune response. Furthermore, success using this approach could be adapted to find ligands for other orphan receptors as well as regulatory pathways associated with their upregulation.

Results

Design and characterization of chimeric antigen receptor T cells expressing human NCRs.

In order to generate T cells capable of killing via NK cell NCRs, chimeric antigen receptor constructs containing the extracellular signaling domains of human NKp30, NKp44, or NKp46 were fused to the transmembrane and intracellular signaling domain of human CD28, followed by the intracellular signaling domain of human CD3ζ (NKp30 CAR, NKp44 CAR, and NKp46 CAR, respectively) (Figure 36A). The CAR constructs were then cloned into a lentiviral vector backbone upstream of an IRES-mCherry sequence and driven by the EF-1α promoter. Viral vector particles, pseudotyped with the VSV-G envelope glycoprotein, were then generated. To transduce human T cells, PBMCs were stimulated with beads containing anti-CD3 and anti-CD28 followed by spinfection with viral supernatants in the presence of polybrene. Transduced NK CAR T cells were then single-cell sorted based on mCherry positivity and CAR expression was verified by flow cytometry (Figure 36B). To test if the transduced NK CAR constructs could

stimulate T cell responses, we stimulated the NK CAR T cells with plate-bound antibodies specific for each NCR. NK CAR T cells stimulated with an antibody specific to their individual NCR expressed both CD107a and IFN-γ, while T cells transduced with empty vector had no response (Figure 36C), indicating that the transduced CARs could stimulate T cell responses.

We next tested if the NK CAR T cells could respond to coculture with tumor cells. Coculturing all three NK CAR T cells with the HAP1 cell line (Carette et al., 2011; Gowen et al., 2015) resulted in robust TNF-α and IFN-γ production, while no responses were seen in T cells transduced with empty vector alone (Figure 36D). Similar responses were seen upon coculture with the colorectal carcinoma cell line, HCT116, although the NKp30 NK CAR T cells responded very poortly to the those cells (Figure 36D), indicating that HCT116 cells may not display NKp30 ligands robustly. In addition, NKp44 and NKp46 CAR T cells, but not NKp30 CAR T cells, exhibited potent *in vitro* cytotoxicity against HCT116 cells, consistent with the effects seen in the cytokine production assay (Figure 36E). Overall these data show that our NCR CAR T cells promote CAR-specific T cell activation and can potently kill tumor cells *in vitro,* suggesting that these cells will be appropriate tools for screens to identify currently unknown NCR ligands.

NKp46 is the only NCR expressed on both mouse and human NK cells, suggesting it is key to NK cell function in multiple species. Previous reports have indicated that NKp46 ligands are found on many tumor cell lines from multiple tissue origins (Arnon et al., 2004; Pende et al., 1999; Pessino et al., 1998; Sivori et al., 2000; Sivori et al., 1999; Vitale et al., 1998), suggesting that it is especially important for tumor cell recognition. Consistent with these reports, nearly every human tumor cell line we tested induced the production of TNF-α from the NKp46 CAR T cells (Figure 36F). Some studies had indicated that human NKp46 could also interact with ligands on mouse tumor cell lines, especially B16 melanoma cells (Glasner et al., 2012; Lakshmikanth et al., 2009), but we did not detect activation of our human NKp46 CAR T cells upon coculture with any mouse cell line tested, including two B16 variants (Figure 36F). Overall these data support previous studies suggesting that many tumors express NKp46 ligands and that NKp46 ligands are important for NK-mediated tumor recognition, underscoring the great need to identify the currently unknown ligand(s) for this receptor.

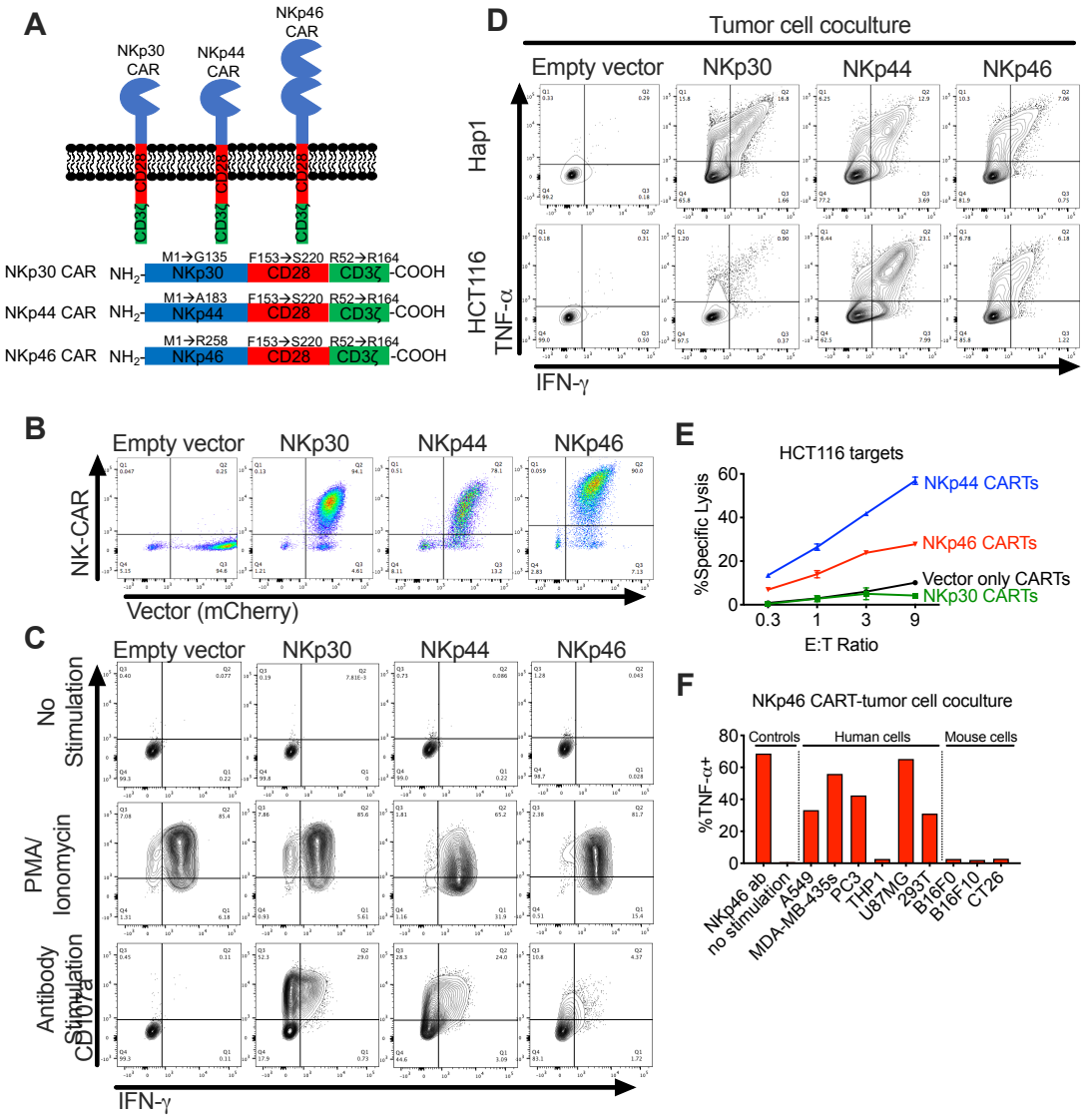

Fig. 36. Design and characterization of chimeric antigen receptor T cells expressing human NCRs. (A) Schematic depicting the design of NK-CARs. Amino acid residues for each domain are shown. **(B)** Expression of human NKp30, NKp44, and NKp46 on sorted mCherry^{+} T cells. Empty vector control stained negative for all NCRs. **(C-D)** Sorted NK-CAR T cells, or empty vector control T cells, were stimulated with either NCR-specific plate-bound antibody, PMA+Ionomycin, or left unstimulated, for 5 hours, in the presence of Brefeldin A, Monensin and anti-CD107a, followed by intracellular staining for IFN-γ. **(D)** Sorted NK-CAR T cells or an empty vector controls were stimulated with the indicated tumor cell line for 5 hours in the presence of Brefeldin A and Monensin followed by intracellular staining for IFN-γ and TNF-α. **(E)** Sorted NK-CAR or empty vector T cells were used as effectors in a ^{51}Cr cytotoxicity assay with HCT116 target cells. Assay was performed in technical triplicate. Error bars are shown but are too small to see. **(F)** Sorted NKp46 CAR T cells were stimulated with the indicated tumor cell lines as in D, followed by intracellular staining for TNF-α. B-D are representative of 3 independent experiments. E is representative of 2 independent experiments. F as only been done once.

CRISPRi-based screens in HCT116 cells to identify novel NKp46 ligands.

Given its broad expression profile and that there are no known cellular ligands for NKp46 we decided to focus on screens using the NKp46 CAR T cells. We previously showed that coculture with HCT116 tumor cells triggered activation of the NKp46 CAR T cells (Figure 36D) and HCT116 cells were efficiently killed *in vitro* by NKp46 CAR T cells (Figure 36E). Based on this data, we initially chose HCT116 cells cells as a screening line.

In order to perform screens on a large scale we needed to develop a protocol that would efficiently expand the NKp46 CAR T cells so as to have enough cells to perform the screen. Initially we tried repeated stimulation with anti-CD3/anti-CD28 beads. This gave us modest expansion (~10-fold) but did not result in the numbers needed to easily perform screens. Eventually we contacted Tom Schmitt in Phil Greenberg's lab at Fred Hutchinson Cancer Research Center in Seattle and he shared with us their T cell expansion protocol. Using the Greenberg Lab's Rapid Expansion Protocol (REP) (detailed in methods) we achieved CAR T cell expansion on the order of 500-1000-fold, thus enabling us to generate enough T cells to perform the screen. Interestingly, at first we were unable to generate $CD8^+$ NKp46 CAR T cells. After the REP, only $CD4^+$ NKp46 cells remained. In contrast, the other NK CAR T cells, such as NKp44 CAR T cells, included both $CD4^+$ and $CD8^+$ populations after the REP. This finding was corroborated using T cells from a different donor, leading us to speculate that activated $CD8^+$ T cells may possess a ligand for NKp46, thus triggering fratricide among the $CD8^+$ NKp46 CAR T cells. This would be consistent with the previous finding that NK cells can kill activated T cells to help regulate immune responses (Waggoner et al., 2011). Fortunately, $CD4^+$ NKp46 CAR T cells efficiently killed HCT116 cells (Figure 37A) and these cells were therefore used for the initial screen. Note that for later screens we were able to generate $CD8^+$ NKp46 CAR T cells after the REP. These were created from separate donors from the first two used. Why we were initially unable to generate CD8+ NKp46 CAR T cells remains an unresolved question although it is interesting to speculate that variable expression of the NKp46 ligand on T cells from different donors may play a role.

For the first screen we used a CRISPRi-based approach in collaboration with the Innovative Genomics Institute (IGI) at UC Berkeley. Unlike conventional CRISPR-Cas9, which causes DNA double stranded breaks, CRISPRi utilizes a catalytically inactive form of Cas9 (dCas9) fused to a transcriptional silencing KRAB domain (dCas9-KRAB), thus repressing transcription of guide-targeted genes rather than knocking them out (Gilbert et al., 2014). dCas9-KRAB was stably expressed in HCT116 cells and single cell clones capable of robust silencing were generated by the IGI (available at the UC Berkeley TC Facility). In collaboration with Benjamin Gowen (IGI) and Natalie Wolf (Raulet laboratory), HCT116-dCas9 cells were transduced, in duplicate, with a lentiviral CRISPRi guide library containing ~100,000 guides (5 guides/gene), obtained from the Weisman Lab at UCSF (Gilbert et al., 2014). After selection in puromycin for 7 days, a total of 100×10^6 HCT116-dCas9 cells for each replicate were seeded into two T175 flasks at 50×10^6 per flask. An additional flask of 50×10^6 cells of each replicate was plated for controls. The next morning the media was removed and fresh media containing 50×10^6 $CD4^+$ NKp46 CAR T cells was added to each flask (100×10^6 total CAR T cells for each replicate). No CAR T cells were added to the control flasks. After 6 hours, approximately 50% of the HCT116-dCas9 cells were dead based on remaining adherent cells. At this time the CAR

T cells were removed, the cells washed with PBS, and fresh media added. Surviving cells were then expanded for 5 days, with PBS washed and media changes occurring every day. Over the next few days, continued death was observed in the remaining cells, as evidenced by their lifting from the plate. The cells were then pelleted and genomic DNA was extracted from 5 x 10^6 NKp46 CAR T-selected cells and 30 x 10^6 unselected cells followed by sequencing. The top 50 hits, sorted by phenotype score (recommended by IGI), are shown in Figure 37B.

Initially, the top 10 hits were chosen for validation and HCT116-dCas9 cells were generated with a single guide specific for each of the hits. The chosen guides were the ones that gave the maximal effects in the screen. Two assays were chosen for guide validation. One assay was to examine HCT116-dCas9 survival upon CAR T cell coculture and the other was to assess CAR T cell effector functions (ie TNFα production) after stimulation with HCT116-dCas9 cells in a coculture.

To assess each guide's impact on tumor cell survival we used a flow cytometry-based killing assay. For this experiment equal numbers of BFP^+ $guide^+$ HCT116-dCas9 cells were mixed with GFP^+ no guide cells. Impact on killing was measured by examining the ratio of BFP^+ cells to GFP^+ cells. For example, if a guide had no effect on survival, BFP^+ and GFP^+ cells would be killed equally well, thus yielding a BFP/GFP ratio of ~1. If a guide caused the cell to become more resistant to killing, then the ratio would be expected to be >1, as the GFP^+ cells would be killed more readily than the BFP^+ cells. Figure 37C depicts the outcome of the assay on the top 10 hits. Cells expressing BFP without a guide were used as controls. Guides targeting CASP8, BID, and FADD led to a BFP/GFP ratio of >1 (Figure 37C), which is expected given their known role in promoting cell death. Suppression of KHDRBS1, also known as Sam68, also enhanced tumor survival. A previous report indicated that Sam68 is part of the cytoplasmic caspase-8-FADD complex and helps promote apoptosis (Ramakrishnan and Baltimore, 2011), which would be consistent with enhanced survival upon its inhibition. Targeting STAT1, which is important for IFN-γ-mediated signaling, also led to enhanced tumor cell survival (Figure 37C). IFN-γ is known to promote a variety of antitumor effects, including sensitizing cells to apoptosis (Castro et al., 2018), and our results are consistent with such a role. Several other components of the IFN-γ signaling pathway were also represented among the hits (Figure 37B), further implicating its importance.

It did not escape our attention that cells may become resistant to CAR T killing but still retain expression of the NKp46 ligand(s). To address this issue, we also performed NKp46 CAR T cell-HCT116-dCas9+guide cell coculture experiments. If the CAR T cells lost the ability to recognize the tumor cells (as might be expected for guides targeting a NKp46 ligand or genes involved in its regulation) they should become less activated in the cocultures, and produce less cytokine. We selected TNF-α production as a readout because its expression was typically higher than other cytokines, such as IFN-γ (Figure 36D). In contrast to our findings using the killing assay, we did not observe a reduction in TNF-α production for any of the top 10 screen hits (Figure 37D), suggesting that these genes are important for promoting cell death in general but are not important for NKp46-mediated tumor recognition.

We next tested the top 100 predicted membrane-bound hits from the screen to extend the analysis. Again, the top guide in the screen for each gene was cloned into a viral vector and 100

different knockdown HCT116-dCas9 cell lines were generated. Each knockdown cell line was then tested individually by analyzing TNF-α production by NKp46 CAR T cells in a coculture assay as described above. Unfortunately, only 2 of the 100 guides tested resulted in a robust reduction in TNF-α. These were guides targeting ICAM1 and CR2 (Figure 37E). Furthermore, ICAM1 and CR2 knockdown also resulted in reduced HCT116-dCas9 killing in a ^{51}Cr assay (Figure 37F). These data indicate that expression of these genes is important for both recognition and killing by NKp46 CAR T cells. ICAM-1 is an important adhesion molecule that binds LFA-1 on immune cells and is important for mediating cell-cell interactions (including cytotoxicity) and is therefore not a surprising hit in the screen. CR2, also known as complement receptor 2, is a receptor for derivatives of C3, such as C3d, of the complement pathway and is important for promoting B cell responses to antigens covalently attached to C3d (Hannan, 2016). CR2 has also been reported to be a receptor for Epstein-Barr virus (Fingeroth et al., 1984) making it an interesting potential ligand for NK cell activating receptors, given the important role of NK cells during viral infections. However, upon further research we found that complement receptor inhibition has been shown to reduce ICAM-1 expression, although mechanistically how this occurs was not shown (Atkinson et al., 2010). We then examined ICAM-1 expression on CR2-knockdown HCT116 cells and found that ICAM-1 was greatly reduced in these cells (data not shown). Therefore, a likely explanation as to why CR2 knockdown causes reduced NKp46 CAR T cell activation and killing is due to a reduction in surface ICAM-1 expression and not because CR2 is a ligand for NKp46, although we have not ruled out this possibility.

Because of the lack of progress on hits from this, CRISPRi-based, screen we decided to carry out a second screen, using a haploid cell line, that has been used successfully by previous members of the lab (Gowen et al., 2015).

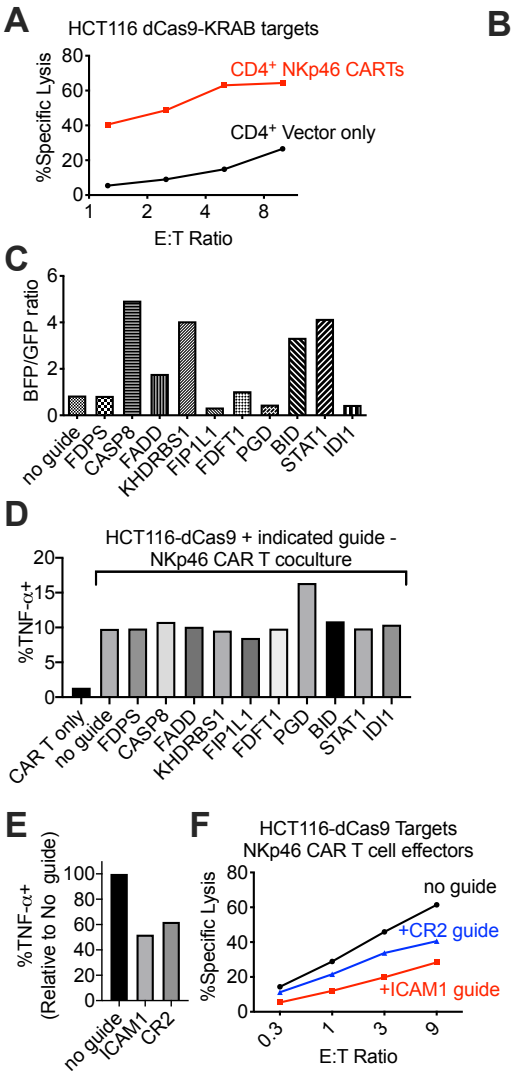

B

Gene	average phenotype of strongest 3	Mann-Whitney p-value
FDPS	4.911297801	0.002734201
CASP8	4.608218108	0.000110564
FADD	3.225923782	0.06545688
KHDRBS1	2.997504134	0.011089663
FIP1L1	2.925354284	0.000112909
FDFT1	2.807716312	0.001256913
PGD	2.676361739	0.000112515
BID	2.606157907	0.010379618
STAT1	2.598075348	0.0001485
IDI1	2.591865143	0.000216648
PRPF38B	2.586287182	0.000121491
IFNGR1	2.492551271	0.001758316
EIF4G1	2.443122059	0.000731065
IFNGR2	2.438981812	0.007967462
JAK2	2.409603287	0.000141019
ILF2	2.316315635	0.000866326
TRRAP	2.312582351	0.000157971
SRPRB	2.28531565	0.020881022
RPS13	2.164029154	0.014891898
NFKB2	2.159913673	0.000586374
NONO	2.125500785	0.000130685
ICAM1	2.112508079	0.000124054
WDR75	2.090758745	0.017865016
SCAF8	2.065954483	0.000119394
YLPM1	2.020326826	0.000120648
NEDD8	2.015743672	0.176769967
MAX	1.989880648	0.008528772
RPP40	1.974312958	0.002865592
RNF41	1.904602812	0.000137175
LEO1	1.891741819	0.009125179
CHD2	1.891605869	0.000155818
SFPQ	1.885607343	0.000424206
SP1	1.851277645	0.000146974
MTOR	1.837693082	0.001582971
RPRD2	1.820038328	0.00378997
SRFBP1	1.812792622	0.001044194
TRMT61A	1.807627639	0.04595038
VN1R4	1.803712626	0.005938979
ELAVL1	1.786736577	0.018333735
RPS6	1.742203993	0.004621243
KTI12	1.732306943	0.003718411
UTP11L	1.71868777	0.000207365
FUT6	1.696794816	0.040615252
TAF15	1.696575953	0.090031196
PNISR	1.692360257	0.000586374
STX1A	1.664431433	0.057407089
JAK1	1.642803026	0.003387999
RPS24	1.634535626	0.000703593
GNPAT	1.629184458	0.000468633
pseudo_3165	1.612285101	0.019776383

Fig. 37. HCT116 CRISPRi screen with NKp46 CAR T cells. (A) CD4$^+$ NK-CAR T cells were used as effector cells in a ^{51}Cr cytotoxicity assay with HCT116-dCas9-KRAB target cells. Assay was performed with technical triplicates. Error bars are shown but are too small to see. Representative of 3 independent experiments. **(B)** Genes hits that were found to be significant in the CD4$^+$ NKp46 CAR T cell HCT116 CRISPRi screen. **(C)** 2.5 x 10^4 HCT116-dCas9-KRAB cells expressing GFP were seeded in a flat bottom 96 well plate along with 2.5 x 10^4 HCT116-dCas9-KRAB cells expressing BFP and transduced with a lentivirus expressing guide sequences for the indicated genes. The next day the

media was removed and fresh media containing 10^5 $CD4^+$ NKp46 CAR T cells was added and killing was allowed to continue for 8 hours after which the cells were washed with PBS and fresh media was added. 3 days later the surviving cells were analyzed by flow cytometry and the BFP/GFP ratio was calculated. Only one well per condition and experiment only done once. **(D)** 10^5 $CD4^+$ NKp46 CAR T cells were stimulated with 10^5 HCT116-dCas9-KRAB cells expressing the indicated guide sequences for 5 hours followed by intracellular staining for TNF-α. Data shown is from one well and is representative of 2 independent experiments **(E)** 10^5 $CD4^+$ NKp46 CAR T cells were stimulated with 10^5 HCT116-dCas9-KRAB cells expressing the indicated guide sequences for 5 hours followed by intracellular staining for TNF-α. Data shown is from one well and is representative of 3 independent experiments. **(F)** $CD4^+$ NK-CAR T cells were used as effector cells in a ^{51}Cr cytotoxicity assay with HCT116-dCas9-KRAB cells expressing guide sequences for the indicated gene as target cells. Assay was performed with technical triplicates. Error bars are shown but are too small to see. This experiment was only done once.

Retroviral gene-trap mutagenesis screen in HAP1 cells to identify novel NKp46 ligands.

After failing to find a ligand for NKp46 using the CRISPRi-based screen we decided to take a different approach. HAP1 cells are a near-haploid human cell line that has been used successful in retroviral gene-trap mutagenesis screens (Carette et al., 2009; Carette et al., 2011; Gowen et al., 2015). In Figure 36D, we showed that coculture with HAP1 tumor cells triggered activation of NKp46 CAR T cells so we decided to try these cells as targets for NKp46 CAR T cell-based screens.

Consistent with activation data in Figure 36D, HAP1 cells were efficiently killed *in vitro* by $CD4^+$ NKp46 CAR T cells (Figure 38A). Thus, we set about performing the screen using HAP1 cells. Mutagenized HAP1 cells, previously frozen by Benjamin Gowen and used successfully in his screen (Gowen et al., 2015), were thawed and expanded and 225 x 10^6 cells were seeded into 3x T175 flasks (75 x 10^6/flask). The next day, in the evening, the media was removed from each flask and replaced with fresh media containing 100 x 10^6 $CD4^+$ NKp46 CAR T cells/flask. The coculture was allowed to happen overnight (~15 hours) and the media containing the NKp46 CAR T cells and dead (floating) HAP1 cells was removed. The remaining adherent HAP1 cells were washed with PBS and fresh media was added. Approximately 95% killing was observed at this time point. Interestingly, over the next few days in culture, the remaining HAP1 cells continued to die, even with repeated media changes. This prompted us to question whether HAP1 killing could be mediated independently of direct cell-cell killing. We hypothesized that a soluble, CAR T cell-produced, factor was responsible for some of the killing, and consistent with this hypothesis, supernatant taken from NKp46 CAR T cell-HAP1 coculture was able to kill HAP1 cells after prolonged culture *in vitro* (data not shown). Activated NKp46 CAR T cells produce IFN-γ (Figure 36) and although not classically known as a cytotoxic molecule, we found that IFN-γ was capable of killing HAP1 cells *in vitro* (Figure 38B).

Despite finding that IFN-γ was toxic to HAP1 cells, we decided to repeat the screen, but for the second round to coculture the HAP1 and CART cells for a maximum of 8 hours so as to limit the amount of IFN-γ-mediated killing. This time point was chosen because we found that exposure of HAP1 cells to IFN-γ for short periods (8 hours) was not toxic (data not shown). For this screen we would also employ NKp46 CAR T cells sorted to be either homogeneously $CD4^+$

or CD8$^+$, which were both capable of killing HAP1 cells similarly *in vitro* (Figure 38C). Note that by the time of this screen we had no trouble getting CD8$^+$ NKp46 CAR T cells after the REP. We performed the screen as described above, but this time we serially killed the mutagenized HAP1 cells 5 times for the CD4$^+$ NKp46 CAR T cells and 6 times for the CD8$^+$ NKp46 CAR T cells. Unfortunately, after several rounds of killing the surviving HAP1 cells were not any more resistant to killing than the parental HAP1 cells (Figure 38C), suggesting that the selections were ineffective. Nevertheless, we extracted genomes from 50 x 10^6 of the surviving HAP1 cells as described previously (Gowen et al., 2015) and sent them to our collaborator, Dr. Jan Carette, for sequencing. Significant results from the sequencing data are shown in Figure 38D. As of the writing of this thesis, attempts to validate the hits have not yet been performed.

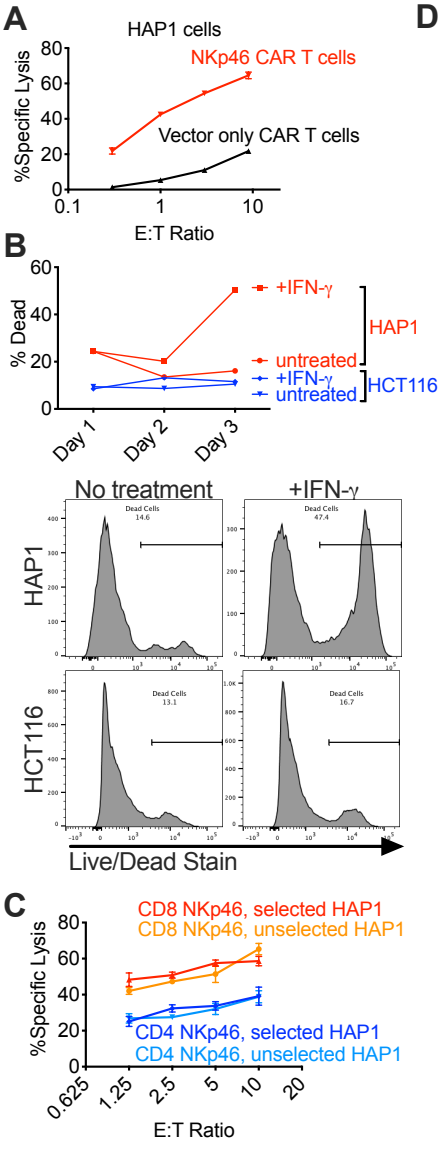

D

CD4$^+$ NKp46 CAR T cell screen hits

Gene	p-value	Carette's Notes
RPRD2	3.85E-43	Comes up in many of our screens (viral, IFN-based, and TNF-based)
WAC	1.68E-20	Comes up in many of our screens (viral, IFN-based, and TNF-based)
MLL	3.33E-13	Comes up in many of our screens (viral, IFN-based, drug, and TNF-based)
EPC2	2.58E-12	**Specific to this screen**
CASP8	1.10E-09	Comes up in our TNF-based screens
ARID2	0.0012736	Comes up in our IFN-based screens
PACS1	0.00146887	**Specific to this screen**
KAT5	0.00174838	**Specific to this screen**
NF2	0.0041819	Comes up in our IFN-based screens
CHORDC1	0.00972373	Comes up in only one other of our IFN-based screens
FADD	0.02299297	Comes up in our TNF-based screens
FEM1A	0.02524882	**Specific to this screen**
AKNAD1	0.04208535	**Specific to this screen**

CD8$^+$ NKp46 CAR T cell screen hits

Gene	p-value	Carette's Notes
PBRM1	1.08E-81	Comes up in almost every screen
RPRD2	1.30E-18	Comes up in many of our screens (viral, IFN-based, and TNF-based)
MLL	3.21E-18	Comes up in many of our screens (viral, IFN-based, drug, and TNF-based)
EPC2	5.58E-18	**Specific to this screen**
PMAIP1	2.29E-14	Comes up in almost every screen
CCDC101	1.19E-11	Comes up in multiple unrelated screens
BCL2L1	1.76E-11	Comes up in multiple unrelated screens
FADD	1.55E-09	Comes up in our TNF-based screens
CASP8	3.91E-06	Comes up in our TNF-based screens
SLFN11	3.91E-06	Comes up in a few screens, but was a hit in an IFN-gamma screen
CDK13	6.98E-06	Comes up in a drug screen
BID	1.36E-05	Comes up in our TNF-based screens
MEAF6	5.44E-05	Comes up a few of our IFN-based screens
UNK	0.00022773	Comes up in two unrelated screens
BRD7	0.0002716	Comes up in two TNF-based screens
ZNF292	0.00038215	Comes up in a single IFN-gamma screen
ATP2C1	0.00041151	Comes up in multiple unrelated screens
MGA	0.00089937	Comes up in multiple unrelated screens
FAS	0.00372884	**Specific to this screen**
TMUB1	0.00672352	Comes up in multiple unrelated screens
DICER1	0.00903567	Comes up in two TNF-based screens
ZC3H4	0.01598513	Comes up in three screens
PHF12	0.01605952	Comes up in multiple unrelated screens
CDC73	0.0256116	**Specific to this screen**
MALAT1	0.02630191	Comes up in multiple unrelated screens

Fig. 38. HAP1 screen with NKp46 CAR T cells. (A) Sorted $CD8^+$ NKp46-CAR or empty vector T cells were used as effectors in a ^{51}Cr cytotoxicity assay with HAP1 target cells. Assay was performed in technical triplicate. Error bars are shown but are too small to see. Representative of 3 independent experiments. **(B)** HAP1 or HCT116 cells were treated overnight with 100 ng/ml recombinant IFN-γ. The next day (Day 1) the cells were washed and placed in fresh media. Cell death was assessed by flow cytometry on Day 1, 2, and 3. Flow plots are from day 3. Experiment only done once. **(C)** Standard ^{51}Cr assay on 5x $CD4^+$ NKp46 CAR T cell-selected and 6x $CD8^+$ NKp46 CAR T cell-selected mutagenized HAP1 cells compared to unselected controls. Experiments with $CD8^+$ effectors shown in Red and Orange and $CD4^+$ effectors shown in Light and Dark Blue. **(D)** Genes hits that were found to be significant in the $CD4^+$ and $CD8^+$ NKp46 CAR T cell screen.

Conventional CRISPR-based screens in HCT116 cells to identify novel NKp44 and NKp46 ligands.

Upon learning that IFN-γ could kill HAP1 cells *in vitro* (Figure 37B), in addition to performing a second screen in HAP1 cells we also decide to pivot to a third screen utilizing conventional CRISPR-Cas9 in HCT116 cells. This was done in collaboration with Moritz Gaidt from the Vance Lab, who had previous success with this screening system. As with the previously described CRISPRi screen, we selected HCT116 cells for this screen because they are efficiently killed by both NKp44 and NKp46 CAR T cells *in vitro* (Figure 36E and 37A) and are not killed by culturing in IFN-γ (Figure 38B). Using a lentiviral vector, CAS9 was stably expressed in HCT116 cells, followed by single cell sorting to generate individual clones, which were then expanded. Several of the clones were screened for knockout ability by transducing a vector encoding a guide sequence targeting ICAM1 and then examining loss of ICAM-1 on the cell surface. The clone achieving the highest knockout percentage was then selected to be used for the screen (Figure 39A).

The HCT116-Cas9 clone was expanded and 20 x 10^6 cells were transduced, in triplicate, with a ~200,000 guide library targeting ~20,500 protein-coding genes with ~10 guides/gene (Morgens et al., 2017). The cells were then placed under puromycin selection (the guide vector encodes a puromycin resistance gene) for one week to ensure enough time for loss of gene expression. After one week the three puromycin selected transduction replicates were expanded and 100 x 10^6 total cells from each replicate were seeded into two T175 flasks (50 x 10^6 for each each) for each treatment group (NKp44 CAR T selection, NKp46 CAR T selection, and unselected controls). The next day the media was removed and replaced with fresh media containing 100 x 10^6 CAR T cells/replicate (50 x 10^6 for each T175 flask). The HCT116 cells and CAR T cells were incubated together overnight. The next morning the CAR T cells were removed, and the flasks were washed with PBS and fresh media was added. At this timepoint we estimated that ~10% of the NKp46 CAR T-selected and ~1% of the NKp44 CAR T-selected HCT116-Cas9 cells remained adhered to the plate, indicating we achieved >90% killing under these conditions. The remaining adherent cells were then expanded with daily PBS washing followed by fresh media addition.

To examine if the CAR T selected HCT116-Cas9 cells were resistant to CAR T cell killing we compared the unselected cells to selected cells in a standard ^{51}Cr assay. Unfortunately, the CAR T-selected HCT116 cells and the unselected controls were killed similarly (Figure 39B

and 38C), indicating that the guides conferring resistance to NKp44 and NKp46-mediated killing were not appreciably enriched within the sample. We then repeated the killing four additional times. This was done by expanding the surviving cells as described above, plating 50 x 10^6 in a T175 flask, and adding 50 x 10^6 CAR T cells the next day. As before, the coculture was allowed to continue for 8-24 hours and the cells were then washed with PBS and fresh media was added. After the 5^{th} killing we repeated the ^{51}Cr assay. Notably, in this assay both the NKp44 and NKp46 CAR T cell-selected HCT11-Cas9+guide cells were more resistant to killing than the unselected control cells (Figure 39D and 39E). We then pelleted 5 x 10^6 HCT116 cells from all three replicates from all three treatment groups (NKp44-selected, NKp46-selected, and unselected), and gave them to Moritz for genomic DNA extraction and sequencing. The results of the sequencing are shown in Figure 39F. As of the writing of this thesis, none of the hits have been subjected to validation analysis

One issue with this screen was that the unselected guide-containing control cells had greatly reduced guide representation than what would be expected. It is unclear exactly why this was the case but may be because the cells were passaged for several months while the screen was taking place. There were also issues in overall cell health at one point during passage which likely played a major role. In any case the NKp44 and NKp46 CAR T-selected cells were compared to the plasmid guide library in order to generate a list of enriched guides in the selected cells. This is obviously not ideal and future screens will be necessary to move this project forward.

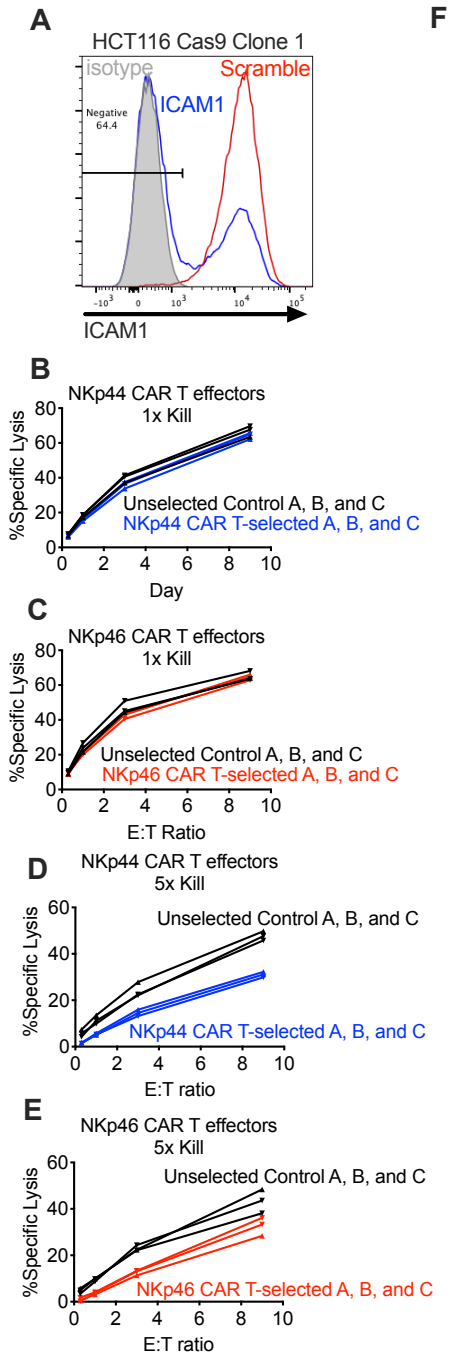

F

NKp44 CAR T-selected

Number	Gene	Score
1	FADD	12.39259058
2	PDCD10	9.05130779
3	FRYL	8.580195996
4	CASP8	7.258773002
5	ZNF792	3.699048178
6	POLR2G	3.602157709
7	LUZP1	3.398096358
8	HMCN1	3.346963379
9	TEX33	3.301225433
10	MSANTD3	3.259852292
11	NF2	3.187340714
12	SPANXN4	3.155175575
13	PRKACG	3.125231896
14	ANKRD36	3.097222718
15	RIPK4	3.046109285
16	PPIE	3.022647734
17	SLC39A8	3.000390885
18	DEGS1	2.979221131
19	OR14C36	2.95903729
20	TRIB1	2.93975168
21	PRSS38	2.92128782
22	EFCAB10	2.903578599
23	AMBRA1	2.886564805
24	ETNK1	2.854419214
25	MLYCD	2.839198793
26	SGCB	2.824495082
27	MAST1	2.81027419
28	ABRA	2.796505451
29	COQ5	2.783161036
30	GUSB	2.770215606
31	NTN5	2.757646025
32	TEC	2.745431115
33	FAM71A	2.733551439
34	DCAF5	2.721989113
35	VPS4B	2.699751813
36	REEP1	2.689047494
37	MXRA7	2.678601608
38	EPB41L5	2.66840199
39	USP46	2.658437317
40	CPA6	2.648697027
41	SLC12A4	2.639171257
42	PLEKHH3	2.629850779
43	NAA25	2.620726947
44	ABCD1	2.611791652
45	GPR82	2.603037276
46	MRPL37	2.594456653
47	RNASE8	2.586043033
48	TTL	2.569691714
49	PPARD	2.546269264
50	GCNT7	2.538735675

NKp46 CAR T-selected

Number	Gene	Score
1	FADD	14.29757096
2	FRYL	10.86593144
3	PDCD10	8.894219599
4	CASP8	6.540885472
5	ZNF792	4.301049539
6	POLR2G	3.823967371
7	LUZP1	3.699048178
8	PRKACG	3.456068761
9	PPIE	3.398096358
10	FAM71A	3.259852292
11	NF2	3.222083276
12	NAA25	3.187340714
13	RIPK4	3.070913324
14	TEX35	3.046109285
15	HMCN1	3.022647734
16	GPR26	3.000390885
17	PRSS38	2.979221131
18	YWHAB	2.95903729
19	PRKD2	2.93975168
20	TEX33	2.92128782
21	AMBRA1	2.903578599
22	EFCAB10	2.886564805
23	MLYCD	2.854419214
24	ETNK1	2.839198793
25	MLNR	2.824495082
26	ABRA	2.81027419
27	BOD1L1	2.796505451
28	MAST1	2.783161036
29	MSANTD3	2.770215606
30	GMPR	2.757646025
31	COQ5	2.745431115
32	GOLGA6D	2.733551439
33	DLG3	2.721989113
34	GUSB	2.71072765
35	PREX1	2.699751813
36	NTN5	2.689047494
37	TEC	2.678601608
38	DCAF5	2.66840199
39	MXRA7	2.648697027
40	REEP1	2.639171257
41	VPS4B	2.629850779
42	SPANXN4	2.620726947
43	EPB41L5	2.611791652
44	USP46	2.603037276
45	PLEKHH3	2.594456653
46	MRPL37	2.586043033
47	CPA6	2.577790056
48	JAK2	2.569691714
49	ABCD1	2.561742333
50	ANKRD36	2.553936544

Fig. 39. HCT116 CRISPR screen with NKp44 and NKp46 CAR T cells. (A) HCT116 cells expressing Cas9 were cloned and transduced with a lentivurus expressing guide sequences for *Icam1* or a non-targeting "scramble" sequence. Shown is the ICAM1 or isotype staining for the clone exhibiting the best knockout phenotype. **(B-E)** $CD8^+$ NKp44 (B and D) or NKp46 (C and E) CAR T cells were used as effectors in a ^{51}Cr cytotoxicity assay with 1x-selected (B and C), 5x-selected (D and E), or unselected control (B-E) HCT116-Cas9+guide target cells. Assay was performed in technical triplicate. Error bars are shown but are too small to see. Experiment only done once. **(F)** Genes hits that were found to be significant in the HCT116 CRISPR $CD8^+$ NKp44 and NKp46 CAR T cell screens.

Discussion

In this chapter we describe a screening method utilizing CAR T cells as selecting agents in order to find novel NK cell activating ligands on human tumor cells. In this approach, T cell killing is directed against cells expressing ligands for the desired receptor. In a population of mutagenized or Cas9+guide library-expressing cells some will have lost or downregulated expression of the ligand, making them resistant to killing, and these will become enriched in the surviving population after CAR T cell coculture. We believe that this method of using CAR T cells in screens can be applied to search for unknown surface ligands for any orphan receptor, and thus has broad applicability and relevance outside of this project and dissertation. There are many cell surface receptors that have ligands that are currently unknown, and similar approaches could be done to enable their discovery.

For this project we performed 3 different screens and for the first, CRISPRi-based, screen we tested the top 100 predicted-to-be membrane-bound hits. Out of those 100 hits only two were found to consistently affect NKp46 CAR T cell killing and effector functions: ICAM1 and CR2. ICAM-1 is a well-known surface molecule and is important for cellular adhesion and therefore it is not surprising that this gene was a hit. Interestingly, CR2 expression also influenced CAR T cell effector functions. However, we subsequently learned that CR2 downregulation also negatively affects ICAM-1 expression, and it is likely that this accounts for its impact on the CART response, although we have not directly ruled out that CR2 is a ligand for NKp46. It is perhaps noteworthy that CR2 was not a hit in any of the other screens performed with the NKp46 CAR T cells.

In addition to the CRISPRi-based screen, we also performed screens using mutagenized HAP1 cells and conventional CRISPR-Cas9. As of now we have yet to validate any of the hits from these screens and future work should be directed at examining if any of the candidate genes are ligands for NKp44 and NKp46.

Several genes did consistently come out of each screen and were validated to increase cell survival after CAR T cell coculture. These include genes associated with promoting cell death, such as CASP8 and FADD. Because of their known role in cell death, it is not surprising, that these were hits in our killing-based screens.

NK cells are important effectors for antitumor and antiviral immunity. They express many activating receptors but the cellular ligands for several remain poorly defined. Therefore, a major focus of NK cell research should be devoted to uncovering these mysterious ligands in order to gain a better understanding of NK cell biology. This chapter details a method and several screens aimed at identifying unknown ligands for the activating receptors NKp44 and NKp46. Future work will be needed to validate most of the hits uncovered in this chapter and perform additional screens as necessary. We believe this type of screening approach has great potential for uncovering ligands for many other orphan cellular receptors, as well.

References

Ablasser, A., and Z.J. Chen. 2019. cGAS in action: Expanding roles in immunity and inflammation. *Science* 363:

Ablasser, A., M. Goldeck, T. Cavlar, T. Deimling, G. Witte, I. Rohl, K.P. Hopfner, J. Ludwig, and V. Hornung. 2013a. cGAS produces a 2'-5'-linked cyclic dinucleotide second messenger that activates STING. *Nature* 498:380-384.

Ablasser, A., J.L. Schmid-Burgk, I. Hemmerling, G.L. Horvath, T. Schmidt, E. Latz, and V. Hornung. 2013b. Cell intrinsic immunity spreads to bystander cells via the intercellular transfer of cGAMP. *Nature*

Alexandrov, L.B., S. Nik-Zainal, D.C. Wedge, S.A. Aparicio, S. Behjati, A.V. Biankin, G.R. Bignell, N. Bolli, A. Borg, A.L. Borresen-Dale, S. Boyault, B. Burkhardt, A.P. Butler, C. Caldas, H.R. Davies, C. Desmedt, R. Eils, J.E. Eyfjord, J.A. Foekens, M. Greaves, F. Hosoda, B. Hutter, T. Ilicic, S. Imbeaud, M. Imielinski, N. Jager, D.T. Jones, D. Jones, S. Knappskog, M. Kool, S.R. Lakhani, C. Lopez-Otin, S. Martin, N.C. Munshi, H. Nakamura, P.A. Northcott, M. Pajic, E. Papaemmanuil, A. Paradiso, J.V. Pearson, X.S. Puente, K. Raine, M. Ramakrishna, A.L. Richardson, J. Richter, P. Rosenstiel, M. Schlesner, T.N. Schumacher, P.N. Span, J.W. Teague, Y. Totoki, A.N. Tutt, R. Valdes-Mas, M.M. van Buuren, L. van 't Veer, A. Vincent-Salomon, N. Waddell, L.R. Yates, I. Australian Pancreatic Cancer Genome, I.B.C. Consortium, I.M.-S. Consortium, I. PedBrain, J. Zucman-Rossi, P.A. Futreal, U. McDermott, P. Lichter, M. Meyerson, S.M. Grimmond, R. Siebert, E. Campo, T. Shibata, S.M. Pfister, P.J. Campbell, and M.R. Stratton. 2013. Signatures of mutational processes in human cancer. *Nature* 500:415-421.

Alexandrov, L.B., and M.R. Stratton. 2014. Mutational signatures: the patterns of somatic mutations hidden in cancer genomes. *Curr Opin Genet Dev* 24:52-60.

Alspach, E., D.M. Lussier, A.P. Miceli, I. Kizhvatov, M. DuPage, A.M. Luoma, W. Meng, C.F. Lichti, E. Esaulova, A.N. Vomund, D. Runci, J.P. Ward, M.M. Gubin, R.F.V. Medrano, C.D. Arthur, J.M. White, K.C.F. Sheehan, A. Chen, K.W. Wucherpfennig, T. Jacks, E.R. Unanue, M.N. Artyomov, and R.D. Schreiber. 2019. MHC-II neoantigens shape tumour immunity and response to immunotherapy. *Nature* 574:696-701.

Andre, P., C. Denis, C. Soulas, C. Bourbon-Caillet, J. Lopez, T. Arnoux, M. Blery, C. Bonnafous, L. Gauthier, A. Morel, B. Rossi, R. Remark, V. Breso, E. Bonnet, G. Habif, S. Guia, A.I. Lalanne, C. Hoffmann, O. Lantz, J. Fayette, A. Boyer-Chammard, R. Zerbib, P. Dodion, H. Ghadially, M. Jure-Kunkel, Y. Morel, R. Herbst, E. Narni-Mancinelli, R.B. Cohen, and E. Vivier. 2018. Anti-NKG2A mAb Is a Checkpoint Inhibitor that Promotes Anti-tumor Immunity by Unleashing Both T and NK Cells. *Cell* 175:1731-1743 e1713.

Ardolino, M., C.S. Azimi, A. Iannello, T.N. Trevino, L. Horan, L. Zhang, W. Deng, A.M. Ring, S. Fischer, K.C. Garcia, and D.H. Raulet. 2014. Cytokine therapy reverses NK cell anergy in MHC-deficient tumors. *J Clin Invest* 124:4781-4794.

Arnon, T.I., H. Achdout, N. Lieberman, R. Gazit, T. Gonen-Gross, G. Katz, A. Bar-Ilan, N. Bloushtain, M. Lev, A. Joseph, E. Kedar, A. Porgador, and O. Mandelboim. 2004. The mechanisms controlling the recognition of tumor- and virus-infected cells by NKp46. *Blood* 103:664-672.

Atkinson, C., S. He, K. Morris, F. Qiao, S. Casey, M. Goddard, and S. Tomlinson. 2010. Targeted complement inhibitors protect against posttransplant cardiac ischemia and reperfusion injury and reveal an important role for the alternative pathway of complement activation. *J Immunol* 185:7007-7013.

Balkwill, F. 2009. Tumour necrosis factor and cancer. *Nat Rev Cancer* 9:361-371.
Barrow, A.D., M.A. Edeling, V. Trifonov, J. Luo, P. Goyal, B. Bohl, J.K. Bando, A.H. Kim, J. Walker, M. Andahazy, M. Bugatti, L. Melocchi, W. Vermi, D.H. Fremont, S. Cox, M. Cella, C. Schmedt, and M. Colonna. 2017. Natural Killer Cells Control Tumor Growth by Sensing a Growth Factor. *Cell*
Barry, K.C., J. Hsu, M.L. Broz, F.J. Cueto, M. Binnewies, A.J. Combes, A.E. Nelson, K. Loo, R. Kumar, M.D. Rosenblum, M.D. Alvarado, D.M. Wolf, D. Bogunovic, N. Bhardwaj, A.I. Daud, P.K. Ha, W.R. Ryan, J.L. Pollack, B. Samad, S. Asthana, V. Chan, and M.F. Krummel. 2018. A natural killer-dendritic cell axis defines checkpoint therapy-responsive tumor microenvironments. *Nat Med* 24:1178-1191.
Baumeister, S.H., G.J. Freeman, G. Dranoff, and A.H. Sharpe. 2016. Coinhibitory Pathways in Immunotherapy for Cancer. *Annu Rev Immunol* 34:539-573.
Baychelier, F., A. Sennepin, M. Ermonval, K. Dorgham, P. Debre, and V. Vieillard. 2013. Identification of a cellular ligand for the natural cytotoxicity receptor NKp44. *Blood* 122:2935-2942.
Becknell, B., and M.A. Caligiuri. 2005. Interleukin-2, interleukin-15, and their roles in human natural killer cells. *Adv Immunol* 86:209-239.
Bekisz, J., S. Baron, C. Balinsky, A. Morrow, and K.C. Zoon. 2010. Antiproliferative Properties of Type I and Type II Interferon. *Pharmaceuticals (Basel)* 3:994-1015.
Blake, S.J., W.C. Dougall, J.J. Miles, M.W. Teng, and M.J. Smyth. 2016. Molecular Pathways: Targeting CD96 and TIGIT for Cancer Immunotherapy. *Clinical cancer research : an official journal of the American Association for Cancer Research* 22:5183-5188.
Boehm, U., T. Klamp, M. Groot, and J.C. Howard. 1997. Cellular responses to interferon-gamma. *Annu Rev Immunol* 15:749-795.
Borst, J., T. Ahrends, N. Babala, C.J.M. Melief, and W. Kastenmuller. 2018. CD4(+) T cell help in cancer immunology and immunotherapy. *Nat Rev Immunol* 18:635-647.
Bottcher, J.P., E. Bonavita, P. Chakravarty, H. Blees, M. Cabeza-Cabrerizo, S. Sammicheli, N.C. Rogers, E. Sahai, S. Zelenay, and E.S.C. Reis. 2018. NK Cells Stimulate Recruitment of cDC1 into the Tumor Microenvironment Promoting Cancer Immune Control. *Cell* 172:1022-1037 e1014.
Brandt, C.S., M. Baratin, E.C. Yi, J. Kennedy, Z. Gao, B. Fox, B. Haldeman, C.D. Ostrander, T. Kaifu, C. Chabannon, A. Moretta, R. West, W. Xu, E. Vivier, and S.D. Levin. 2009. The B7 family member B7-H6 is a tumor cell ligand for the activating natural killer cell receptor NKp30 in humans. *J Exp Med* 206:1495-1503.
Brinkmann, V., T. Geiger, S. Alkan, and C.H. Heusser. 1993. Interferon alpha increases the frequency of interferon gamma-producing human CD4+ T cells. *J Exp Med* 178:1655-1663.
Carette, J.E., C.P. Guimaraes, M. Varadarajan, A.S. Park, I. Wuethrich, A. Godarova, M. Kotecki, B.H. Cochran, E. Spooner, H.L. Ploegh, and T.R. Brummelkamp. 2009. Haploid genetic screens in human cells identify host factors used by pathogens. *Science* 326:1231-1235.
Carette, J.E., M. Raaben, A.C. Wong, A.S. Herbert, G. Obernosterer, N. Mulherkar, A.I. Kuehne, P.J. Kranzusch, A.M. Griffin, G. Ruthel, P. Dal Cin, J.M. Dye, S.P. Whelan, K. Chandran, and T.R. Brummelkamp. 2011. Ebola virus entry requires the cholesterol transporter Niemann-Pick C1. *Nature* 477:340-343.

Castro, F., A.P. Cardoso, R.M. Goncalves, K. Serre, and M.J. Oliveira. 2018. Interferon-Gamma at the Crossroads of Tumor Immune Surveillance or Evasion. *Frontiers in immunology* 9:847.

Cerwenka, A., and L.L. Lanier. 2001. Natural killer cells, viruses and cancer. *Nature Rev Immunol* 1:41-49.

Chen, Q., L. Sun, and Z.J. Chen. 2016. Regulation and function of the cGAS-STING pathway of cytosolic DNA sensing. *Nat Immunol* 17:1142-1149.

Chesebro, B., K. Wehrly, K. Chesebro, and J. Portis. 1976. Characterization of Ia8 antigen, thy-1.2 antigen, complement receptors, and virus production in a group of murine virus-induced leukemia cell lines. *J Immunol* 117:1267-1274.

Cooper, M.A., J.M. Elliott, P.A. Keyel, L. Yang, J.A. Carrero, and W.M. Yokoyama. 2009. Cytokine-induced memory-like natural killer cells. *Proc Natl Acad Sci U S A*

Corrales, L., L.H. Glickman, S.M. McWhirter, D.B. Kanne, K.E. Sivick, G.E. Katibah, S.R. Woo, E. Lemmens, T. Banda, J.J. Leong, K. Metchette, T.W. Dubensky, Jr., and T.F. Gajewski. 2015. Direct Activation of STING in the Tumor Microenvironment Leads to Potent and Systemic Tumor Regression and Immunity. *Cell Rep* 11:1018-1030.

Corthay, A., D.K. Skovseth, K.U. Lundin, E. Rosjo, H. Omholt, P.O. Hofgaard, G. Haraldsen, and B. Bogen. 2005. Primary antitumor immune response mediated by CD4+ T cells. *Immunity* 22:371-383.

Costello, R.T., S. Sivori, E. Marcenaro, M. Lafage-Pochitaloff, M.J. Mozziconacci, D. Reviron, J.A. Gastaut, D. Pende, D. Olive, and A. Moretta. 2002. Defective expression and function of natural killer cell-triggering receptors in patients with acute myeloid leukemia. *Blood* 99:3661-3667.

Critchley-Thorne, R.J., D.L. Simons, N. Yan, A.K. Miyahira, F.M. Dirbas, D.L. Johnson, S.M. Swetter, R.W. Carlson, G.A. Fisher, A. Koong, S. Holmes, and P.P. Lee. 2009. Impaired interferon signaling is a common immune defect in human cancer. *Proc Natl Acad Sci U S A* 106:9010-9015.

Curran, E., X. Chen, L. Corrales, D.E. Kline, T.W. Dubensky, Jr., P. Duttagupta, M. Kortylewski, and J. Kline. 2016. STING Pathway Activation Stimulates Potent Immunity against Acute Myeloid Leukemia. *Cell Rep* 15:2357-2366.

Curran, M.A., T.L. Geiger, W. Montalvo, M. Kim, S.L. Reiner, A. Al-Shamkhani, J.C. Sun, and J.P. Allison. 2013. Systemic 4-1BB activation induces a novel T cell phenotype driven by high expression of Eomesodermin. *J Exp Med* 210:743-755.

Curran, M.A., W. Montalvo, H. Yagita, and J.P. Allison. 2010. PD-1 and CTLA-4 combination blockade expands infiltrating T cells and reduces regulatory T and myeloid cells within B16 melanoma tumors. *Proc Natl Acad Sci U S A* 107:4275-4280.

Degli-Esposti, M.A., and M.J. Smyth. 2005. Close encounters of different kinds: dendritic cells and NK cells take centre stage. *Nat Rev Immunol* 5:112-124.

Demaria, O., A. De Gassart, S. Coso, N. Gestermann, J. Di Domizio, L. Flatz, O. Gaide, O. Michielin, P. Hwu, T.V. Petrova, F. Martinon, R.L. Modlin, D.E. Speiser, and M. Gilliet. 2015. STING activation of tumor endothelial cells initiates spontaneous and therapeutic antitumor immunity. *Proc Natl Acad Sci U S A* 112:15408-15413.

Deng, L., H. Liang, M. Xu, X. Yang, B. Burnette, A. Arina, X.D. Li, H. Mauceri, M. Beckett, T. Darga, X. Huang, T.F. Gajewski, Z.J. Chen, Y.X. Fu, and R.R. Weichselbaum. 2014. STING-Dependent Cytosolic DNA Sensing Promotes Radiation-Induced Type I

Interferon-Dependent Antitumor Immunity in Immunogenic Tumors. *Immunity* 41:843-852.

Deng, W., B.G. Gowen, L. Zhang, L. Wang, S. Lau, A. Iannello, J. Xu, T.L. Rovis, N. Xiong, and D.H. Raulet. 2015. Antitumor immunity. A shed NKG2D ligand that promotes natural killer cell activation and tumor rejection. *Science* 348:136-139.

Diamond, M.S., M. Kinder, H. Matsushita, M. Mashayekhi, G.P. Dunn, J.M. Archambault, H. Lee, C.D. Arthur, J.M. White, U. Kalinke, K.M. Murphy, and R.D. Schreiber. 2011. Type I interferon is selectively required by dendritic cells for immune rejection of tumors. *J Exp Med* 208:1989-2003.

Diefenbach, A., A.M. Jamieson, S.D. Liu, N. Shastri, and D.H. Raulet. 2000. Ligands for the murine NKG2D receptor: expression by tumor cells and activation of NK cells and macrophages. *Nat Immunol* 1:119-126.

Diner, E.J., D.L. Burdette, S.C. Wilson, K.M. Monroe, C.A. Kellenberger, M. Hyodo, Y. Hayakawa, M.C. Hammond, and R.E. Vance. 2013. The innate immune DNA sensor cGAS produces a noncanonical cyclic dinucleotide that activates human STING. *Cell Rep* 3:1355-1361.

Dunn, G.P., C.M. Koebel, and R.D. Schreiber. 2006. Interferons, immunity and cancer immunoediting. *Nat Rev Immunol* 6:836-848.

Epling-Burnette, P.K., F. Bai, J.S. Painter, D.E. Rollison, H.R. Salih, M. Krusch, J. Zou, E. Ku, B. Zhong, D. Boulware, L. Moscinski, S. Wei, J.Y. Djeu, and A.F. List. 2007. Reduced natural killer (NK) function associated with high-risk myelodysplastic syndrome (MDS) and reduced expression of activating NK receptors. *Blood* 109:4816-4824.

Eroglu, Z., D.W. Kim, X. Wang, L.H. Camacho, B. Chmielowski, E. Seja, A. Villanueva, K. Ruchalski, J.A. Glaspy, K.B. Kim, W.J. Hwu, and A. Ribas. 2015. Long term survival with cytotoxic T lymphocyte-associated antigen 4 blockade using tremelimumab. *Eur J Cancer* 51:2689-2697.

Fingeroth, J.D., J.J. Weis, T.F. Tedder, J.L. Strominger, P.A. Biro, and D.T. Fearon. 1984. Epstein-Barr virus receptor of human B lymphocytes is the C3d receptor CR2. *Proc Natl Acad Sci U S A* 81:4510-4514.

Francica, B.J., A. Ghasemzadeh, A.L. Desbien, D. Theodros, K.E. Sivick, G.L. Reiner, L. Hix Glickman, A.E. Marciscano, A.B. Sharabi, M.L. Leong, S.M. McWhirter, T.W. Dubensky, Jr., D.M. Pardoll, and C.G. Drake. 2018. TNFalpha and Radioresistant Stromal Cells Are Essential for Therapeutic Efficacy of Cyclic Dinucleotide STING Agonists in Nonimmunogenic Tumors. *Cancer Immunol Res* 6:422-433.

Fu, J., D.B. Kanne, M. Leong, L.H. Glickman, S.M. McWhirter, E. Lemmens, K. Mechette, J.J. Leong, P. Lauer, W. Liu, K.E. Sivick, Q. Zeng, K.C. Soares, L. Zheng, D.A. Portnoy, J.J. Woodward, D.M. Pardoll, T.W. Dubensky, Jr., and Y. Kim. 2015. STING agonist formulated cancer vaccines can cure established tumors resistant to PD-1 blockade. *Science translational medicine* 7:283ra252.

Fuertes, M.B., A.K. Kacha, J. Kline, S.R. Woo, D.M. Kranz, K.M. Murphy, and T.F. Gajewski. 2011. Host type I IFN signals are required for antitumor CD8+ T cell responses through CD8{alpha}+ dendritic cells. *J Exp Med* 208:2005-2016.

Fuertes, M.B., S.R. Woo, B. Burnett, Y.X. Fu, and T.F. Gajewski. 2013. Type I interferon response and innate immune sensing of cancer. *Trends Immunol* 34:67-73.

Gall, A., P. Treuting, K.B. Elkon, Y.M. Loo, M. Gale, Jr., G.N. Barber, and D.B. Stetson. 2012. Autoimmunity initiates in nonhematopoietic cells and progresses via lymphocytes in an interferon-dependent autoimmune disease. *Immunity* 36:120-131.

Garrido, F., and I. Algarra. 2001. MHC antigens and tumor escape from immune surveillance. *Adv Cancer Res* 83:117-158.

Garrido, F., N. Aptsiauri, E.M. Doorduijn, A.M. Garcia Lora, and T. van Hall. 2016. The urgent need to recover MHC class I in cancers for effective immunotherapy. *Current opinion in immunology* 39:44-51.

Gasteiger, G., and A.Y. Rudensky. 2014. Interactions between innate and adaptive lymphocytes. *Nat Rev Immunol* 14:631-639.

Gauthier, L., A. Morel, N. Anceriz, B. Rossi, A. Blanchard-Alvarez, G. Grondin, S. Trichard, C. Cesari, M. Sapet, F. Bosco, H. Rispaud-Blanc, F. Guillot, S. Cornen, A. Roussel, B. Amigues, G. Habif, F. Caraguel, S. Arrufat, R. Remark, F. Romagne, Y. Morel, E. Narni-Mancinelli, and E. Vivier. 2019. Multifunctional Natural Killer Cell Engagers Targeting NKp46 Trigger Protective Tumor Immunity. *Cell* 177:1701-1713 e1716.

Gilbert, L.A., M.A. Horlbeck, B. Adamson, J.E. Villalta, Y. Chen, E.H. Whitehead, C. Guimaraes, B. Panning, H.L. Ploegh, M.C. Bassik, L.S. Qi, M. Kampmann, and J.S. Weissman. 2014. Genome-Scale CRISPR-Mediated Control of Gene Repression and Activation. *Cell* 159:647-661.

Glasner, A., H. Ghadially, C. Gur, N. Stanietsky, P. Tsukerman, J. Enk, and O. Mandelboim. 2012. Recognition and prevention of tumor metastasis by the NK receptor NKp46/NCR1. *J Immunol* 188:2509-2515.

Gleason, M.K., M.R. Verneris, D.A. Todhunter, B. Zhang, V. McCullar, S.X. Zhou, A. Panoskaltsis-Mortari, L.M. Weiner, D.A. Vallera, and J.S. Miller. 2012. Bispecific and trispecific killer cell engagers directly activate human NK cells through CD16 signaling and induce cytotoxicity and cytokine production. *Mol Cancer Ther* 11:2674-2684.

Gowen, B.G., B. Chim, C.D. Marceau, T.T. Greene, P. Burr, J.R. Gonzalez, C.R. Hesser, P.A. Dietzen, T. Russell, A. Iannello, L. Coscoy, C.L. Sentman, J.E. Carette, S.A. Muljo, and D.H. Raulet. 2015. A forward genetic screen reveals novel independent regulators of ULBP1, an activating ligand for natural killer cells. *Elife* 4:e08474.

Gray, E.E., P.M. Treuting, J.J. Woodward, and D.B. Stetson. 2015. Cutting Edge: cGAS Is Required for Lethal Autoimmune Disease in the Trex1-Deficient Mouse Model of Aicardi-Goutieres Syndrome. *J Immunol* 195:1939-1943.

Greenberg, P.D., D.E. Kern, and M.A. Cheever. 1985. Therapy of disseminated murine leukemia with cyclophosphamide and immune Lyt-1+,2- T cells. Tumor eradication does not require participation of cytotoxic T cells. *J Exp Med* 161:1122-1134.

Guerra, N., Y.X. Tan, N.T. Joncker, A. Choy, F. Gallardo, N. Xiong, S. Knoblaugh, D. Cado, N.R. Greenberg, and D.H. Raulet. 2008. NKG2D-deficient mice are defective in tumor surveillance in models of spontaneous malignancy. *Immunity* 28:571-580.

Guillerey, C., N.D. Huntington, and M.J. Smyth. 2016. Targeting natural killer cells in cancer immunotherapy. *Nat Immunol* 17:1025-1036.

Hanahan, D., and R.A. Weinberg. 2000. The hallmarks of cancer. *Cell* 100:57-70.

Hanahan, D., and R.A. Weinberg. 2011. Hallmarks of cancer: the next generation. *Cell* 144:646-674.

Hannan, J.P. 2016. The Structure-Function Relationships of Complement Receptor Type 2 (CR2; CD21). *Curr Protein Pept Sci* 17:463-487.

Harrington, L.E., R.D. Hatton, P.R. Mangan, H. Turner, T.L. Murphy, K.M. Murphy, and C.T. Weaver. 2005. Interleukin 17-producing CD4+ effector T cells develop via a lineage distinct from the T helper type 1 and 2 lineages. *Nat Immunol* 6:1123-1132.

Haynes, N.M., E.D. Hawkins, M. Li, N.M. McLaughlin, G.J. Hammerling, R. Schwendener, A. Winoto, A. Wensky, H. Yagita, K. Takeda, M.H. Kershaw, P.K. Darcy, and M.J. Smyth. 2010. CD11c+ dendritic cells and B cells contribute to the tumoricidal activity of anti-DR5 antibody therapy in established tumors. *J Immunol* 185:532-541.

Herberman, R.B., M.E. Nunn, and D.H. Lavrin. 1975. Natural cytotoxic reactivity of mouse lymphoid cells against syngeneic and allogeneic tumors. I. Distribution of reactivity and specificity. *International Journal of Cancer* 16:216-229.

Hildner, K., B.T. Edelson, W.E. Purtha, M. Diamond, H. Matsushita, M. Kohyama, B. Calderon, B.U. Schraml, E.R. Unanue, M.S. Diamond, R.D. Schreiber, T.L. Murphy, and K.M. Murphy. 2008. Batf3 deficiency reveals a critical role for CD8alpha+ dendritic cells in cytotoxic T cell immunity. *Science* 322:1097-1100.

Hirano, F., K. Kaneko, H. Tamura, H. Dong, S. Wang, M. Ichikawa, C. Rietz, D.B. Flies, J.S. Lau, G. Zhu, K. Tamada, and L. Chen. 2005. Blockade of B7-H1 and PD-1 by monoclonal antibodies potentiates cancer therapeutic immunity. *Cancer Res* 65:1089-1096.

Ho, S.S., W.Y. Zhang, N.Y. Tan, M. Khatoo, M.A. Suter, S. Tripathi, F.S. Cheung, W.K. Lim, P.H. Tan, J. Ngeow, and S. Gasser. 2016. The DNA Structure-Specific Endonuclease MUS81 Mediates DNA Sensor STING-Dependent Host Rejection of Prostate Cancer Cells. *Immunity* 44:1177-1189.

Hodi, F.S., S.J. O'Day, D.F. McDermott, R.W. Weber, J.A. Sosman, J.B. Haanen, R. Gonzalez, C. Robert, D. Schadendorf, J.C. Hassel, W. Akerley, A.J. van den Eertwegh, J. Lutzky, P. Lorigan, J.M. Vaubel, G.P. Linette, D. Hogg, C.H. Ottensmeier, C. Lebbe, C. Peschel, I. Quirt, J.I. Clark, J.D. Wolchok, J.S. Weber, J. Tian, M.J. Yellin, G.M. Nichol, A. Hoos, and W.J. Urba. 2010. Improved survival with ipilimumab in patients with metastatic melanoma. *N Engl J Med* 363:711-723.

Hsu, J., J.J. Hodgins, M. Marathe, C.J. Nicolai, M.C. Bourgeois-Daigneault, T.N. Trevino, C.S. Azimi, A.K. Scheer, H.E. Randolph, T.W. Thompson, L. Zhang, A. Iannello, N. Mathur, K.E. Jardine, G.A. Kirn, J.C. Bell, M.W. McBurney, D.H. Raulet, and M. Ardolino. 2018. Contribution of NK cells to immunotherapy mediated by PD-1/PD-L1 blockade. *J Clin Invest* 128:4654-4668.

Huber, J.P., H.J. Ramos, M.A. Gill, and J.D. Farrar. 2010. Cutting edge: Type I IFN reverses human Th2 commitment and stability by suppressing GATA3. *J Immunol* 185:813-817.

Hung, K., R. Hayashi, A. Lafond-Walker, C. Lowenstein, D. Pardoll, and H. Levitsky. 1998. The central role of CD4(+) T cells in the antitumor immune response. *J Exp Med* 188:2357-2368.

Ikeda, H., L.J. Old, and R.D. Schreiber. 2002. The roles of IFN gamma in protection against tumor development and cancer immunoediting. *Cytokine & growth factor reviews* 13:95-109.

Ishikawa, H., and G.N. Barber. 2008. STING is an endoplasmic reticulum adaptor that facilitates innate immune signalling. *Nature* 455:674-678.

Ishikawa, H., Z. Ma, and G.N. Barber. 2009. STING regulates intracellular DNA-mediated, type I interferon-dependent innate immunity. *Nature* 461:788-792.

Jamieson, A.M., A. Diefenbach, C.W. McMahon, N. Xiong, J.R. Carlyle, and D.H. Raulet. 2002. The role of the NKG2D immunoreceptor in immune cell activation and natural killing. *Immunity* 17:19-29.

Johnson, D.B., M.V. Estrada, R. Salgado, V. Sanchez, D.B. Doxie, S.R. Opalenik, A.E. Vilgelm, E. Feld, A.S. Johnson, A.R. Greenplate, M.E. Sanders, C.M. Lovly, D.T. Frederick, M.C. Kelley, A. Richmond, J.M. Irish, Y. Shyr, R.J. Sullivan, I. Puzanov, J.A. Sosman, and J.M. Balko. 2016. Melanoma-specific MHC-II expression represents a tumour-autonomous phenotype and predicts response to anti-PD-1/PD-L1 therapy. *Nat Commun* 7:10582.

June, C.H., R.S. O'Connor, O.U. Kawalekar, S. Ghassemi, and M.C. Milone. 2018. CAR T cell immunotherapy for human cancer. *Science* 359:1361-1365.

June, C.H., and M. Sadelain. 2018. Chimeric Antigen Receptor Therapy. *N Engl J Med* 379:64-73.

Kagi, D., B. Ledermann, K. Burki, P. Seiler, B. Odermatt, K.J. Olsen, E.R. Podack, R.M. Zinkernagel, and H. Hengartner. 1994. Cytotoxicity mediated by T cells and natural killer cells is greatly impaired in perforin-deficient mice. *Nature* 369:31-37.

Karlhofer, F.M., R.K. Ribaudo, and W.M. Yokoyama. 1992. MHC class I alloantigen specificity of Ly-49^{+} IL-2 activated natural killer cells. *Nature* 358:66-70.

Karo, J.M., D.G. Schatz, and J.C. Sun. 2014. The RAG recombinase dictates functional heterogeneity and cellular fitness in natural killer cells. *Cell* 159:94-107.

Karre, K. 2008. Natural killer cell recognition of missing self. *Nat Immunol* 9:477-480.

Karre, K., H.G. Ljunggren, G. Piontek, and R. Kiessling. 1986. Selective rejection of H-2-deficient lymphoma variants suggests alternative immune defence strategy. *Nature* 319:675-678.

Kerdiles, Y., S. Ugolini, and E. Vivier. 2013. T cell regulation of natural killer cells. *J Exp Med* 210:1065-1068.

Khan, O., J.R. Giles, S. McDonald, S. Manne, S.F. Ngiow, K.P. Patel, M.T. Werner, A.C. Huang, K.A. Alexander, J.E. Wu, J. Attanasio, P. Yan, S.M. George, B. Bengsch, R.P. Staupe, G. Donahue, W. Xu, R.K. Amaravadi, X. Xu, G.C. Karakousis, T.C. Mitchell, L.M. Schuchter, J. Kaye, S.L. Berger, and E.J. Wherry. 2019. TOX transcriptionally and epigenetically programs CD8(+) T cell exhaustion. *Nature* 571:211-218.

Kiessling, R., E. Klein, and H. Wigzell. 1975. "Natural" killer cells in the mouse. I. Cytotoxic cells with specificity for mouse Moloney leukemia cells. Specificity and distribution according to genotype. *Eur J Immunol* 5:112-117.

Kitamura, D., J. Roes, R. Kuhn, and K. Rajewsky. 1991. A B cell-deficient mouse by targeted disruption of the membrane exon of the immunoglobulin mu chain gene. *Nature* 350:423-426.

Klarquist, J., C.M. Hennies, M.A. Lehn, R.A. Reboulet, S. Feau, and E.M. Janssen. 2014. STING-Mediated DNA Sensing Promotes Antitumor and Autoimmune Responses to Dying Cells. *J Immunol*

Koka, R., P. Burkett, M. Chien, S. Chai, D.L. Boone, and A. Ma. 2004. Cutting edge: murine dendritic cells require IL-15R alpha to prime NK cells. *J Immunol* 173:3594-3598.

Kreiter, S., M. Vormehr, N. van de Roemer, M. Diken, M. Lower, J. Diekmann, S. Boegel, B. Schrors, F. Vascotto, J.C. Castle, A.D. Tadmor, S.P. Schoenberger, C. Huber, O. Tureci, and U. Sahin. 2015. Mutant MHC class II epitopes drive therapeutic immune responses to cancer. *Nature* 520:692-696.

Krummel, M.F., and J.P. Allison. 1995. CD28 and CTLA-4 have opposing effects on the response of T cells to stimulation. *J. Exp. Med.* 182:459-465.

Kruse, P.H., J. Matta, S. Ugolini, and E. Vivier. 2014. Natural cytotoxicity receptors and their ligands. *Immunol Cell Biol* 92:221-229.

Lakshmikanth, T., S. Burke, T.H. Ali, S. Kimpfler, F. Ursini, L. Ruggeri, M. Capanni, V. Umansky, A. Paschen, A. Sucker, D. Pende, V. Groh, R. Biassoni, P. Hoglund, M. Kato, K. Shibuya, D. Schadendorf, A. Anichini, S. Ferrone, A. Velardi, K. Karre, A. Shibuya, E. Carbone, and F. Colucci. 2009. NCRs and DNAM-1 mediate NK cell recognition and lysis of human and mouse melanoma cell lines in vitro and in vivo. *J Clin Invest* 119:1251-1263.

Lam, A.R., N. Le Bert, S.S. Ho, Y.J. Shen, M.L. Tang, G.M. Xiong, J.L. Croxford, C.X. Koo, K.J. Ishii, S. Akira, D.H. Raulet, and S. Gasser. 2014. RAE1 ligands for the NKG2D receptor are regulated by STING-dependent DNA sensor pathways in lymphoma. *Cancer Res* 74:2193-2203.

Larkin, J., V. Chiarion-Sileni, R. Gonzalez, J.J. Grob, C.L. Cowey, C.D. Lao, D. Schadendorf, R. Dummer, M. Smylie, P. Rutkowski, P.F. Ferrucci, A. Hill, J. Wagstaff, M.S. Carlino, J.B. Haanen, M. Maio, I. Marquez-Rodas, G.A. McArthur, P.A. Ascierto, G.V. Long, M.K. Callahan, M.A. Postow, K. Grossmann, M. Sznol, B. Dreno, L. Bastholt, A. Yang, L.M. Rollin, C. Horak, F.S. Hodi, and J.D. Wolchok. 2015. Combined Nivolumab and Ipilimumab or Monotherapy in Untreated Melanoma. *N Engl J Med* 373:23-34.

Le, D.T., J.N. Uram, H. Wang, B.R. Bartlett, H. Kemberling, A.D. Eyring, A.D. Skora, B.S. Luber, N.S. Azad, D. Laheru, B. Biedrzycki, R.C. Donehower, A. Zaheer, G.A. Fisher, T.S. Crocenzi, J.J. Lee, S.M. Duffy, R.M. Goldberg, A. de la Chapelle, M. Koshiji, F. Bhaijee, T. Huebner, R.H. Hruban, L.D. Wood, N. Cuka, D.M. Pardoll, N. Papadopoulos, K.W. Kinzler, S. Zhou, T.C. Cornish, J.M. Taube, R.A. Anders, J.R. Eshleman, B. Vogelstein, and L.A. Diaz, Jr. 2015. PD-1 Blockade in Tumors with Mismatch-Repair Deficiency. *N Engl J Med* 372:2509-2520.

Leach, D.R., M.F. Krummel, and J.P. Allison. 1996. Enhancement of antitumor immunity by CTLA-4 blockade. *Science* 271:1734-1736.

Li, T., and Z.J. Chen. 2018. The cGAS-cGAMP-STING pathway connects DNA damage to inflammation, senescence, and cancer. *J Exp Med* 215:1287-1299.

Lucas, M., W. Schachterle, K. Oberle, P. Aichele, and A. Diefenbach. 2007. Dendritic cells prime natural killer cells by trans-presenting interleukin 15. *Immunity* 26:503-517.

Luteijn, R.D., S.A. Zaver, B.G. Gowen, S.K. Wyman, N.E. Garelis, L. Onia, S.M. McWhirter, G.E. Katibah, J.E. Corn, J.J. Woodward, and D.H. Raulet. 2019. SLC19A1 transports immunoreactive cyclic dinucleotides. *Nature* 573:434-438.

Mach, B., V. Steimle, E. Martinez-Soria, and W. Reith. 1996. Regulation of MHC class II genes: lessons from a disease. *Annu Rev Immunol* 14:301-331.

Maciejewski, J., C. Selleri, S. Anderson, and N.S. Young. 1995. Fas antigen expression on CD34+ human marrow cells is induced by interferon gamma and tumor necrosis factor alpha and potentiates cytokine-mediated hematopoietic suppression in vitro. *Blood* 85:3183-3190.

Mandelboim, O., N. Lieberman, M. Lev, L. Paul, T.I. Arnon, Y. Bushkin, D.M. Davis, J.L. Strominger, J.W. Yewdell, and A. Porgador. 2001. Recognition of haemagglutinins on virus-infected cells by NKp46 activates lysis by human NK cells. *Nature* 409:1055-1060.

Mangsbo, S.M., L.C. Sandin, K. Anger, A.J. Korman, A. Loskog, and T.H. Totterman. 2010. Enhanced tumor eradication by combining CTLA-4 or PD-1 blockade with CpG therapy. *J Immunother* 33:225-235.

Marcus, A., B.G. Gowen, T.W. Thompson, A. Iannello, M. Ardolino, W. Deng, L. Wang, N. Shifrin, and D.H. Raulet. 2014. Recognition of tumors by the innate immune system and natural killer cells. *Adv Immunol* 122:91-128.

Marcus, A., A.J. Mao, M. Lensink-Vasan, L. Wang, R.E. Vance, and D.H. Raulet. 2018. Tumor-Derived cGAMP Triggers a STING-Mediated Interferon Response in Non-tumor Cells to Activate the NK Cell Response. *Immunity* 49:754-763 e754.

Martinez, J., X. Huang, and Y. Yang. 2008. Direct action of type I IFN on NK cells is required for their activation in response to vaccinia viral infection in vivo. *J Immunol* 180:1592-1597.

McCarthy, E.F. 2006. The toxins of William B. Coley and the treatment of bone and soft-tissue sarcomas. *Iowa Orthop J* 26:154-158.

McGranahan, N., R. Rosenthal, C.T. Hiley, A.J. Rowan, T.B.K. Watkins, G.A. Wilson, N.J. Birkbak, S. Veeriah, P. Van Loo, J. Herrero, C. Swanton, and T.R. Consortium. 2017. Allele-Specific HLA Loss and Immune Escape in Lung Cancer Evolution. *Cell* 171:1259-1271 e1211.

Meazza, R., B. Azzarone, A.M. Orengo, and S. Ferrini. 2011. Role of common-gamma chain cytokines in NK cell development and function: perspectives for immunotherapy. *J Biomed Biotechnol* 2011:861920.

Meric-Bernstam, F., S.K. Sandhu, O. Hamid, A. Spreafico, S. Kasper, R. Dummer, T. Shimizu, N. Steeghs, N. Lewis, C.C. Talluto, S. Dolan, A. Bean, R. Brown, D. Trujillo, N. Nair, and J.J. Luke. 2019. Phase Ib study of MIW815 (ADU-S100) in combination with spartalizumab (PDR001) in patients (pts) with advanced/metastatic solid tumors or lymphomas. *Journal of Clinical Oncology* 37:2507-2507.

Mizutani, T., N. Neugebauer, E.M. Putz, N. Moritz, O. Simma, E. Zebedin-Brandl, D. Gotthardt, W. Warsch, E. Eckelhart, H.P. Kantner, U. Kalinke, S. Lienenklaus, S. Weiss, B. Strobl, M. Muller, V. Sexl, and D. Stoiber. 2012. Conditional IFNAR1 ablation reveals distinct requirements of Type I IFN signaling for NK cell maturation and tumor surveillance. *Oncoimmunology* 1:1027-1037.

Mlecnik, B., G. Bindea, H.K. Angell, M.S. Sasso, A.C. Obenauf, T. Fredriksen, L. Lafontaine, A.M. Bilocq, A. Kirilovsky, M. Tosolini, M. Waldner, A. Berger, W.H. Fridman, A. Rafii, V. Valge-Archer, F. Pages, M.R. Speicher, and J. Galon. 2014. Functional network pipeline reveals genetic determinants associated with in situ lymphocyte proliferation and survival of cancer patients. *Science translational medicine* 6:228ra237.

Montoya, M., G. Schiavoni, F. Mattei, I. Gresser, F. Belardelli, P. Borrow, and D.F. Tough. 2002. Type I interferons produced by dendritic cells promote their phenotypic and functional activation. *Blood* 99:3263-3271.

Moretta, A., C. Bottino, M. Vitale, D. Pende, R. Biassoni, M.C. Mingari, and L. Moretta. 1996. Receptors for HLA class-I molecules in human natural killer cells. *Ann. Rev. Immunol.* 14:619-648.

Moretta, A., C. Bottino, M. Vitale, D. Pende, C. Cantoni, M.C. Mingari, R. Biassoni, and L. Moretta. 2001. Activating receptors and coreceptors involved in human natural killer cell-mediated cytolysis. *Annu Rev Immunol* 19:197-223.

Morgens, D.W., M. Wainberg, E.A. Boyle, O. Ursu, C.L. Araya, C.K. Tsui, M.S. Haney, G.T. Hess, K. Han, E.E. Jeng, A. Li, M.P. Snyder, W.J. Greenleaf, A. Kundaje, and M.C. Bassik. 2017. Genome-scale measurement of off-target activity using Cas9 toxicity in high-throughput screens. *Nat Commun* 8:15178.

Mortier, E., R. Advincula, L. Kim, S. Chmura, J. Barrera, B. Reizis, B.A. Malynn, and A. Ma. 2009. Macrophage- and dendritic-cell-derived interleukin-15 receptor alpha supports homeostasis of distinct CD8+ T cell subsets. *Immunity* 31:811-822.

Mortier, E., T. Woo, R. Advincula, S. Gozalo, and A. Ma. 2008. IL-15R{alpha} chaperones IL-15 to stable dendritic cell membrane complexes that activate NK cells via trans presentation. *J Exp Med* 205:1213-1225.

Mumberg, D., P.A. Monach, S. Wanderling, M. Philip, A.Y. Toledano, R.D. Schreiber, and H. Schreiber. 1999. CD4(+) T cells eliminate MHC class II-negative cancer cells in vivo by indirect effects of IFN-gamma. *Proc Natl Acad Sci U S A* 96:8633-8638.

Narni-Mancinelli, E., J. Chaix, A. Fenis, Y.M. Kerdiles, N. Yessaad, A. Reynders, C. Gregoire, H. Luche, S. Ugolini, E. Tomasello, T. Walzer, and E. Vivier. 2011. Fate mapping analysis of lymphoid cells expressing the NKp46 cell surface receptor. *Proc Natl Acad Sci U S A* 108:18324-18329.

Narni-Mancinelli, E., L. Gauthier, M. Baratin, S. Guia, A. Fenis, A.E. Deghmane, B. Rossi, P. Fourquet, B. Escaliere, Y.M. Kerdiles, S. Ugolini, M.K. Taha, and E. Vivier. 2017. Complement factor P is a ligand for the natural killer cell-activating receptor NKp46. *Science immunology* 2:

Ni, J., M. Miller, A. Stojanovic, N. Garbi, and A. Cerwenka. 2012. Sustained effector function of IL-12/15/18-preactivated NK cells against established tumors. *J Exp Med* 209:2351-2365.

O'Sullivan, T., G.P. Dunn, D.Y. Lacoursiere, R.D. Schreiber, and J.D. Bui. 2011. Cancer immunoediting of the NK group 2D ligand H60a. *J Immunol* 187:3538-3545.

Ohkuri, T., A. Ghosh, A. Kosaka, J. Zhu, M. Ikeura, M. David, S.C. Watkins, S.N. Sarkar, and H. Okada. 2014. STING contributes to antiglioma immunity via triggering type I IFN signals in the tumor microenvironment. *Cancer Immunol Res* 2:1199-1208.

Oppenheim, D.E., S.J. Roberts, S.L. Clarke, R. Filler, J.M. Lewis, R.E. Tigelaar, M. Girardi, and A.C. Hayday. 2005. Sustained localized expression of ligand for the activating NKG2D receptor impairs natural cytotoxicity in vivo and reduces tumor immunosurveillance. *Nat Immunol* 6:928-937.

Ossendorp, F., E. Mengede, M. Camps, R. Filius, and C.J. Melief. 1998. Specific T helper cell requirement for optimal induction of cytotoxic T lymphocytes against major histocompatibility complex class II negative tumors. *J Exp Med* 187:693-702.

Park, J.H., M.B. Geyer, and R.J. Brentjens. 2016. CD19-targeted CAR T-cell therapeutics for hematologic malignancies: interpreting clinical outcomes to date. *Blood* 127:3312-3320.

Pende, D., S. Parolini, A. Pessino, S. Sivori, R. Augugliaro, L. Morelli, E. Marcenaro, L. Accame, A. Malaspina, R. Biassoni, C. Bottino, L. Moretta, and A. Moretta. 1999. Identification and molecular characterization of NKp30, a novel triggering receptor involved in natural cytotoxicity mediated by human natural killer cells. *Journal of Experimental Medicine* 190:1505-1516.

Pessino, A., S. Sivori, C. Bottino, A. Malaspina, L. Morelli, L. Moretta, R. Biassoni, and A. Moretta. 1998. Molecular cloning of NKp46: a novel member of the immunoglobulin

superfamily involved in triggering of natural cytotoxicity. *Journal of Experimental Medicine* 188:953-960.
Pipkin, M.E., A. Rao, and M.G. Lichtenheld. 2010. The transcriptional control of the perforin locus. *Immunol Rev* 235:55-72.
Platten, M., W. Wick, and B.J. Van den Eynde. 2012. Tryptophan catabolism in cancer: beyond IDO and tryptophan depletion. *Cancer Res* 72:5435-5440.
Pogge von Strandmann, E., V.R. Simhadri, B. von Tresckow, S. Sasse, K.S. Reiners, H.P. Hansen, A. Rothe, B. Boll, V.L. Simhadri, P. Borchmann, P.J. McKinnon, M. Hallek, and A. Engert. 2007. Human leukocyte antigen-B-associated transcript 3 is released from tumor cells and engages the NKp30 receptor on natural killer cells. *Immunity* 27:965-974.
Qin, Z., and T. Blankenstein. 2000. CD4+ T cell--mediated tumor rejection involves inhibition of angiogenesis that is dependent on IFN gamma receptor expression by nonhematopoietic cells. *Immunity* 12:677-686.
Quezada, S.A., T.R. Simpson, K.S. Peggs, T. Merghoub, J. Vider, X. Fan, R. Blasberg, H. Yagita, P. Muranski, P.A. Antony, N.P. Restifo, and J.P. Allison. 2010. Tumor-reactive CD4+ T cells develop cytotoxic activity and eradicate large established melanoma after transfer into lymphopenic hosts. *J Exp Med*
Ramakrishnan, P., and D. Baltimore. 2011. Sam68 is required for both NF-kappaB activation and apoptosis signaling by the TNF receptor. *Mol Cell* 43:167-179.
Raulet, D.H., S. Gasser, B.G. Gowen, W. Deng, and H. Jung. 2013. Regulation of ligands for the NKG2D activating receptor. *Annu Rev Immunol* 31:413-441.
Raulet, D.H., and N. Guerra. 2009. Oncogenic stress sensed by the immune system: role of natural killer cell receptors. *Nat Rev Immunol* 9:568-580.
Raulet, D.H., and R.E. Vance. 2006. Self-tolerance of natural killer cells. *Nat Rev Immunol* 6:520-531.
Restifo, N.P., F.M. Marincola, Y. Kawakami, J. Taubenberger, J.R. Yannelli, and S.A. Rosenberg. 1996. Loss of functional beta 2-microglobulin in metastatic melanomas from five patients receiving immunotherapy. *J Natl Cancer Inst* 88:100-108.
Ribas, A., and J.D. Wolchok. 2018. Cancer immunotherapy using checkpoint blockade. *Science* 359:1350-1355.
Ritchie, C., A.F. Cordova, G.T. Hess, M.C. Bassik, and L. Li. 2019. SLC19A1 Is an Importer of the Immunotransmitter cGAMP. *Mol Cell* 75:372-381 e375.
Rizvi, N.A., M.D. Hellmann, A. Snyder, P. Kvistborg, V. Makarov, J.J. Havel, W. Lee, J. Yuan, P. Wong, T.S. Ho, M.L. Miller, N. Rekhtman, A.L. Moreira, F. Ibrahim, C. Bruggeman, B. Gasmi, R. Zappasodi, Y. Maeda, C. Sander, E.B. Garon, T. Merghoub, J.D. Wolchok, T.N. Schumacher, and T.A. Chan. 2015. Cancer immunology. Mutational landscape determines sensitivity to PD-1 blockade in non-small cell lung cancer. *Science* 348:124-128.
Rodig, S.J., D. Gusenleitner, D.G. Jackson, E. Gjini, A. Giobbie-Hurder, C. Jin, H. Chang, S.B. Lovitch, C. Horak, J.S. Weber, J.L. Weirather, J.D. Wolchok, M.A. Postow, A.C. Pavlick, J. Chesney, and F.S. Hodi. 2018. MHC proteins confer differential sensitivity to CTLA-4 and PD-1 blockade in untreated metastatic melanoma. *Science translational medicine* 10:
Roemer, M.G., R.H. Advani, R.A. Redd, G.S. Pinkus, Y. Natkunam, A.H. Ligon, C.F. Connelly, C.J. Pak, C.D. Carey, S.E. Daadi, B. Chapuy, D. de Jong, R.T. Hoppe, D.S. Neuberg, M.A. Shipp, and S.J. Rodig. 2016. Classical Hodgkin Lymphoma with Reduced

beta2M/MHC Class I Expression Is Associated with Inferior Outcome Independent of 9p24.1 Status. *Cancer Immunol Res* 4:910-916.

Romagne, F., P. Andre, P. Spee, S. Zahn, N. Anfossi, L. Gauthier, M. Capanni, L. Ruggeri, D.M. Benson, Jr., B.W. Blaser, M. Della Chiesa, A. Moretta, E. Vivier, M.A. Caligiuri, A. Velardi, and N. Wagtmann. 2009. Preclinical characterization of 1-7F9, a novel human anti-KIR receptor therapeutic antibody that augments natural killer-mediated killing of tumor cells. *Blood* 114:2667-2677.

Rosenberg, S.A. 2014. IL-2: the first effective immunotherapy for human cancer. *J Immunol* 192:5451-5458.

Rosenberg, S.A., and N.P. Restifo. 2015. Adoptive cell transfer as personalized immunotherapy for human cancer. *Science* 348:62-68.

Sade-Feldman, M., Y.J. Jiao, J.H. Chen, M.S. Rooney, M. Barzily-Rokni, J.P. Eliane, S.L. Bjorgaard, M.R. Hammond, H. Vitzthum, S.M. Blackmon, D.T. Frederick, M. Hazar-Rethinam, B.A. Nadres, E.E. Van Seventer, S.A. Shukla, K. Yizhak, J.P. Ray, D. Rosebrock, D. Livitz, V. Adalsteinsson, G. Getz, L.M. Duncan, B. Li, R.B. Corcoran, D.P. Lawrence, A. Stemmer-Rachamimov, G.M. Boland, D.A. Landau, K.T. Flaherty, R.J. Sullivan, and N. Hacohen. 2017. Resistance to checkpoint blockade therapy through inactivation of antigen presentation. *Nat Commun* 8:1136.

Schadendorf, D., F.S. Hodi, C. Robert, J.S. Weber, K. Margolin, O. Hamid, D. Patt, T.T. Chen, D.M. Berman, and J.D. Wolchok. 2015. Pooled Analysis of Long-Term Survival Data From Phase II and Phase III Trials of Ipilimumab in Unresectable or Metastatic Melanoma. *J Clin Oncol* 33:1889-1894.

Schietinger, A., M. Philip, V.E. Krisnawan, E.Y. Chiu, J.J. Delrow, R.S. Basom, P. Lauer, D.G. Brockstedt, S.E. Knoblaugh, G.J. Hammerling, T.D. Schell, N. Garbi, and P.D. Greenberg. 2016. Tumor-Specific T Cell Dysfunction Is a Dynamic Antigen-Driven Differentiation Program Initiated Early during Tumorigenesis. *Immunity* 45:389-401.

Schumacher, T.N., and R.D. Schreiber. 2015. Neoantigens in cancer immunotherapy. *Science* 348:69-74.

Scott, A.C., F. Dundar, P. Zumbo, S.S. Chandran, C.A. Klebanoff, M. Shakiba, P. Trivedi, L. Menocal, H. Appleby, S. Camara, D. Zamarin, T. Walther, A. Snyder, M.R. Femia, E.A. Comen, H.Y. Wen, M.D. Hellmann, N. Anandasabapathy, Y. Liu, N.K. Altorki, P. Lauer, O. Levy, M.S. Glickman, J. Kaye, D. Betel, M. Philip, and A. Schietinger. 2019. TOX is a critical regulator of tumour-specific T cell differentiation. *Nature* 571:270-274.

Seaman, W.E., M. Sleisenger, E. Eriksson, and G.C. Koo. 1987. Depletion of natural killer cells in mice by monoclonal antibody to NK-1.1. Reduction in host defense against malignancy without loss of cellular or humoral immunity. *J Immunol* 138:4539-4544.

Seo, H., J. Chen, E. Gonzalez-Avalos, D. Samaniego-Castruita, A. Das, Y.H. Wang, I.F. Lopez-Moyado, R.O. Georges, W. Zhang, A. Onodera, C.J. Wu, L.F. Lu, P.G. Hogan, A. Bhandoola, and A. Rao. 2019. TOX and TOX2 transcription factors cooperate with NR4A transcription factors to impose CD8(+) T cell exhaustion. *Proc Natl Acad Sci U S A* 116:12410-12415.

Shankaran, V., H. Ikeda, A.T. Bruce, J.M. White, P.E. Swanson, L.J. Old, and R.D. Schreiber. 2001. IFN gamma and lymphocytes prevent primary tumour development and shape tumour immunogenicity. *Nature* 410:1107-1111.

Sharma, P., and J.P. Allison. 2015a. The future of immune checkpoint therapy. *Science* 348:56-61.

Sharma, P., and J.P. Allison. 2015b. Immune checkpoint targeting in cancer therapy: toward combination strategies with curative potential. *Cell* 161:205-214.
Shen, Y.J., N. Le Bert, A.A. Chitre, C.X. Koo, X.H. Nga, S.S. Ho, M. Khatoo, N.Y. Tan, K.J. Ishii, and S. Gasser. 2015. Genome-derived cytosolic DNA mediates type I interferon-dependent rejection of B cell lymphoma cells. *Cell Rep* 11:460-473.
Sheng, Y., F. Li, and Z. Qin. 2018. TNF Receptor 2 Makes Tumor Necrosis Factor a Friend of Tumors. *Frontiers in immunology* 9:1170.
Shimasaki, N., A. Jain, and D. Campana. 2020. NK cells for cancer immunotherapy. *Nat Rev Drug Discov*
Shimizu, T., H. Uenishi, Y. Teramura, M. Iwashiro, K. Kuribayashi, H. Tamamura, N. Fujii, and H. Yamagishi. 1994. Fine structure of a virus-encoded helper T-cell epitope expressed on FBL-3 tumor cells. *J Virol* 68:7704-7708.
Sivick, K.E., A.L. Desbien, L.H. Glickman, G.L. Reiner, L. Corrales, N.H. Surh, T.E. Hudson, U.T. Vu, B.J. Francica, T. Banda, G.E. Katibah, D.B. Kanne, J.J. Leong, K. Metchette, J.R. Bruml, C.O. Ndubaku, J.M. McKenna, Y. Feng, L. Zheng, S.L. Bender, C.Y. Cho, M.L. Leong, A. van Elsas, T.W. Dubensky, Jr., and S.M. McWhirter. 2018. Magnitude of Therapeutic STING Activation Determines CD8(+) T Cell-Mediated Anti-tumor Immunity. *Cell Rep* 25:3074-3085 e3075.
Sivori, S., S. Parolini, E. Marcenaro, R. Castriconi, D. Pende, R. Millo, and A. Moretta. 2000. Involvement of natural cytotoxicity receptors in human natural killer cell-mediated lysis of neuroblastoma and glioblastoma cell lines. *J Neuroimmunol* 107:220-225.
Sivori, S., D. Pende, C. Bottino, E. Marcenaro, A. Pessino, R. Biassoni, L. Moretta, and A. Moretta. 1999. NKp46 is the major triggering receptor involved in the natural cytotoxicity of fresh or cultured human NK cells. Correlation between surface density of NKp46 and natural cytotoxicity against autologous, allogeneic or xenogeneic target cells. *Eur J Immunol* 29:1656-1666.
Smyth, M.J., E. Cretney, J.M. Kelly, J.A. Westwood, S.E. Street, H. Yagita, K. Takeda, S.L. van Dommelen, M.A. Degli-Esposti, and Y. Hayakawa. 2005. Activation of NK cell cytotoxicity. *Mol Immunol* 42:501-510.
Smyth, M.J., N.Y. Crowe, and D.I. Godfrey. 2001. NK cells and NKT cells collaborate in host protection from methylcholanthrene-induced fibrosarcoma. *International immunology* 13:459-463.
Spranger, S., R. Bao, and T.F. Gajewski. 2015. Melanoma-intrinsic beta-catenin signalling prevents anti-tumour immunity. *Nature* 523:231-235.
Sun, J.C., and L.L. Lanier. 2008. Cutting edge: viral infection breaks NK cell tolerance to "missing self". *J Immunol* 181:7453-7457.
Swann, J.B., Y. Hayakawa, N. Zerafa, K.C. Sheehan, B. Scott, R.D. Schreiber, P. Hertzog, and M.J. Smyth. 2007. Type I IFN contributes to NK cell homeostasis, activation, and antitumor function. *J Immunol* 178:7540-7549.
Tanaka, A., and S. Sakaguchi. 2017. Regulatory T cells in cancer immunotherapy. *Cell Res* 27:109-118.
Thompson, T.W., A.B. Kim, P.J. Li, J. Wang, B.T. Jackson, K.T.H. Huang, L. Zhang, and D.H. Raulet. 2017. Endothelial cells express NKG2D ligands and desensitize anti-tumor NK responses. *Elife* 6:e30881.
Trapani, J.A., and M.J. Smyth. 2002. Functional significance of the perforin/granzyme cell death pathway. *Nat Rev Immunol* 2:735-747.

Ulloa-Montoya, F., J. Louahed, B. Dizier, O. Gruselle, B. Spiessens, F.F. Lehmann, S. Suciu, W.H. Kruit, A.M. Eggermont, J. Vansteenkiste, and V.G. Brichard. 2013. Predictive gene signature in MAGE-A3 antigen-specific cancer immunotherapy. *J Clin Oncol* 31:2388-2395.

Vallera, D.A., M. Felices, R. McElmurry, V. McCullar, X. Zhou, J.U. Schmohl, B. Zhang, A.J. Lenvik, A. Panoskaltsis-Mortari, M.R. Verneris, J. Tolar, S. Cooley, D.J. Weisdorf, B.R. Blazar, and J.S. Miller. 2016. IL15 Trispecific Killer Engagers (TriKE) Make Natural Killer Cells Specific to CD33+ Targets While Also Inducing Persistence, In Vivo Expansion, and Enhanced Function. *Clinical cancer research : an official journal of the American Association for Cancer Research* 22:3440-3450.

van Hall, T., J. van Bergen, P.A. van Veelen, M. Kraakman, L.C. Heukamp, F. Koning, C.J. Melief, F. Ossendorp, and R. Offringa. 2000. Identification of a novel tumor-specific CTL epitope presented by RMA, EL-4, and MBL-2 lymphomas reveals their common origin. *J Immunol* 165:869-877.

Vance, R.E., J.R. Kraft, J.D. Altman, P.E. Jensen, and D.H. Raulet. 1998. Mouse CD94/NKG2A is a natural killer cell receptor for the nonclassical MHC class I molecule Qa-1^{b}. *J Exp Med* 188:1841-1848.

Vey, N., J.H. Bourhis, N. Boissel, D. Bordessoule, T. Prebet, A. Charbonnier, A. Etienne, P. Andre, F. Romagne, D. Benson, H. Dombret, and D. Olive. 2012. A phase 1 trial of the anti-inhibitory KIR mAb IPH2101 for AML in complete remission. *Blood* 120:4317-4323.

Vitale, M., C. Bottino, S. Sivori, L. Sanseverino, R. Castraconi, E. Marcenaro, R. Augugliaro, L. Moretta, and A. Moretta. 1998. NKp44, a novel triggering surface molecule specifically expressed by activated natural killer cells, is involved in non-major histocompatibility complex-restricted tumor cell lysis. *J. Exp. Med.* 187:2065-2072.

Vivier, E., D.H. Raulet, A. Moretta, M.A. Caligiuri, L. Zitvogel, L.L. Lanier, W.M. Yokoyama, and S. Ugolini. 2011. Innate or adaptive immunity? The example of natural killer cells. *Science* 331:44-49.

Voskoboinik, I., M.J. Smyth, and J.A. Trapani. 2006. Perforin-mediated target-cell death and immune homeostasis. *Nat Rev Immunol* 6:940-952.

Waggoner, S.N., M. Cornberg, L.K. Selin, and R.M. Welsh. 2011. Natural killer cells act as rheostats modulating antiviral T cells. *Nature*

Weiner, L.M., R. Surana, and S. Wang. 2010. Monoclonal antibodies: versatile platforms for cancer immunotherapy. *Nat Rev Immunol* 10:317-327.

Wherry, E.J., and M. Kurachi. 2015. Molecular and cellular insights into T cell exhaustion. *Nat Rev Immunol* 15:486-499.

Wolchok, J.D., H. Kluger, M.K. Callahan, M.A. Postow, N.A. Rizvi, A.M. Lesokhin, N.H. Segal, C.E. Ariyan, R.A. Gordon, K. Reed, M.M. Burke, A. Caldwell, S.A. Kronenberg, B.U. Agunwamba, X. Zhang, I. Lowy, H.D. Inzunza, W. Feely, C.E. Horak, Q. Hong, A.J. Korman, J.M. Wigginton, A. Gupta, and M. Sznol. 2013. Nivolumab plus ipilimumab in advanced melanoma. *N Engl J Med* 369:122-133.

Woo, S.R., M.B. Fuertes, L. Corrales, S. Spranger, M.J. Furdyna, M.Y. Leung, R. Duggan, Y. Wang, G.N. Barber, K.A. Fitzgerald, M.L. Alegre, and T.F. Gajewski. 2014. STING-dependent cytosolic DNA sensing mediates innate immune recognition of immunogenic tumors. *Immunity* 41:830-842.

Wu, J., and L.L. Lanier. 2003. Natural killer cells and cancer. *Adv Cancer Res* 90:127-156.

Xie, Y., A. Akpinarli, C. Maris, E.L. Hipkiss, M. Lane, E.K. Kwon, P. Muranski, N.P. Restifo, and P.A. Antony. 2010. Naive tumor-specific CD4(+) T cells differentiated in vivo eradicate established melanoma. *J Exp Med* 207:651-667.

Yang, H., W.S. Lee, S.J. Kong, C.G. Kim, J.H. Kim, S.K. Chang, S. Kim, G. Kim, H.J. Chon, and C. Kim. 2019. STING activation reprograms tumor vasculatures and synergizes with VEGFR2 blockade. *J Clin Invest* 130:4350-4364.

Yarchoan, M., A. Hopkins, and E.M. Jaffee. 2017. Tumor Mutational Burden and Response Rate to PD-1 Inhibition. *N Engl J Med* 377:2500-2501.

Zaretsky, J.M., A. Garcia-Diaz, D.S. Shin, H. Escuin-Ordinas, W. Hugo, S. Hu-Lieskovan, D.Y. Torrejon, G. Abril-Rodriguez, S. Sandoval, L. Barthly, J. Saco, B. Homet Moreno, R. Mezzadra, B. Chmielowski, K. Ruchalski, I.P. Shintaku, P.J. Sanchez, C. Puig-Saus, G. Cherry, E. Seja, X. Kong, J. Pang, B. Berent-Maoz, B. Comin-Anduix, T.G. Graeber, P.C. Tumeh, T.N. Schumacher, R.S. Lo, and A. Ribas. 2016. Mutations Associated with Acquired Resistance to PD-1 Blockade in Melanoma. *N Engl J Med* 375:819-829.

Zhang, Q., J. Bi, X. Zheng, Y. Chen, H. Wang, W. Wu, Z. Wang, Q. Wu, H. Peng, H. Wei, R. Sun, and Z. Tian. 2018. Blockade of the checkpoint receptor TIGIT prevents NK cell exhaustion and elicits potent anti-tumor immunity. *Nat Immunol* 19:723-732.

Zhao, L., L.M. Ching, P. Kestell, and B.C. Baguley. 2002. The antitumour activity of 5,6-dimethylxanthenone-4-acetic acid (DMXAA) in TNF receptor-1 knockout mice. *British journal of cancer* 87:465-470.

Zhou, C., X. Chen, R. Planells-Cases, J. Chu, L. Wang, L. Cao, Z. Li, K.I. Lopez-Cayuqueo, Y. Xie, S. Ye, X. Wang, F. Ullrich, S. Ma, Y. Fang, X. Zhang, Z. Qian, X. Liang, S.Q. Cai, Z. Jiang, D. Zhou, Q. Leng, T.S. Xiao, K. Lan, J. Yang, H. Li, C. Peng, Z. Qiu, T.J. Jentsch, and H. Xiao. 2020. Transfer of cGAMP into Bystander Cells via LRRC8 Volume-Regulated Anion Channels Augments STING-Mediated Interferon Responses and Anti-viral Immunity. *Immunity*

Zhu, J., and W.E. Paul. 2008. CD4 T cells: fates, functions, and faults. *Blood* 112:1557-1569.

Zhu, Q., S.M. Man, P. Gurung, Z. Liu, P. Vogel, M. Lamkanfi, and T.D. Kanneganti. 2014. Cutting edge: STING mediates protection against colorectal tumorigenesis by governing the magnitude of intestinal inflammation. *J Immunol* 193:4779-4782.

Zitvogel, L., L. Galluzzi, O. Kepp, M.J. Smyth, and G. Kroemer. 2015. Type I interferons in anticancer immunity. *Nat Rev Immunol* 15:405-414.